



New global steel industry study shows how to shrink the environmental footprint of next-generation car bodies by up to nearly 70 percent with use of new steels, latest design optimization techniques and electrified powertrain

## FutureSteelVehicle

*Nature's Way to Mobility*

### Overview Report



April 2011

---

**FutureSteelVehicle (FSV)** is a programme of WorldAutoSteel, the automotive group of the World Steel Association comprised of seventeen major global steel producers from around the world:

- Anshan Iron & Steel Group Corporation
- ArcelorMittal
- Baoshan Iron & Steel Co. Ltd.
- China Steel Corporation
- Hyundai-Steel Company
- JFE Steel Corporation
- Kobe Steel, Ltd.
- Nippon Steel Corporation
- Nucor Corporation
- POSCO
- Severstal
- Sumitomo Metal Industries, Ltd.
- Tata Steel
- ThyssenKrupp Steel Europe AG (SE-AG)
- United States Steel Corporation
- Usinas Siderurgicas de Minas Gerais S.A.
- voestalpine Stahl GmbH

WorldAutoSteel's mission is to advance and communicate steel's unique ability to meet the automotive industry's needs and challenges in a sustainable and environmentally responsible way. We are committed to a low carbon future, the principles of which are embedded in continuous research in and advancement of automotive steel products, for the benefit of society and future generations. To learn more about WorldAutoSteel and its projects, visit [www.worldautosteel.org](http://www.worldautosteel.org).

The FSV programme is the most recent addition to the global steel industry's series of initiatives offering steel solutions to the challenges facing automakers around the world to increase the fuel efficiency of automobiles and reduce greenhouse gas emissions, while improving safety and performance and maintaining affordability. This programme follows the UltraLight Steel Auto Body 1998, the UltraLight Steel Auto Closures 2000, UltraLight Steel Auto Suspension 2000, and ULSAB-AVC (Advanced Vehicle Concepts) 2001, representing nearly €60 million in research and demonstration investment.

WorldAutoSteel commissioned EDAG, Inc., Auburn Hills, Michigan, USA, to conduct an advanced powertrain technology assessment, and to provide vehicle design and program engineering management for the FutureSteelVehicle program. For the FutureSteelVehicle program, EDAG, along with its engineering partners ETA and LMS, applied a holistic approach to vehicle layout design using advanced future powertrains and creating a new vehicle architecture that offers mass efficient, steel-intensive solutions. The future advanced powertrains that have major influence on vehicle layout and body structure architecture are: Battery Electric Vehicles, (BEV), Plug-In Hybrid Electric Vehicle (PHEV) and Fuel Cell Electric Vehicle (FCEV).

*This work may not be edited or modified without the express permission of WorldAutoSteel.  
FutureSteelVehicle™ and WorldAutoSteel™ are trademarks of WorldAutoSteel.*

#### **Acknowledgments:**

##### **FutureSteelVehicle Technology Partners (Phase 2):**

- EDAG AG
- Engineering Technologies Associates Inc.
- LMS Engineering Services

**FSV Programme Chair:** Jody Shaw, United States Steel Corporation

**FSV Programme Manager:** Harry Singh, EDAG, Inc.

##### **FSV Steering Team Members:**

T. Chen	China Steel Corporation	M. Lambriks	Tata Steel Europe
K. Fukui	Sumitomo Metal Industries, Ltd.	J. Meng	Anshan Iron & Steel Group Corporation
A. Gauriat	ArcelorMittal	E. Opbroek	WorldAutoSteel
O. Hoffmann	ThyssenKrupp Steel Europe	M. Peruzzi	voestalpine Stahl GmbH
S. Hong	Hyundai Steel Company	J. Powers	Severstal
T. Inazumi	JFE Steel Corporation	E. Taiss	Usinas Siderúrgicas de Minas Gerais S.A.
D. Kanelos	Nucor Corporation	C. ten Broek	WorldAutoSteel
J. Kim	POSCO	K. Watanabe	Kobe Steel, Ltd.
R. Krupitzer	AISI's Steel Market Development Institute	W. Xu	Baoshan Iron & Steel Co. Ltd.
Y. Kuriyama	Nippon Steel Corporation		

## Table of Contents

	PAGE
<b>0.0 Seven Key Achievements</b>	<b>4</b>
0.1 Body Structure Steel Technologies	5
0.2 Results "At A Glance"	6
<b>1.0 Project Objectives</b>	<b>7</b>
1.1 FSV Advanced Powertrains Options and Performance	7
1.2 Body Structure Mass Targets	8
1.3 Steel Materials and Manufacturing Processes Portfolios	8
1.3.1 Steel Designations	9
1.3.2 FSV Steel Technologies	10
1.4 State-of-the-Future Design Optimisation Methodologies – Nature's Way to Mobility	10
1.5 Noise, Vibration and Harshness Analysis	10
1.6 CAE Analysis	10
1.7 Total Life Cycle Emissions	11
<b>2.0 Phase 2 Design Methodology, T1-T5</b>	<b>12</b>
2.1 T1: Packing, Styling & CFD Simulations	12
2.2 T2: Topology Optimisation	14
2.3 T3: Low Fidelity 3G Optimisation	15
2.4 T4: Body Structure Sub-Systems Optimisation	16
2.4.1 3G Optimisation of Sub-Systems	17
2.5 T5: Detailed Body Structure Design	18
2.5.1 BEV Sub-System Selection	18
2.5.2 Mass/Cost Paradigm Shift	19
2.5.3 Carbon (GHG) Cost Effect	20
2.5.4 Selection Example for FSV Rocker Solutions	20
2.6 Selected Sub-Systems	22
2.7 Sub-System Integration into Body Design	23
2.8 Final 2G (Grade and Gauge) Full System Design Optimisation	24
2.8.1 Hardening Effects	26
2.8.2 Bead Optimisation	26
2.9 Noise, Vibration and Harshness Analysis	27
<b>3.0 FSV BEV Body Structure Design, Performance and Assembly</b>	<b>28</b>
3.1 FSV BEV Final Light Weight Body Structure	28
3.2 Nature's Way to Mobility	31
3.2.1 Front Rail Sub-System	31
3.2.2 Shot Gun	32
3.2.3 Rocker	33
3.3 Load Paths for Crash Management	33
3.3.1 Front End for Front Impact	33
3.3.2 Side Structure for Side Impact	34
3.3.3 Rear Structure for Rear Impact	36

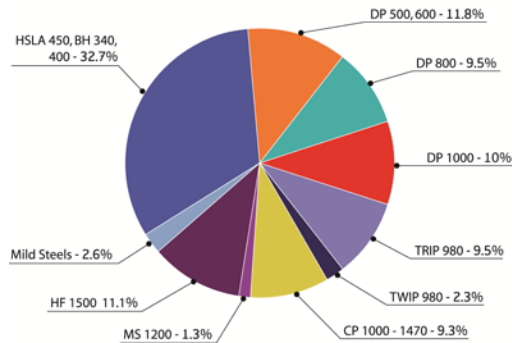
---

	<b>PAGE</b>
3.4 Body Structure Performance CAE Analysis	37
3.4.1 Crash Events	39
3.5 Manufacturing Process Simulation Results	40
3.5.1 One Step Metal Stamping Simulation	40
3.5.2 One Step Hot Stamping Simulation	40
3.5.3 Incremental Forming Simulation	41
3.5.3.1 Front Rail Lower	41
3.5.3.2 Front Rail Upper	43
3.5.3.3 Body Side Outer	44
3.6 Body Structure Joining and Assembly	46
3.6.1 Joining Technology	46
3.6.2 Weldability of Advanced High-Strength Steels	47
3.6.2.1 Laser Welding of Zinc-Coated Steels	47
3.6.2.2 Laser Welding of Three Material Thicknesses	47
3.6.3 Body Assembly Flow Chart	48
<b>4.0 Cost Assessment</b>	<b>49</b>
4.1 Increase Volumes and Comparison to ULSAB-AVC	50
4.2 Sensitivity Analysis	51
<b>5.0 Environmental Assessments</b>	<b>52</b>
5.1 Life Cycle Assessment	53
5.1.1 Methodology	53
5.1.2 Results	54
5.2 Fuel Assessments	56
5.2.1 Pump-to-Wheel CO <sub>2</sub> e Emissions Assessment	56
5.2.2 Well-to-Wheel Analysis	57
<b>6.0 Extension to Plug-In-Hybrid and Fuel Cell Variants</b>	<b>58</b>
6.1 FSV-1 PHEV <sub>20</sub>	58
6.2 FSV-2 Variants	59
6.2.1 FSV-2 PHEV <sub>40</sub>	59
6.2.2 FSV-2 FCEV	60
<b>References</b>	<b>61</b>
<b>Appendices</b>	<b>62</b>
1. FSV Materials Portfolio	63
2. FSV Design Flow Chart	64
3. FSV BEV Exploded View and Parts List	65
4. FSV-1 PHEV <sub>20</sub> Exploded View and Parts List	70
5. FSV-2 Exploded View and Parts List	75

## 0.0 Seven Key Achievements



FSV BEV Steel Types  
as % of Body Structure Mass



### 1. State-of-the-future design innovations that exploit steel's versatility and strength

Steel's design flexibility makes best use of the award-winning "state of the future" design optimisation process that develops non-intuitive solutions for structural performance. The resulting optimised shapes and component configurations often mimic Mother Nature's own design efficiency where structure and strength is placed exactly where it is needed for the intended function. FSV's steel portfolio is utilised with the aid of full vehicle analysis to determine material grade and thickness optimisation. Consequently, FSV vehicles are very efficient and very light weight.

### 2. Achieves 35% body structure mass savings compared to a benchmark vehicle

Compared to a highly efficient A-/ B-Class current production vehicle whose ICE powertrain mass is nearly 100 kg lighter than the BEV, the FSV BEV weighs just 188 kg compared to the production vehicle's 230 kg. And compared to a benchmark body structure weighing 290 kg, FSV reduces mass by 35%.

### 3. Uses 97% High-Strength (HSS) and Advanced High-Strength Steel (AHSS)

The FSV programme brings yet more advanced steel and steel technologies to its portfolio, and consequently to the tool sets of automotive engineers around the world. It includes over 20 new AHSS grades, representing materials expected to be commercially available in the 2015 – 2020 technology horizon.

### 4. Uses nearly 50% GigaPascal steels

The FSV material portfolio includes Dual Phase, TRIP, TWIP, Complex Phase, and Hot Formed steels, which reach into GigaPascal strength levels and are the newest in steel technology offered by the global industry. These steels answer the call of automakers for stronger, yet formable steels needed for lighter structures that meet ever increasing crash requirements and are evidence of steel's continual reinvention of itself to meet automotive design challenges.

### 5. Enables 5-star safety ratings

Included as an integral part of the design optimisation process are crash analyses according to a set of stringent analyses that encompass the most severe global requirements. FSV meets or exceeds the structural requirements for each of these analyses, and thereby enables the achievement of five-star safety ratings in final production vehicles.

### 6. Reduces total Lifetime Emissions by nearly 70%

The data show that, using the U.S. energy grid and the previously noted production vehicle comparison, AHSS combined with an electrified powertrain reduces total life cycle emissions by 56%. In regions where energy grid sources are more efficient, such as Europe, this grows to nearly 70% reduction in total life cycle emissions.

### 7. Reduces mass and emissions at no cost penalty

Dramatic mass reduction is achieved at no cost penalty over current steel body structures. The FSV BEV can be manufactured and assembled for an estimated cost of US\$1,115.

## 0.1 Body Structure Steel Technologies

FSV's design optimisation process identified a number of options that were viable solutions for light weight body structure applications. The charts below represent the results of those selected by FSV's engineering team based on the programme's selection criteria for the final demonstration vehicle. A wide variety of steel material and technology options are possible, depending on the selection criteria imposed.

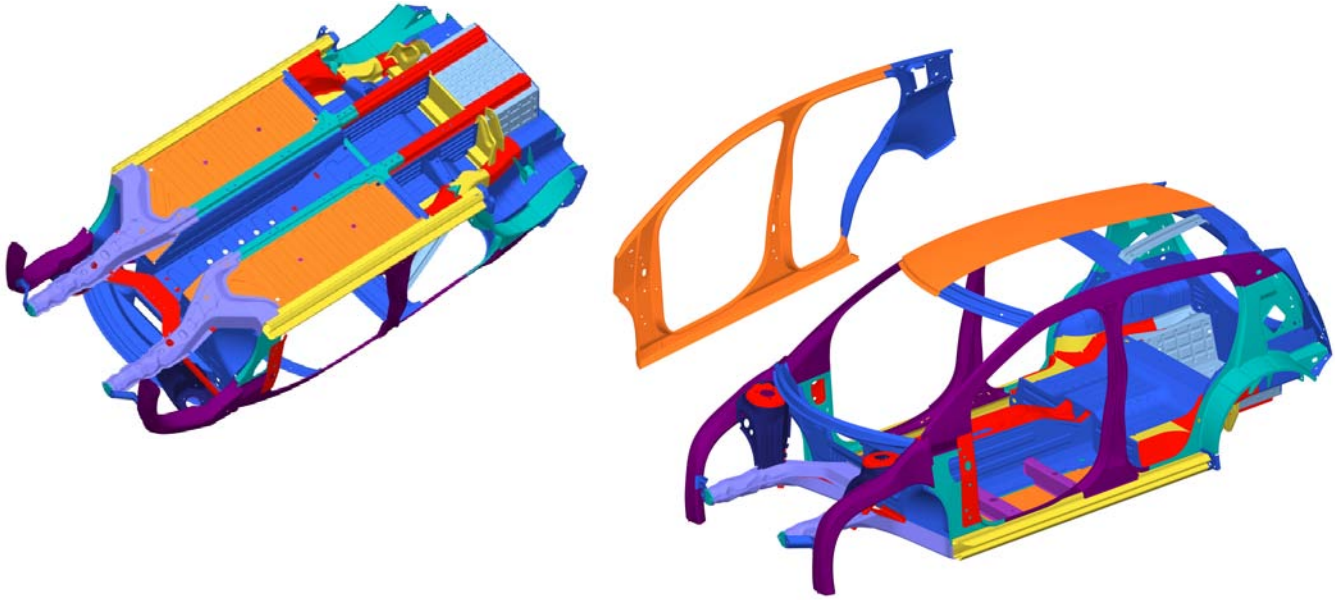


Figure 0-2: Battery Electric Vehicle (BEV) Body Structure (colour-coded by steel type)

### FSV BEV Steel Types as % of Body Structure Mass

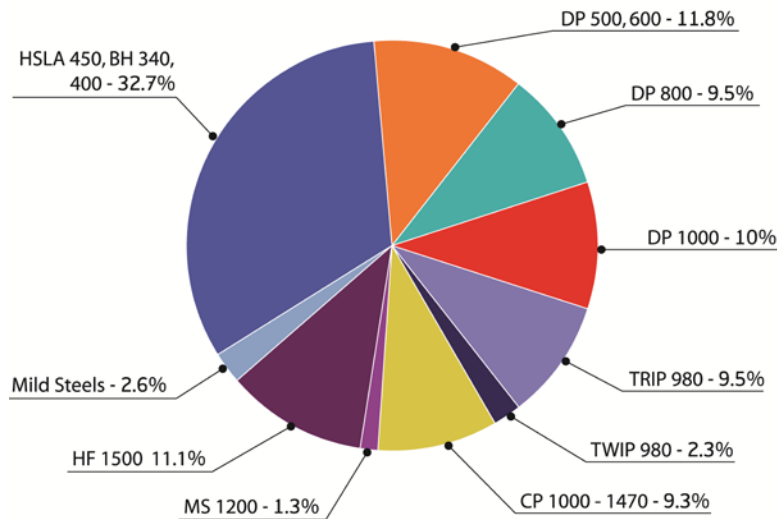


Figure 0-3: FSV BEV Steel Types

## 0.2 Results At-A-Glance

Analysis	FSV1		FSV2	
	BEV	PHEV <sub>20</sub>	PHEV <sub>40</sub>	FCEV
<b>Body Structure Mass (kg)</b>				
Benchmarked Mass	290	269	276	303
Target Mass	190			
Achieved Mass	188	175	201	201
<b>Crash Safety</b>				
US NCAP	Meets or exceeds all structural targets – enables 5-star safety ratings			
Euro NCAP				
IIHS Side Impact				
US SINCAP Side Impact				
FMVSS 301 Rear Impact				
ECE R32				
FMVSS 214 Pole Impact				
Euro NCAP Pole Impact				
FMVSS 216a and IIHS Roof				
RCAR/IIHS Low Speed Impact				
<b>Durability</b>				
3g pot hole	Meets or exceeds all targets			
0.7g cornering				
0.8g forward braking				
<b>Noise, Vibration and Harshness</b>	Meets or exceeds all targets – change from combustion engine to electric motor is compatible with mass reductions and similar or better noise and vibration performances.			
<b>Ride and Handling</b>				
Fish-Hook	Less than 10%			
Double Lane Change Maneuver (ISO 3888-1)	Pass			
<b>Environmental Assessments</b>				
Pump-to-Wheel, Well-to-Wheel Assessments	Less than 95 g CO <sub>2</sub> e/km			
Life Cycle Assessment	15, 373 kg CO <sub>2</sub> e			
<b>Cost Analysis</b>	<b>US\$</b>			
Total Body Parts Manufacturing	\$775			
Body Structure Assembly Cost	\$340			
Total	\$1,115			

## 1.0 Project Objectives

Through the FutureSteelVehicle programme, WorldAutoSteel continues the re-invention process of steel in the automobile. In the quest for more environmentally friendly vehicles, it is necessary to re-think the design of the car to host fundamentally different powertrains such as hybrid, electric, and fuel cell systems, and to ensure that the structure is as environmentally efficient as its powertrain.

The FutureSteelVehicle (FSV) programme, which was launched at the 2007 United Nations Climate Change Conference in Bali, is a multi-million Euro, three-year programme to deliver safe, light weight Advanced High-Strength Steel (AHSS) body structures that address radically different requirements for advanced powertrains and reduce Greenhouse Gas (GHG) emissions over the entire life cycle. FutureSteelVehicle addresses the increased value of mass reduction with solutions that demonstrate steel as the material of choice for vehicle structures.

The engineering team focus, headed by EDAG's Auburn Hills, Mich., USA facility, is a holistic concept development approach to innovative vehicle layout and optimised vehicle body structures, using an expanded portfolio of steels and manufacturing technologies that foretell the future of steel grades readily available in the 2015 to 2020 time frame. The state-of-the-future design methodology used to develop the FSV body structure is at the leading edge of computer-aided optimisation techniques, to achieve an optimal mass efficient design.

Fundamental to ensuring reduced life cycle GHG emissions was the measurement of the total environmental impact. Life Cycle Assessment (LCA) methodology, described in Section 5.0, was applied to measure reduction in total life cycle greenhouse gas (GHG) emissions and drive the selection process of various design options.

Steel technology, design methodology, and LCA combine to realise the best environmental solution for compliance with future vehicle emissions targets.

The FutureSteelVehicle (FSV) programme consists of three phases:

- Phase 1: Engineering Study (completed)
- Phase 2: Concept Designs (completed)
- Phase 3: Demonstration and Implementation (2011-2012)

The content of Phase 1, results of which are documented in a separate report, was a comprehensive assessment and identification of advanced powertrains and future automotive technology applicable to high-volume vehicle production in the 2015-2020 timeframe. This report summarises the completion of Phase 2, designing optimised AHSS body structures for four proposed vehicles: battery electric (BEV) and plug-in hybrid electric (PHEV-20) for A-/ B-Class vehicles; and plug-in hybrid electric (PHEV-40) and fuel cell (FCV) for C-/ D-class vehicles. See Figure 2-1, for an illustration of the programme tasks.

### 1.1 FSV Advanced Powertrain Options & Performances

The deliverables from Phase 1 included complete vehicle technical specifications and vehicle layout showing major components of advanced powertrain modules, and engineering content, which were identified as those most likely to be available in the marketplace in the programme target time frame. Following in Table 1-1 are the powertrain options and performance parameters selected for inclusion in the Phase 2 vehicle concept design development.

**Table 1-1: Powertrain Options and Performance**

<b>FSV 1</b> <b>A-B Class</b> <b>4-door hatchback</b> <b>3700 mm long</b>	<b>Plug-In Hybrid</b> PHEV <sub>20</sub> Electric Range: 32km Total: 500km Max Speed: 150km/h 0-100 km/h 11-13 s	<b>Battery Electric</b> BEV Total Range: 250km Max Speed: 150km/h 0-100 km/h 11-13 s
	<b>Plug-In Hybrid</b> PHEV <sub>40</sub> Electric Range: 64km Total: 500km Max Speed: 161km/h 0-100 km/h 10-12 s	<b>Fuel Cell</b> FCEV Total Range: 500km Max Speed: 161km/h 0-100 km/h 10-12 s
<b>FSV 2</b> <b>C-D Class</b> <b>4-door sedan</b> <b>4350 mm long</b>		

The FSV engineering team recommended the Battery Electric Vehicle (BEV), with a range of 250 km, as the focus of the Phase 2 detailed design. After the BEV detailed design was completed, the design concepts were extended by engineering judgement to the PHEV and FCEV variants as well.

## 1.2 Body Structure Mass Targets

In undertaking FSV, steel members sought to surpass the weight savings targets of production-capable vehicles or concepts in the world today. Consequently, EDAG was tasked with setting a mass reduction target that stretches beyond the limits of what has been currently realised.

EDAG responded with a proposed A/B-Class BEV body structure mass target of 190 kg that meets a stringent set of global safety requirements, and reduces the total life cycle vehicle emissions. This mass target represents a 35% reduction over a baseline vehicle, setting a new goal for vehicle light-weighting beyond the ULSAB-AVC programme's 25% achievement. This baseline vehicle body structure is the same benchmark as used for the ULSAB-AVC, adjusted for a BEV powertrain and year 2020 regulatory requirements. The FSV Phase 2 Engineering Report details how these adjustments were made. Many automakers are now implementing the ULSAB-AVC steel technologies and design concepts in production vehicles today.

As a comparison, the FSV 2015-2020 body structure target, supporting a 329 kg electric powertrain mass, is 41 kg lighter than the body structure of an existing, highly efficient 2010 A-/ B-Class vehicle (VW Polo), whose internal combustion gasoline engine (ICEg) powertrain mass is nearly 100 kg lighter at 233 kg.

## 1.3 Steel Materials and Manufacturing Processes Portfolio

The FSV programme brings yet more advanced steel and steel technologies to its portfolio than ever seen before in steel industry projects, and consequently to the tool sets of automotive engineers around the world. It includes over 20 different new and revolutionary AHSS grades representing materials expected to be commercially available in the 2015–20 technology horizon.

To put this in perspective, the ULSAB-AVC programme, completed in 2002, included 11 AHSS grades. Table 1-2 illustrates available materials for ULSAB-AVC and grades that have been added for FSV.

**Table 1-2: FSV's Expanded Steel Portfolio** (see Table 1-3 for Designator Key)

Mild 140/270	DP 350/600	TRIP 600/980
BH 210/340	TRIP 350/600	TWIP 500/980
BH 260/370	SF 570/640	DP 700/1000
BH 280/400	HSLA 550/650	HSLA 700/780
IF 260/410	TRIP 400/700	CP 800/1000
IF 300/420	SF 600/780	MS 950/1200
DP300/500	CP 500/800	CP 1000/1200
FB 330/450	DP 500/800	DP 1150/1270
HSLA 350/450	TRIP 450/800	MS 1150/1400
HSLA 420/500	CP 600/900	CP 1050/1470
FB 450/600	CP 750/900	HF 1050/1500
		MS 1250/1500

Denotes grades used for ULSAB-AVC	Denotes steel added in FSV
-----------------------------------	----------------------------

The AHSS family of products in the portfolio reflects the demand for improved materials that are required for use in existing and future production methods. AHSS grade development is driven by the ever increasing challenges faced by automakers, such as crash performance requirements, the conflicting need to reduce vehicle mass for fuel efficiency, and the need to enhance AHSS formability. A description of the metallurgy behind many of the AHSS grades can be found in WorldAutoSteel's *Advanced High-Strength Steels Application Guidelines*. FSV's detailed Material Portfolio is included as Appendix 1 to this Overview Report.

### 1.3.1 Steel Designations

Since methods used to classify steel products vary considerably throughout the world, WorldAutoSteel adopted a classification system that defines both Yield Strength (YS) and Ultimate Tensile Strength (UTS) for all steel grades. In this nomenclature, steels are identified as "XX aaa/bbb" where:

XX = Type of Steel  
 aaa = Minimum YS in MPa  
 bbb = Minimum UTS in MPa

The steel-type designator uses classifications shown in Table 1-3. As an example of this classification system, DP 500/800 refers to dual phase steel with 500 MPa minimum yield strength and 800 MPa minimum ultimate tensile strength.

**Table 1-3 Steel Type Designator**

Designator	Classification	Designator	Classification
Mild	Mild Steel	HSLA	High Strength Low Alloy
BH	Bake Hardenable	IF	Interstitial Free
CP	Complex Phase	MS	Martensitic
DP	Dual Phase	SF	Stretch Flangeable
FB	Ferritic Bainitic	TRIP	Transformation Induced Plasticity
HF	Hot Formed	TWIP	Twinning-Induced Plasticity

### 1.3.2 FSV Steel Technologies

Further AHSS mass reduction potential is realised by considering a wide bandwidth of steel technologies as shown in Table 1-4:

**Table 1-4: FSV's Steel Technologies**

Conventional Stamping	Rollforming
Laser Welded Blank	Laser Welded Coil Rollformed
Tailor Rolled Blank	Tailor Rolled Blank Rollformed
Induction Welded Hydroformed Tubes	Rollform with Quench
Laser Welded Hydroformed Tubes	Multi-Walled Hydroformed Tubes
Tailor Rolled Hydroformed Tubes	Multi-Walled Tubes
Hot Stamping (Direct & In-Direct)	Laser Welded Finalised Tubes
Laser Welded Blank Quench Steel	Laser Welded Tube Profiled Sections
Tailor Rolled Blank Quench Steel	

### 1.4 State-of-the-Future Design Optimisation Methodology – Nature's Way to Mobility

Steel's superior attributes were combined with an SAE award-winning "state-of-the-future" holistic design optimisation process that develops non-intuitive solutions for structural performance, including optimised shapes and component configurations that often mimic Mother Nature's own design efficiency. FSV's steel portfolio is utilised during the material selection process with the aid of advanced computerised, full vehicle analysis to determine geometric shape, material grade and thickness optimisation.

### 1.5 Noise, Vibration and Harshness Analysis

Simultaneous to the FSV design tasks, WorldAutoSteel commissioned LMS Engineering Services, Leuven, Belgium, to provide Noise, Vibration and Harshness (NVH) analysis to support the design process. This analysis was conducted as an integrated part of FSV's design and began early in the development tasks.

### 1.6 CAE Analysis

Included as an integral part of the design optimisation process are crash analyses according to a set of requirements that encompass the most stringent regulations around the world. Simulations were included for the events listed in Table 1-5 following.

**Table 1-5: FSV Crash Safety Analysis**

US NCAP	ECE R32 Rear Impact
Euro NCAP/IIHS	FMVSS 214 Pole Impact
IIHS Side Impact	Euro NCAP Pole Impact
US SINCAP Side Impact	FMVSS 216a and IIHS Roof Crush
FMVSS 301 Rear Impact	RCAR/IIHS Low Speed Impact

In addition, the FSV was evaluated for five vehicle durability, ride and handling conditions as follows:

1. Fish-hook test
2. Double lane change maneuver (ISO 3888-1)
3. 3g pothole test
4. 7g constant radius turn test
5. 0.8g forward braking test

Further, Static and Dynamic Stiffness analyses were conducted including torsion and bending stiffness and global modes.

### 1.7 Total Life Cycle Emissions

Life Cycle Assessment (LCA) is a technique to determine the environmental impacts of products, processes or services, through production, usage, and disposal. LCA is the only appropriate way to account for and reduce greenhouse gas emissions attributable to the automotive sector, because it assesses the entire vehicle life including the fuels that power it and the materials from which it is made.

Studies show that Life Cycle Assessment of a vehicle's environmental footprint is critical for material selection decisions. Only through LCA can the use of alternative material in a vehicle body structure be properly evaluated to ensure that increases in material production emissions do not offset the reductions in use phase emissions that may come with mass reduction.

The application of LCA allows automotive engineers to explore the impact of design, material and powertrain choices on life cycle vehicle emissions. This knowledge will help derive optimised solutions for vehicle performance, safety, and our environment. Consequently, the FSV programme design development demonstrates LCA as an integrated part of the design process, using the University of California at Santa Barbara (UCSB), Bren School of Environmental Management's Greenhouse Gas (GHG) Materials Comparison Model.

## 2.0 Phase 2 Design Methodology

An overview of the FSV design process is shown in Figure 2-1. Phase 2 activities are spread across a series of tasks, T1 thru T6, as illustrated in the Figure. To review a complete flow chart of the FSV design process, see Appendix 2.

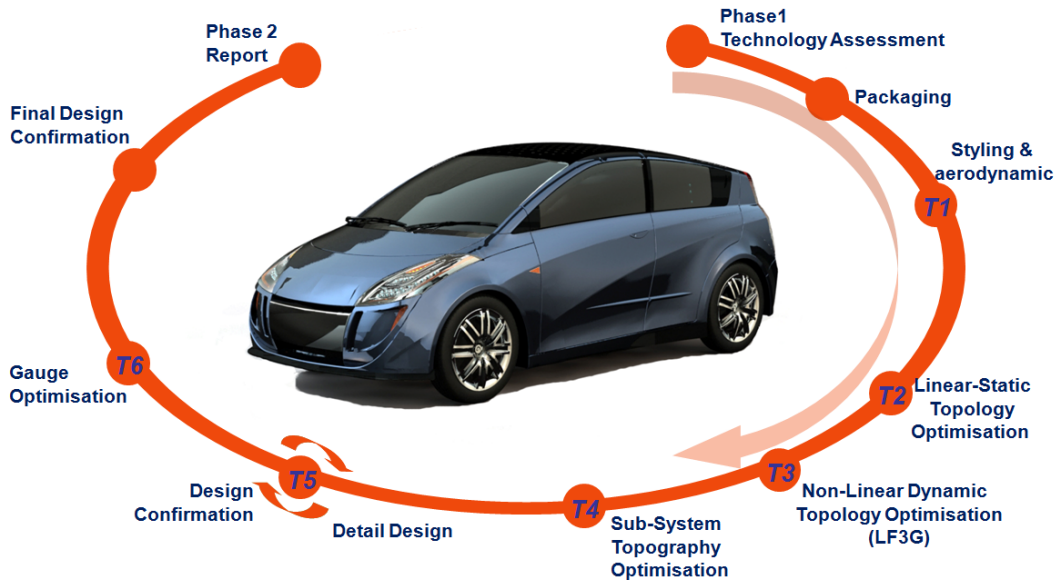


Figure 2-1: FSV Design Process

### 2.1 T1: Packaging, Styling and CFD Simulation

After the Phase 1 technology assessment, studies of powertrain packaging, interior occupant space, ingress/egress requirements, vision/obscuration, luggage volume requirements, and ergonomic and reach studies of interior components (e.g., steering column) established the component and passenger package space requirements, as shown in Figure 2-2.



Figure 2-2: Powertrain Component and Passenger Packaging

An exterior styling was applied to the packaging as shown in Figure 2-3. This styling theme provided the necessary data to derive a rough sketch of the exterior body shape.

This was followed by a Computational Fluid Dynamic (CFD) simulation to improve the aerodynamic drag to achieve the drag coefficient target (Cd) of 0.25. A styling study was completed that maintained the requirements of the previous studies.

The aerodynamic performance results for the original and the new FSV styles are shown in Table 2-1. The Cd value of 0.354 for the original FSV styling model is 42% higher than the required Cd target of 0.25. Through various incremental design changes, the Cd value was reduced to 0.237 for the final proposed style, including rear tire covers. The Cd value of 0.237 for the FSV compares to a typical value of 0.31 for an A-/ B-class vehicle. Final styling for the latest FSV vehicle is shown in Figure 2-4. It does not include rear tire covers, which increases Cd to 0.252 but would possibly be more appealing to buyers in this vehicle segment.

**Table 2-1: Aerodynamic Performance Results**

Model	Drag Force (N)	Lift Force (N)	Drag Coefficient	Lift Coefficient
FSV Baseline CFD Model	485	-113	0.354	-0.082
Modified Original FSV Model	355	224	0.259	0.163
Final FSV Styling Model (with wheel skirts)	325	101	0.237	0.073

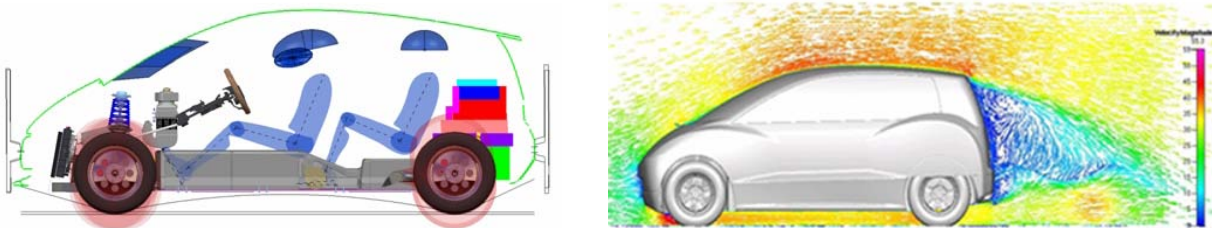


**Figure 2-3: Exterior Styling Theme and Aerodynamic Study**



**Figure 2-4: FSV Styling**

## 2.2 T2: Topology Optimisation

The objective of the topology optimisation is to provide an initial structure based on first principles using the available structure package space. The structural package space is established by the styling surface (Figure 2-4) and what remains after consideration for component and passenger packaging (Figure 2-2). The FSV programme developed this structure by considering the following load cases: three longitudinal load cases (IIHS front 40% ODB, NCAP front impact, FMVSS 301 rear 70% ODB), two lateral load cases (IIHS side impact, FMVSS 214 pole impact), one vertical load case (FMVSS 216 roof crush using the IIHS four-times strength-to-weight ratio), and bending and torsional static stiffnesses.

The topology optimisation is a linear static analysis, with equivalent static loads used as an analogy of these dynamic, non-linear crash events which react against the inertial loading of the vehicle mass, graphically represented in Figure 2-5 A. The linear approximation of the crash loads, as depicted in Figure 2-5 A, react against inertia relief constraints that represent the vehicle components masses. This approach allows load paths to develop within the available structural package space in response to the crash loads applied and the reaction loads of component mass. This is a critical aspect for the FSV programme with a unique mass distribution resulting from the advanced powertrain system.

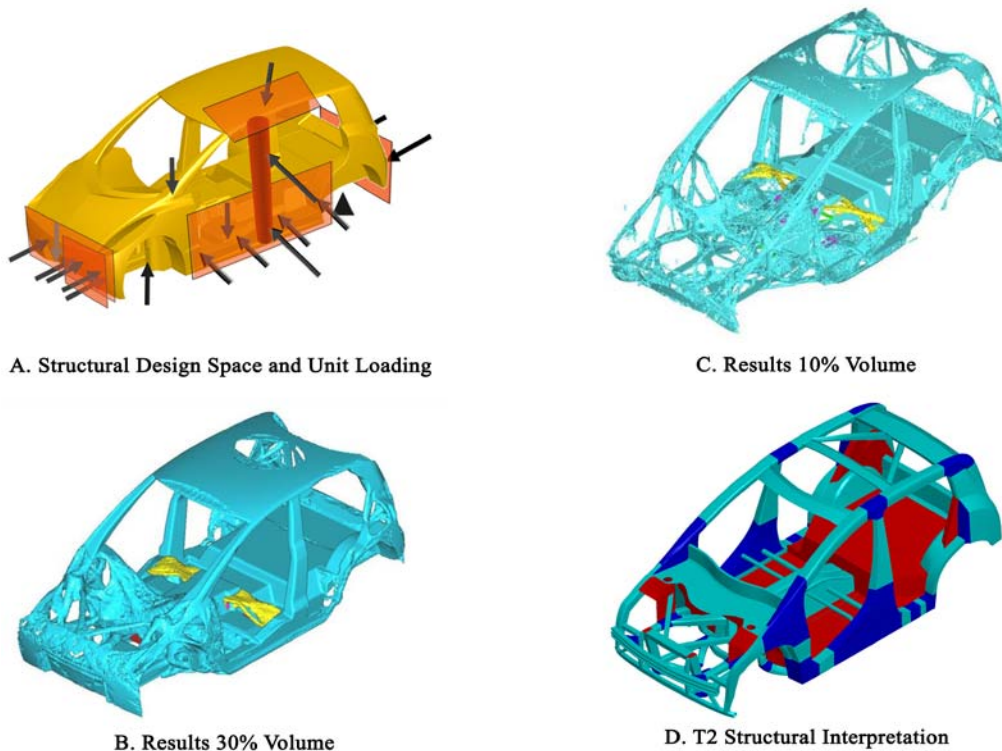


**Figure 2-5: Topology Optimisation Results**

The topology optimisation eliminates elements from a finite element mesh that represents the available structural design space, i.e. the volume within which structure can exist, thereby revealing the optimal load paths. The decision to remove an element is made based on its role in addressing the loading conditions as measured in strain energy, effectively eliminating structure that is not needed while retaining structure that is most effective. A target reduction or mass fraction is defined as a goal for the optimisation. For this analysis, the topology optimisation goals were 30%, 20% and 10% mass fractions.

With the results obtained from the topology optimisation (see Figure 2-5 B, C show the 30% and 10% mass fractions), the geometry is interpreted into a CAD model (see Figure 2-5 D) using engineering judgement. This model represents the initial skeleton geometry of the FSV and forms the basis of the next step in the optimisation process. The different mass fractions support engineering decision-making by providing a better understanding of the load-bearing needs of the structure, which often leads to non-intuitive solutions. This approach gives greater insight into the optimal load paths for translation into a manufacturable structure.

### 2.3 T3: Low Fidelity 3G (Geometry, Grade & Gauge) Optimisation

Though the topology optimisation was able to provide an initial starting point for the FSV's geometry, it is limited by its static approximation of dynamic crash loads and does not consider grade variations of the sheet metal within the structure. As stated, the initial selections of steel grade and gauge were based on engineering judgement and experience. In Task 3 (T3), the load path optimisation is moved to the dynamic design domain (LS Dyna Dynamic Finite Element Programme) and a multi-discipline optimisation programme (HEEDS® Multidisciplinary Design Optimisation Programme) using the T2 static load path optimisation as a starting assumption. T3 also addresses a low fidelity optimisation of the major load path cross-sections, grades, and gauges of the body structure. The output of T3 is designated the Low Fidelity Geometry, Grade & Gauge (LF3G) optimisation.

LF3G design addresses topology and a rough estimate of grade, gauge and geometry (section) in the dynamic domain and provides a starting place for detailed design which will address manufacturing, joint design, and local section geometries. The final FSV body structure attained from the LF3G optimisation is shown in Figure 2-6 B. The T2 Structural interpretation shown again in Figure 2-6 A allows a comparison of the optimisation-driven changes resulting from the translation from the static design domain to the dynamic design domain.

The LF3G optimised geometry (Figure 2-6 B) does not, however, represent section shapes that can necessarily be manufactured and assembled nor are they structurally efficient from a topography perspective. To assist with the interpretation of the design optimisation results, the programme requires a reference representative of a typical state-of-the-art body structure applied to the LF3G architecture.

To create the required reference body structure, the LF3G topology, grade, gauge, and geometry were combined with engineering judgement of current benchmarked designs (Figure 2-6 C). This reference assumes typical manufacturable sections and joint designs combined with extensive use of Advanced High-Strength Steels. It provides the FSV programme with the required reference and includes body structure mass, sub-system mass, part count, and manufacturing costs for comparison through the rest of the design process.

Side-by-side comparison of the first iteration of the sheet steel 'baseline' body structure reference design and LF3G geometry is also shown in Figure 2-6 B and C. The mass of the sheet steel baseline body structure (Fig 2-6 C) is calculated to be 218 kg.

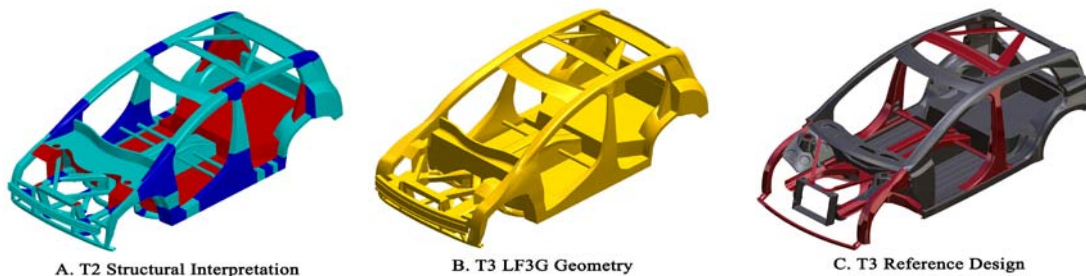


Figure 2-6: FSV Body Structure Comparison – Sheet Steel Design Baseline (C) vs. LF3G Geometry (B)

## 2.4 T4: Body Structure Sub-System Optimisation

The final design attained from the LF3G optimisation was used as the basis for the sub-system optimisation, as well as the source of the boundary conditions. Load path mapping was conducted on the model to identify the most dominant structural sub-systems in the body structure. Load path mapping considers the dominant loads in the structural sub-systems for each of the load cases as shown in Figure 2-7.

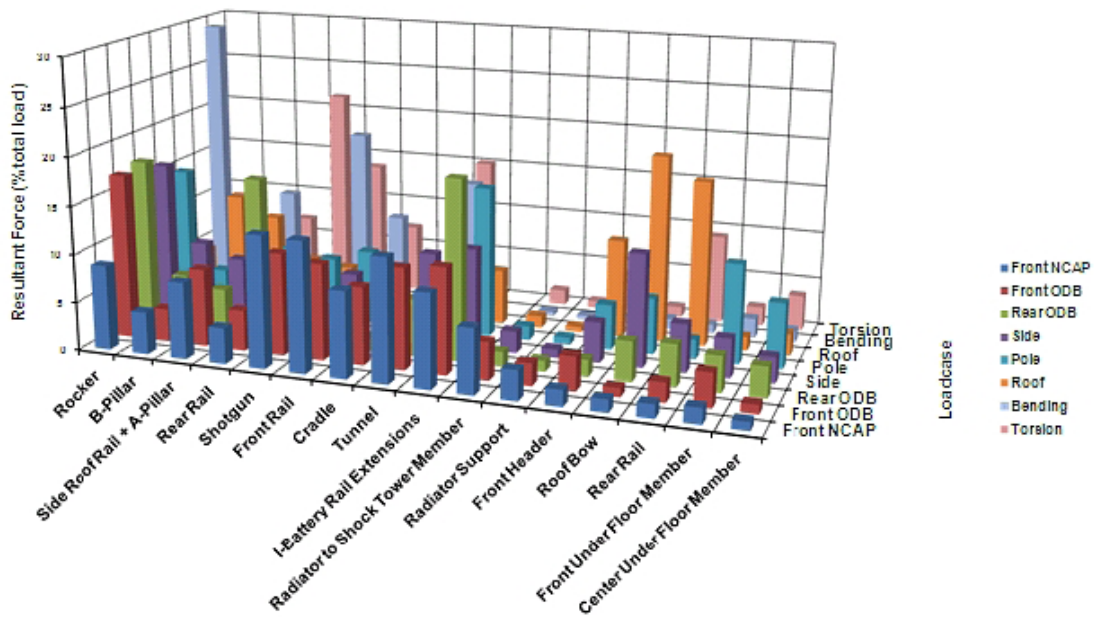


Figure 2-7: T4 Load Path Mapping – Major Load Path Components

Based on load path mapping, seven structural sub-systems (Figure 2-8) were selected for further optimisation using the spectrum of FSV's potential manufacturing technologies.

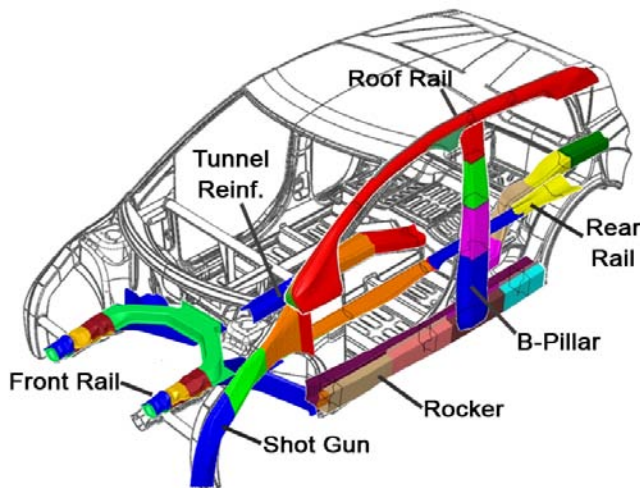


Figure 2-8: Structural Sub-Systems Selected

### 2.4.1 3G Optimisation of Sub-Systems

The optimisation objective was to minimise the mass of each sub-system and simultaneously maintain the sub-systems' total strain energy as that in the full LF3G model for each respective load case.

The solutions obtained from the structural sub-systems multi-discipline 3G optimisation runs had appropriate material strengths and gauges, optimised to give a low mass solution that met the structural performance targets. These solutions were assessed considering the respective general manufacturing technology guidelines to ensure manufacturability of the sub-system; however, detailed manufacturability issues were not yet addressed.

For example, the rocker sub-system model was optimised with AHSS for three different manufacturing methods, which included stamping, rollforming, and hydroforming (Figure 2-9). Also shown is an aluminium solution, which is included as a means for the steel industry to judge product competitiveness in these applications. The aluminum solution for each sub-system was developed by programme engineering contractor EDAG, who have expertise in aluminium automotive structures, using the same aggressive design optimisation and technology approach as the competing steel designs.

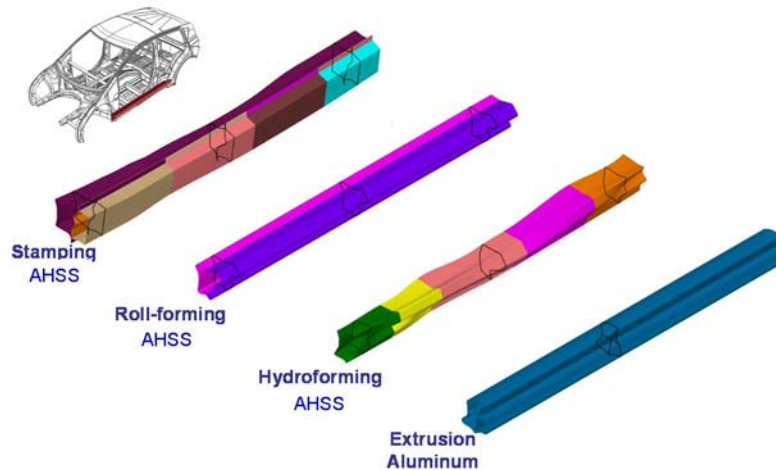


**Figure 2-9: AHSS Rocker Solutions**

Each rocker solution was further developed to consider several alternative manufacturing scenarios as shown in Figure 2-10. Each of the 12 manufacturing interpretations for the rocker structure has equivalent in-vehicle performances.

The manufacturing interpretations of each of the sub-systems formed the basis for determining the blank size, blank mass, part mass and the other related manufacturing parameters. These parameters were used as the input for the technical cost model to determine the sub-systems' manufacturing costs. The assembly costs were not assessed at this stage of the programme.

Each manufacturing interpretation underwent a life cycle assessment using the UCSB GHG Materials Comparison Model previously referenced, which is further addressed in Section 5.0.

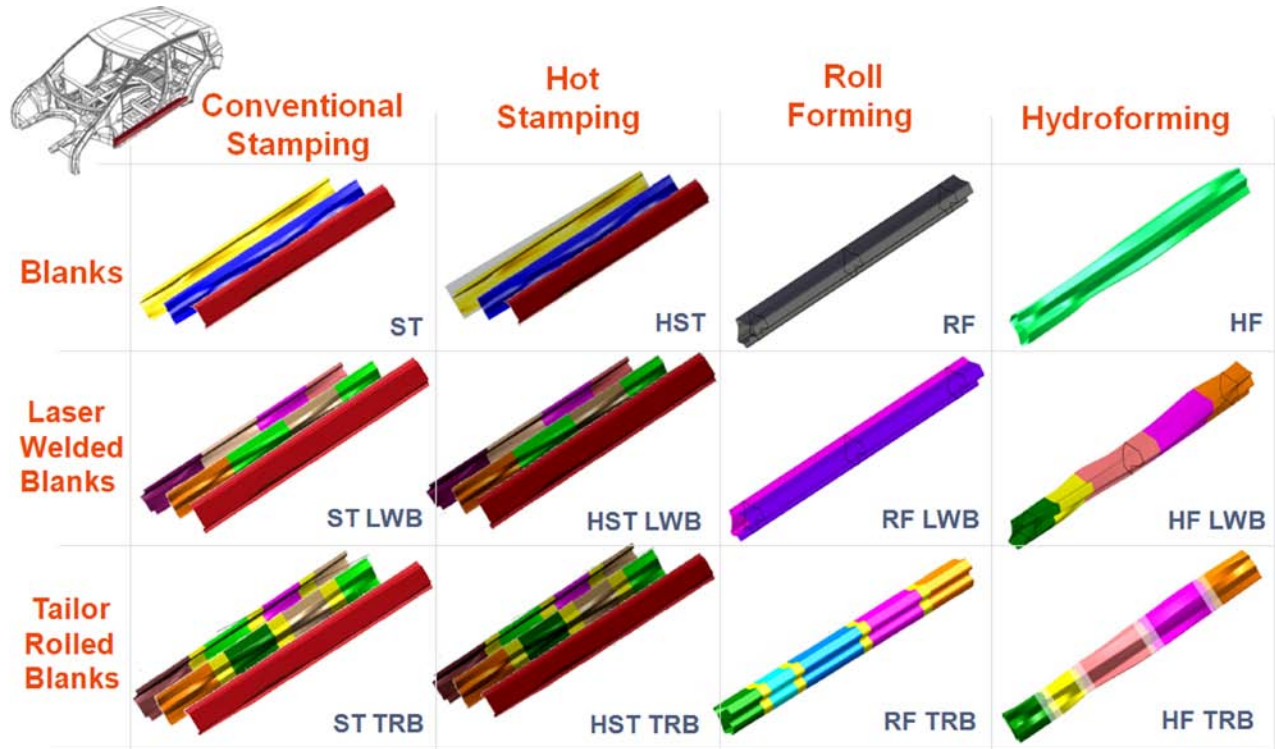


Figure 2-10: Rocker Manufacturing Steel Solutions

## 2.5 T5-Detailed Body Structure Design

### 2.5.1 BEV Sub-Systems Selection

Steel's flexibility enabled the achievement of a variety of solutions for the selected sub-systems. Within this portfolio of solutions are applications that all vehicle manufacturers and segments will find relevant. These solutions demonstrate dramatically reduced mass and GHG emissions in seven optimised sub-system structures, at lower or comparable costs to conventional solutions.

The next step in the FSV design process is to select the most appropriate sub-system options from those developed through the design methodology. The programme engineering team made these decisions based on the following factors:

- **Mass**
- **Cost**  
A "technical cost modeling" approach was applied to all parts to estimate the sub-system manufacturing costs
- **Life Cycle Assessment (LCA) for GHG**  
An analysis of each sub-system's impact on the total LCA of the vehicle conducted with the UCSB GHG Comparison Model.

Beyond these criteria the selection process considered the technology time horizon to be within the 2015-2020 timeframe. It also considered the joining compatibility between the technologies. Hence, the FSV sub-systems recommendations were divided into three categories, based on the level of difficulty of the manufacturing technology, and the time period during which these technologies would be feasible for high-volume production. The three categories were the following:

- 2010-2015 -Conservative approach (C)
- 2015-2020 -Mid-term approach (M)
- 2020-Beyond -Aggressive (A)

The process for this selection criteria approach is explained in Sections 2.5.2 – 2.5.4 following.

**2.5.2 Mass/Cost Paradigm Shift**

There is a new aspect of vehicle design associated with advanced powertrains, such as BEVs, called the “mass-cost paradigm shift.” The high cost of batteries for electrified powertrains has increased the value of mass reduction. Contrary to conventional vehicle design where the low cost structural solution is often the preferred solution, a higher cost, lighter weight solution may be preferred in the electrified vehicle since it will reduce the size, and therefore the cost, of the battery.

As an example, the FSV Phase 1 Engineering Report indicated that for the 2015-2020 timeframe, a light weight solution saving 1 kg can subsequently reduce the battery size by .021 kilowatt hours and battery cost by approximately US\$9.39 (1 kilowatt hour is estimated to cost \$450 by the year 2020), yet maintain the required 250km vehicle range. This means that vehicle manufacturers could spend more on light-weighting technology, and the cost of those solutions would be offset by the battery downsizing and its subsequent reduced cost. Consequently higher cost light weighting solutions become attractive for more vehicle applications since their cost is offset by the reduction in battery and powertrain cost. This weight reduction also could improve the driving or use phase energy efficiency, another desirable outcome.

This is illustrated in the example graph in Figure 2-11 A. The graph is shown with a set of iso-value (angled parallel) lines, enabling evaluation of solutions relative to each other on a total vehicle manufacturing cost basis. Any solutions that fall on the same iso-lines are of equal value to each other due to this off-setting reduction in powertrain costs.

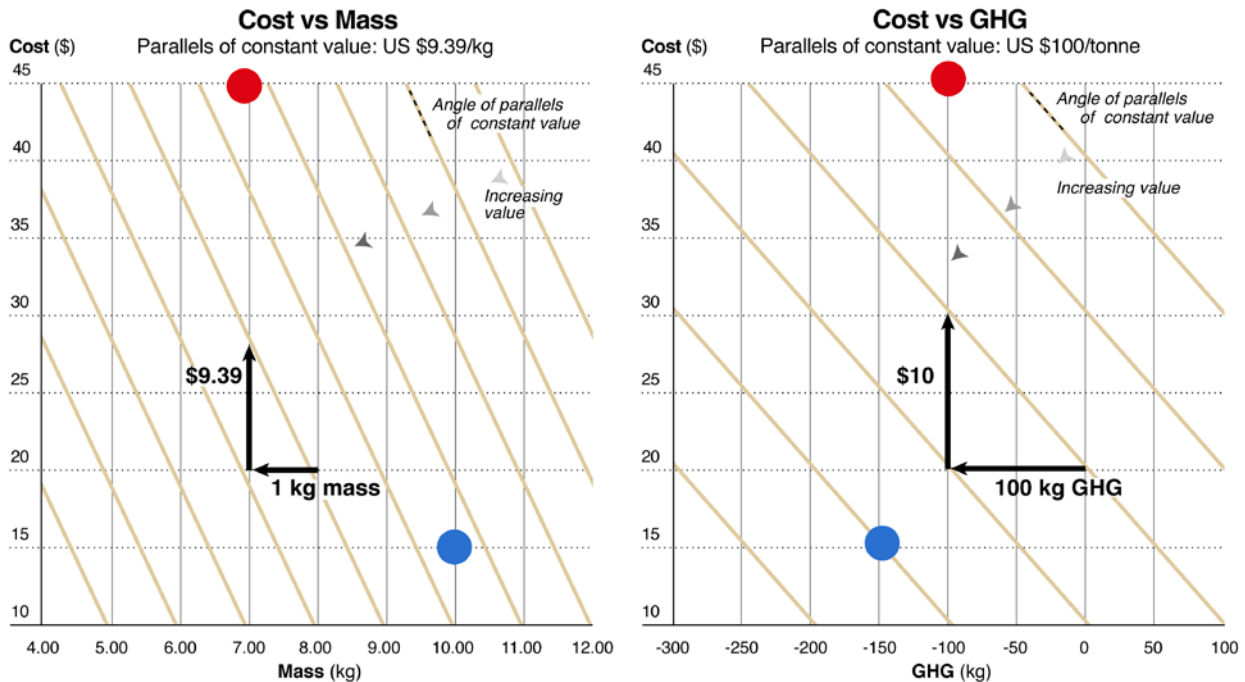


**Figure 2-11: Example Solution Comparison**

For example, in the “Mass vs. Cost” graph in Figure 2-11 A, the red and blue dots show two theoretical solutions. The red solution provides a 30% mass savings over the blue one at three times the cost. But because the red solution is more than 3 kg lighter than the blue solution, the battery cost could be reduced by nearly US\$30, which makes it of equal value to the heavier blue dot US\$15.00 solution. The red dot and the blue dot are of equal value from a total vehicle cost perspective. Therefore, the red dot may be the preferred solution if part mass is a key priority, even though it has a much higher cost.

### 2.5.3 Carbon (GHG) Cost Effect

In a similar manner to the mass-cost paradigm shift, the cost effect of carbon (GHG emissions) reduction can be assessed (see Figure 2-10 B “Cost vs. LCA GHG” graph). Heritage Foundation studies cite future costs for CO<sub>2</sub>e (GHG) emissions of up to US\$100 per metric tonne. Iso-value lines can be constructed to compare the LCA GHG saved by a light weighting solution compared to the ‘carbon cost’ (US\$100 per tonne used for this example). The example illustrates how one solution (blue dot) may not save as much mass (Figure 2-11 A) but can save more GHG (Figure 2-11 B), and therefore be the superior solution from an environmental point of view – even if there is no cost for carbon. Then, if a ‘carbon cost’ is assumed, one can evaluate alternative solutions in Figure 2-11 B using the iso-value lines.

By conducting this comparison, a better decision can be made based on the vehicle design targets. In FutureSteelVehicle’s case, a critical target is the reduction of total life cycle emissions while maintaining affordability, and therefore, the “blue” solution would be the preferred choice. The preferred solution depends on the selection criteria: low cost solution, light weight solution, or low GHG solution.

### 2.5.4 Selection Example for FSV Rocker Solutions

The comparison described in Sections 2.5.1 through 2.5.3 has been applied to all of the FSV sub-systems to evaluate the BEV’s sub-system solutions in terms of mass, cost and life cycle emissions. As an example, following in Figures 2-12 A and 2-12 B are the comparison graphs showing data solutions related to one sub-system: the FSV Rocker sub-system, comparing the 12 solutions described in Figure 2.10 on a mass, cost, and GHG basis.

An engineering judgement baseline solution is shown, representing current state of the art. Also shown is the aluminium solution that was included in the programme work for comparison purposes. In the case of the rocker, the aluminium design (an extruded profile) is not as competitive in mass, cost or GHG emissions LCA as many of the steel designs.

An additional piece of information on these tables is an estimation of manufacturing difficulty. Refer to the key at the bottom of each graph to determine the manufacturing timeframe and degree of difficulty.

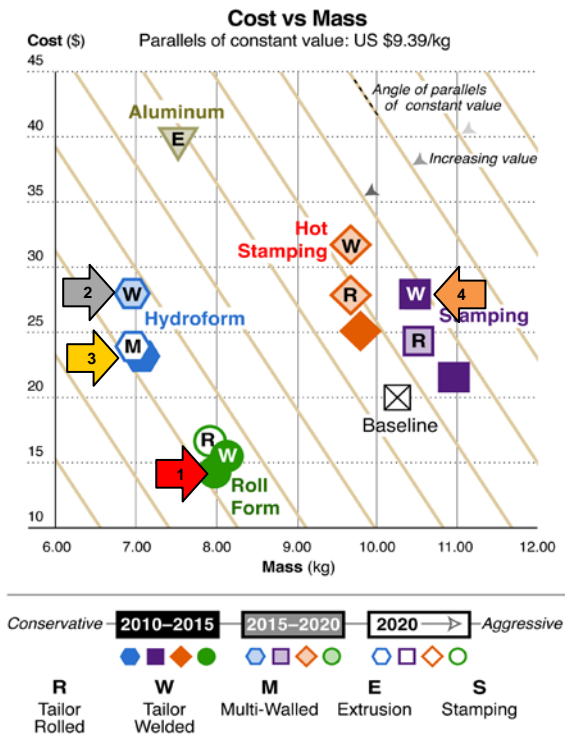


Figure 2-12 A: Rocker Solution Comparison Cost vs. Mass

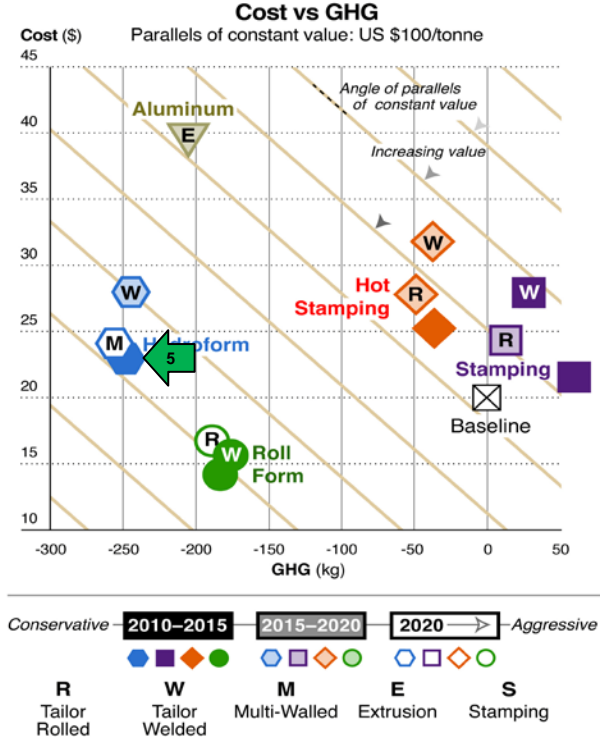


Figure 2-12 B: Rocker Solution Comparison Cost vs. GHG

By using this type of data, the design engineering team can extrapolate solutions based on a range of design drivers, such as:

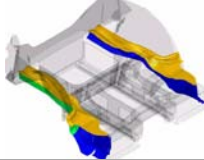
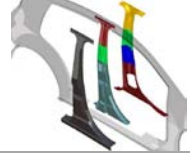
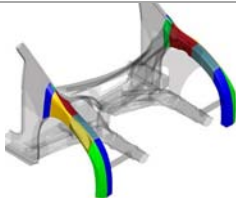
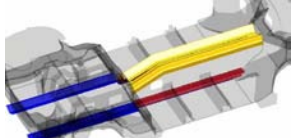
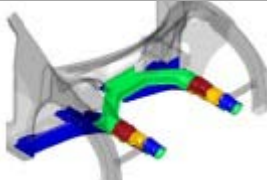
1. Lowest cost (Rollform, **red arrow** in Figure 2-12 A)
2. Lightest weight and therefore best fuel economy (Hydroform Laser Welded Tube **gray arrow**)
3. Lowest total manufacturing cost and best fuel economy (Hydroform or Hydroformed Multi-walled Tube, **yellow arrow**)
4. Reflects the existing manufacturing infrastructure (Stamped Laser Welded Blank, **orange arrow**)
5. Contributes to the lowest carbon foot print (Hydroformed Multi-walled Tube, **green arrow** in Figure 2-11 B)

In the case of FSV's rocker solutions, there are a number of attractive steel rollformed options that are achievable, cost effective and excellent in terms of carbon footprint reduction. In addition, looking at the iso-lines, there also are hydroformed solutions that would meet the design targets. The data graphs are useful tools to allow comparison among the varieties of steel solutions provided by the design methodology. Comparison graphs for all seven sub-systems can be found in the Appendix of the FSV Phase 2 Engineering Report.

## 2.6 Selected Sub-Systems

The sub-systems selected for the FSV BEV are summarised in Table 2-2:

**Table 2-2: FSV BEV sub-system selection summary**

FSV Sub-System	MFG Process (Mid-Term)	Baseline		FSV Selected Sub-System			Illustration
		Weight (kg)	MFG Cost (\$ USD)	Weight (kg)	MFG Cost (\$USD)	LCA CO <sub>2</sub> eq Savings (kg)	
Rocker	Rollformed single thickness or rollformed TWC (with conventional outer)	10.26	\$19.99	7.98/8.07	\$14.27/\$15.70	-183/-177	
Rear Rail	Stamping LWB/TRB	6.28	\$12.73	4.98/5.19	\$16.86/\$12.95	-92/-86	
B-Pillar	Hot stamping LWB w/conventional B-pillar outer	8.79	\$30.84	5.48	\$30.44	-247	
Roof Rail	Hot stamping LWB	12.73	\$27.71	9.31	\$31.71	-256	
Shotgun	Hot stamping LWB (with tailor quench)	4.2	\$14.24	4.98	\$22.11	73	
Tunnel	Open rollform	7.72	\$20.20	4.29	\$11.56	-277	
Front Rail	Stamped LWB	6.24	\$28.91	5.72	\$20.91	-65	

## 2.7 Sub-System Integration into Body Design

The selected sub-systems, as summarised in Table 2-2, formed the basis for the detailed body structure design. The sub-systems designs were further adapted to integrate with the other sub-systems in the complete vehicle, while maintaining the overall sub-system designs. There also were design changes driven by the manufacturability analysis and design for assembly considerations. For example, the solution chosen from the tunnel sub-system 3G optimisation was the open rollformed design, as shown in Figure 2-13. However, the formability analysis results showed that the one-piece tunnel was not a feasible design.

Moreover, strengthening of the side walls required additional stiffening beads, which necessitated that the side walls must be designed as individually stamped parts as illustrated in Figure 2-14. Further, to reduce the assembly costs and to maintain a less complex sub-assembly/assembly structure, it was necessary to integrate the recommended tunnel design with the floor panel and the tunnel side panel. The integration was done such that the section geometry of the tunnel, attained from the 3G optimisation, was maintained. Further, the side impact CAE simulations showed that it was necessary to add an additional stiffening feature along the critical loadpath within the tunnel sub-system. As shown in Figure 2-15, the tunnel bulkhead was added as an additional part to improve the vehicle's side impact performance.

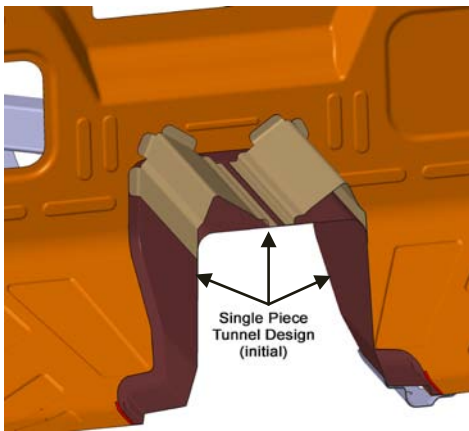


Figure 2-13: Tunnel Sub-System Initial Design

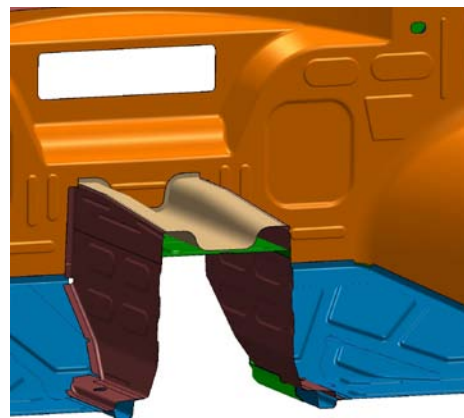


Figure 2-14: Tunnel Sub-System Current Design

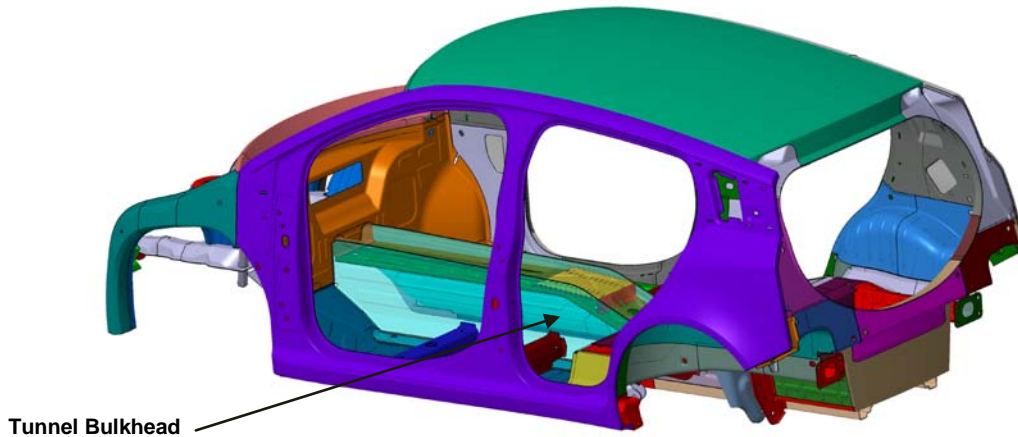


Figure 2-15: Tunnel Sub-System Shown With The Tunnel Bulkhead

## 2.8 Final - 2G (Grade and Gauge) Full System Design Optimisation

The objective of this step in the design development is to apply a 2G (grade and gauge) optimisation process to the FSV full-system vehicle which was designed based on the results of the High Fidelity 3G vehicle structural sub-system optimisation. It established the best combination of material grade, gauge, geometry and manufacturing technologies for the dominant vehicle sub-systems. The challenge was to maintain the design directions provided by the sub-system optimisation while updating it to a full and complete production level design. The re-integration of all sub-systems will naturally cause the full system body structure to become heavier. However, the T6 optimisation objective is to maintain the performance and reduce the mass of the full vehicle system back to the overall vehicle mass target. Consequently, this 2G optimisation is performed to ensure ultimate design efficiency.

The 2G optimisation process follows the same procedure as was applied to 3G (Geometry, Grade & Gauge) optimisation in the previous tasks: T3 Low Fidelity 3G Optimisation and T4 High Fidelity 3G Sub-System Optimisation. This optimisation will track the major load paths that govern Front NCAP, Front ODB, Rear ODB, IIHS Side, Pole Impacts, Roof Crush, Bending and Torsional Stiffness performance. This will provide the final gauge and grade selection for the load path sub-systems and major panels.

The goal of the final optimisation is to use the optimised primary sub-systems as enablers for the whole body structure to lose mass, specifically in the components that are not taking significant loading, such as the large panels. In order to achieve a comprehensive design solution, it is crucial to provide such enablers for the body structure to reach mass targets. Thus based on prior optimisation experience it is necessary to define a set of appropriate design variables (grade and gauge) to be used in the optimisation. For the optimisation to work as effectively as possible, it is also necessary to use its resources (time and CPU) as efficiently as possible. Thus a set of coarsened optimisation models were created and calibrated, which though were less than 50% of the size of the original models, maintained their original performance. Analysis time of the individual load cases also was reduced by reducing their total run times.

The basic steps for the 2G optimisation are show in Figure 2-16 following.

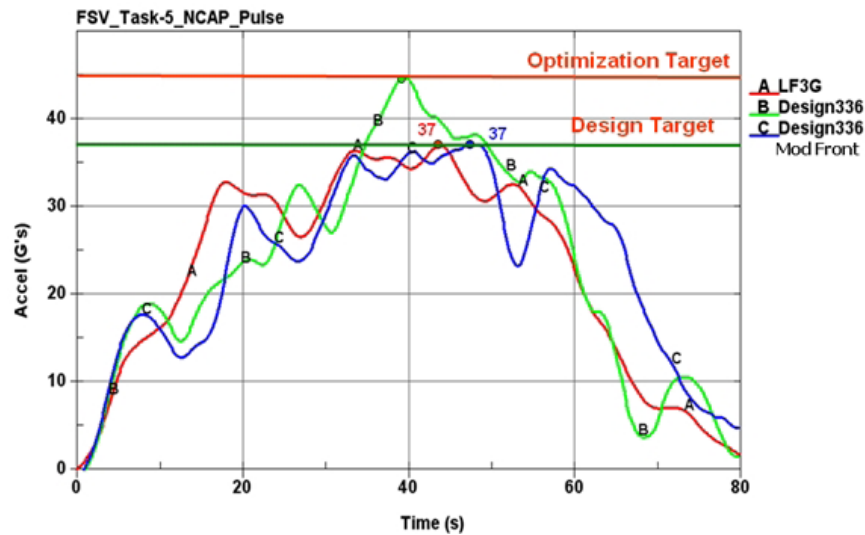


Figure 2-16: Final Optimisation Process

There were 384 optimisation iterations completed. Design #336 marks the best of the design evaluations, having the best performance and lowest mass (Table 2-3) and its gauge and grades were applied to the most updated design. At this point in development, the mass of the body structure was 188.0 kg and the USNCAP full frontal pulse was 45g's. Further analysis of this design showed that by removing the steering rack motor and modifying cradle supports, the pulse could be reduced to 37g. See Figure 2-17 for vehicle Design #336's NCAP pulse and Figure 2-18 for the interpretation to updated design.

**Table 2-3: Design #336 Mass Results**

Baseline Mass (Coarsened Model)	213.7 kg
Current Mass Savings	15.7 kg (8.4%)
Optimised Design #336 Body Structure	188.0 kg



**Figure 2-17: Design #336 USNCAP Full Frontal Vehicle Crash Pulse**

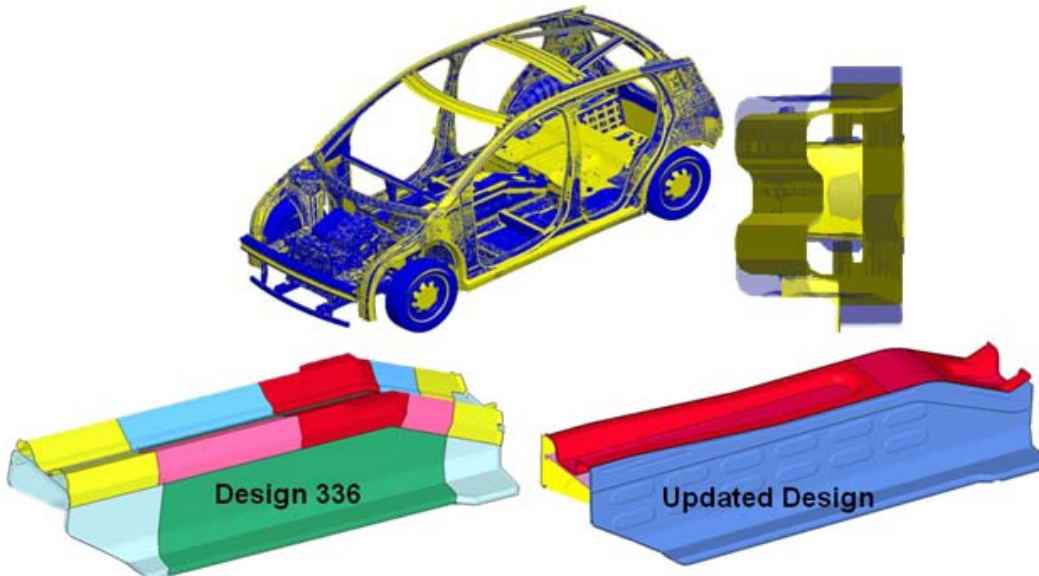


**Figure 2-18: Updated Design #336**

### 2.8.1 Hardening Effects

The gauges and grades of the final Task 5 design, with a mass of 187.7kg, were used as baselines to study the effects of material hardening in all components that use High-Strength Steel (HSS) and Dual Phase (DP) materials. To complete this study, select parts were subjected to One-Step Forming analyses using ETA/DynaForm to calculate the thinning effect, residual stress and strain, as well as to perform full vehicle crash simulations for all load cases. Figure 2-19 shows the parts that were subjected to One-Step Forming.

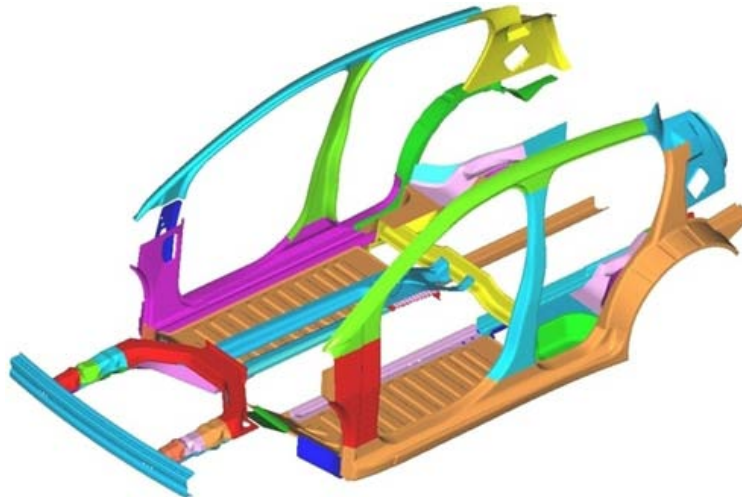


**Figure 2-19: Parts subjected to One-Step Forming analyses**

Data from the analyses were incorporated into the design and adjustments were made to address the results. After changes were made, vehicle performance was re-evaluated and showed slight improvements for IIHS side and pole impact and roof crush events due to the hardening effects. A reduction in performance was noted in the IIHS Front NCAP simulation. This potential for additional mass reduction opportunities could be further studied through continued mass optimisation work.

### 2.8.2 Bead Optimisation

In general, based on benchmark studies and trends in body structure design, the designer-developed stiffening beads are now common on many vehicle components, especially in the larger panels such as the cowl, floor, rear seat pan and trunk floor. These beads usually help in both local and global stiffness of components and body structure. The shape of the beads is usually dictated from design experience (the direction of loads), available space and manufacturing process.

Due to the ease of forming, steel offers considerable flexibility in terms of the size and direction of stiffening beads that can be added to a panel, which can be an advantage in comparison with other materials. A study was conducted to compare between optimised and traditionally designed beading patterns and their impacts on global vehicle performance. The results provided valuable guidance for the future design of large panels and their individual beading patterns. The beading optimisation study was completed by ETA. GENESIS software, which offers two beading optimisation methods (Freeform and Domain), was used in this study, employing a linear static load representation.

The main panels considered for beading optimisation were as follows:

- Cowl
- Transmission tunnel
- Floor LH & RH
- Rear seat pan
- Rear longitudinal
- Spare wheel well

## 2.9 Noise, Vibration and Harshness Analysis

Simultaneous to the FSV design tasks, WorldAutoSteel commissioned LMS Engineering Services, Leuven, Belgium, to provide Noise, Vibration and Harshness (NVH) analysis to support the design process. Documentation of this work can be found in the report entitled, *Electric Motor Noise in a Lightweight Steel Vehicle*, SAE Paper No. 2011-01-1724.

A complete noise and vibration analysis has been performed by LMS for FSV at the concept stage. Measurements were conducted on two small Mitsubishi vehicles that both share the same body, yet one is equipped with an internal combustion engine and the other with an electric motor. The outcome was used as a starting point to identify assets and pitfalls of electric motor noise and draw a set of NVH targets for FSV.

Compared to a combustion engine, the electric motor shows significantly lower sound pressure levels, except for an isolated high frequency peak heard at high speeds (3500 Hz when the vehicle drives at top speed) which is lowered by increased use of acoustic absorbent materials in the motor compartment. For low and mid frequencies, moderate electric motor forces imply less stringent noise and vibration design constraints and a possibility to reduce the body mass.

Finite element simulations at low and mid frequencies led to reshaping the suspension mounts, the rear roof, the front header and the cowl top connection area, each change driving large reductions of noise levels while adding little to no mass. Damping sheets proved unnecessary. Lighter damping solutions, such as vibration damping steels, were examined and proved to be successful in the mid-frequency range.

Overall, the change from combustion engine to electric motor is compatible with mass reductions and similar or better noise and vibration performances. This part of the FSV Programme demonstrated the key benefit of including NVH analysis early in a vehicle programme concept design phase.

### 3.0 BEV Body Structure Design, Performance & Assembly

#### 3.1 FSV BEV Final Light Weight Body Structure

The Battery Electric Vehicle body structure achieved mass savings of 101 kg (-35%) compared to the baseline body structure mass as shown in Table 3-1. Other vehicle specifications are shown in Table 3-2. This mass reduction has been realised through the use of the wide range of available Advanced High-Strength Steel grades combined with an array of steel technologies and the FSV design optimisation methodology. The BEV body structure and its steel grade use are shown in Figure 3-1 and 3-2. Figure 3-3 shows the manufacturing processes employed in the structure. A complete parts list and Body Structure exploded view for each vehicle variant is included in Appendices 3 – 5.

**Table 3-1: FSV Programme Mass Achievement**

Body Structure	FSV1-BEV Mass (kg)
Benchmarked Mass	290
Target Mass	190
Achieved Mass	188

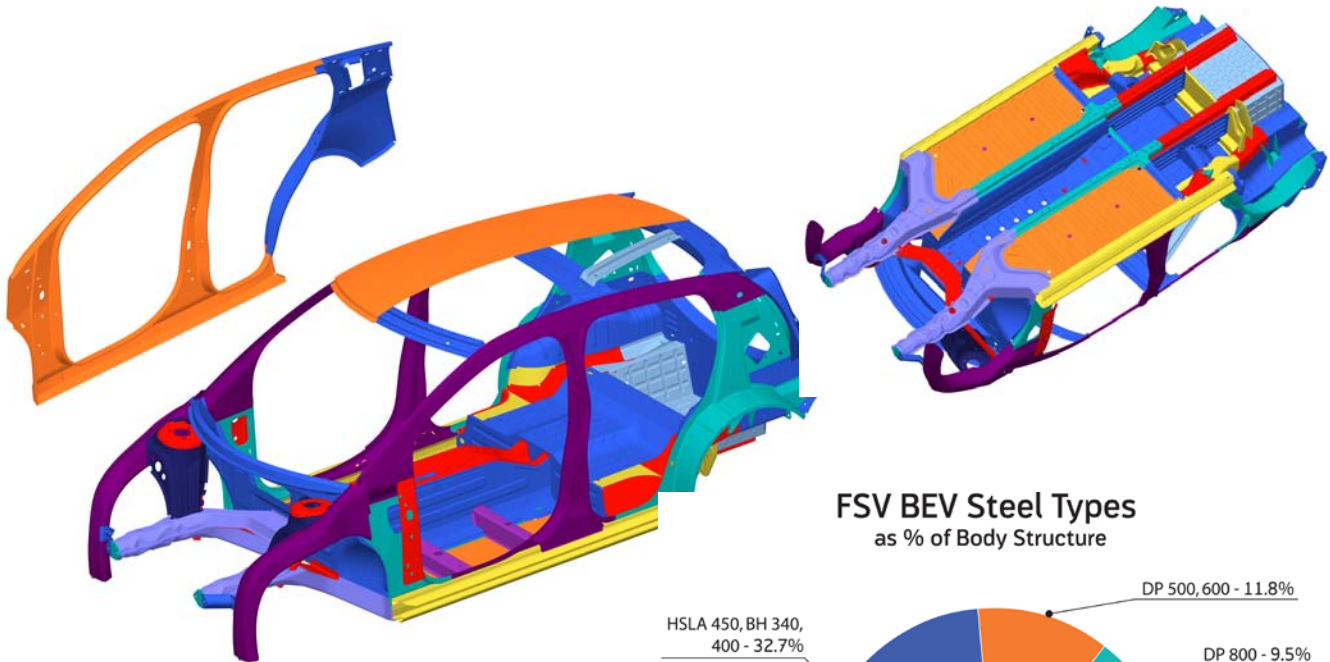


**Figure 3-1: FSV-1 BEV Colour-Coded by Steel Grades**

**FSV BEV Steel Types**  
as % of Body Structure

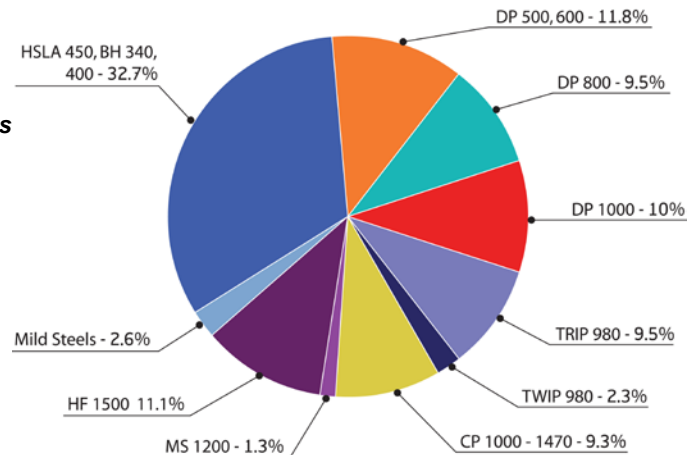


**Figure 3-2: FSV Steel Grades**

Table 3-2: FSV BEV Mass and Specifications

Vehicle	Body Structure Mass (kg)	Length (mm)	Width (mm)	Height (mm)	Wheel Base (mm)	Track Front/Rear (mm)	Powertrain Mass (kg)	Curb Mass (kg)	GVW (kg)
BEV	187.7	3820	1705	1495	2524	1470	328.7	958	1433

### FSV BEV Manufacturing Processes as % of Body Structure Mass

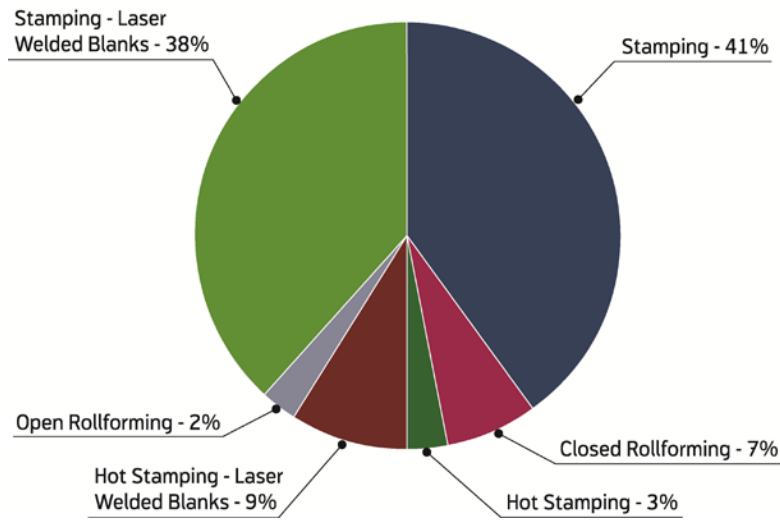


Figure 3-4: Manufacturing processes As % of Body Structure Mass

Figure 3-5 compares the steel gauges used in FSV to those used in the ULSAB-AVC C-Class vehicle.

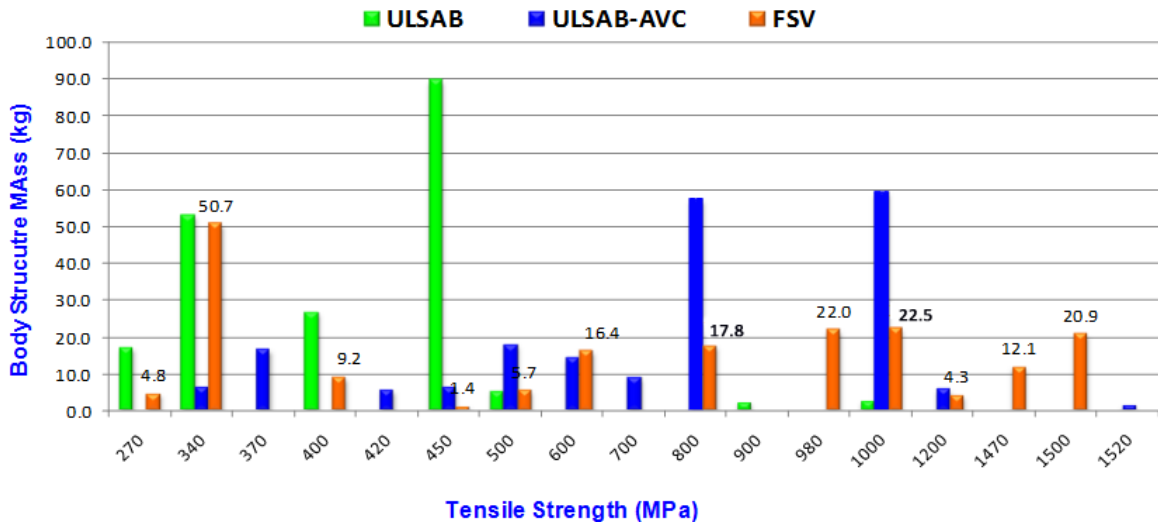
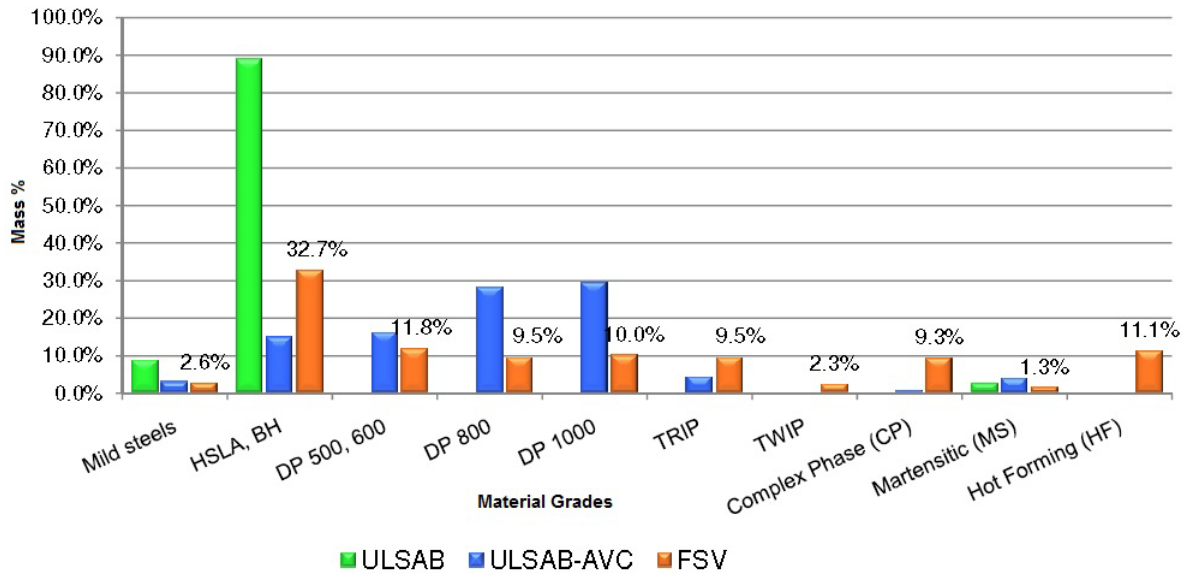


Figure 3-5: FSV Materials Tensile Strengths Compared To ULSAB and ULSAB-AVC

**Table 3-2: FSV Material Mix Tensile Strength Average Compared to ULSAB and ULSAB-AVC**

Vehicle	Tensile Strength (MPa)	Average Material Thickness (mm)
ULSAB	413	1.16
ULSAB-AVC	758	1.0
FSV-BEV	789	0.98



**Figure 3-6: FSV Material Grade Mix Compared to ULSAB and ULSAB-AVC**

Body structure or ‘Body-in-White’ definitions may vary somewhat from one vehicle design to another. Therefore, Table 3-3 shows the comparison of FSV with similar-sized VW Polo and with the ULSAB-AVC C-Class and PNGV Class structures on a ‘Body-in-Prime’ basis (a definition which includes all rigidly bolted-on parts that contribute to vehicle structural performance).

**Table 3-3: FSV Body-in-Prime (BIP) Comparison**

Model Year	ULSAB-AVC Vehicles			
	FSV-BEV (kg)	VW Polo (kg)	C-Class (kg)	PNGV (kg)
2020	2010	2004	2004	
<b>Body Structure with Paint</b>		242.5		
<b>Body Structure minus Paint</b>	187.7	231	201.8	218.1
<b>Engine Cradle</b>	13.9	10.5	44.2	44.2
<b>Bumper Beam Front</b>	5.9	7.5	4.58	4.58
<b>Bumper Beam Rear</b>	3.2	4.7	3.4	3.9
<b>Windshield</b>	15.0	11.1	9.7	9.7
<b>Battery Tray</b>	12.02			
<b>Radiator Support</b>	1.83			
<b>Total</b>	<b>239.5</b>	<b>264.9</b>	<b>263.7</b>	<b>280.5</b>

### 3.2 Nature's Way to Mobility

The design optimisation process used led to several non-intuitive components never before seen in automotive structures. The optimisation process placed structure where it was needed based on the loads each must be designed to support. Engineering judgement refined the initial structures to those that are manufacturable in the real world. The result is a very light weight design that provides excellent crash management yet reduces total life cycle emissions. Following in Sections 3.2.1 – 3.2.3 are highlights of a few of these unique structures. Section 3.3 Load Paths for Crash Management summarises how these structures are enlisted to influence crash management.

#### 3.2.1 Front Rail Sub-System

The Front Rail sub-system, Figure 3-7, is a new design for automotive front crash structures. Traditional design would carry the loads primarily through the rocker and roof rail structures, but the optimisation indicated the need for an additional direct path, such as through the vehicle tunnel, dispersing the load away from the passenger compartment through multiple load paths. As well, the unusual section shape of the rails was a result of the design optimisation methodology that improved the effectiveness of each steel element to achieve minimum mass and best crash management performance. A laser welded blank with varying gauges of TRIP 600/980 material is used to pinpoint where strength is most needed. The mass of the complete sub-system is less than 19 kg. To learn more about the Front Rail load paths for crash management, see Section 3.3.1.

Though the engineering team selected TRIP for the front rail material, based on FSV's particular design goals, these parts also are suitable for production using the very formable Advanced High-Strength Steel (AHSS) grade TWIP 500/980, as well as a Hot Stamped with tailor quenching, HF 1050/1500 grade.

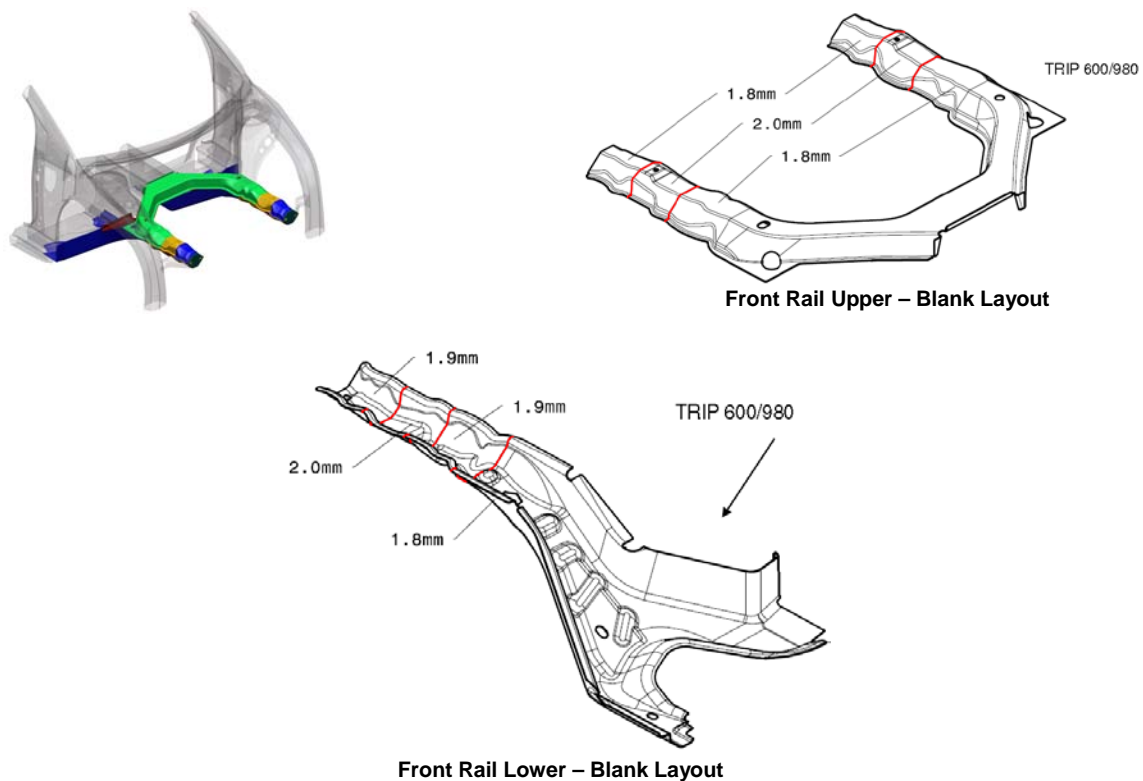


Figure 3-7: Front Rail Stamped LWB Solution

### 3.2.2 Shot Gun

The shot gun is traditionally so named in some parts of the world for its traditional shape that resembles a shot gun-type rifle. But the design optimisation indicated that this very light, trunk-like shaped component (Figure 3-8) was more logical to the load paths; and, consequently, it provides excellent performance in both full frontal and offset crash simulations (See Section 3.3.1 and 3.5). The shot gun is comprised of a three-piece HF 1050/1500 tailor welded blank of varying thicknesses, manufactured using Hot Stamping. As these parts are required to absorb energy without premature failure, during the Hot Stamping process the parts are tailor quenched to achieve the required amount of material elongation for the energy absorption function. The shot gun outer and inner components, left and right side, has a total mass of 8.5 kg.

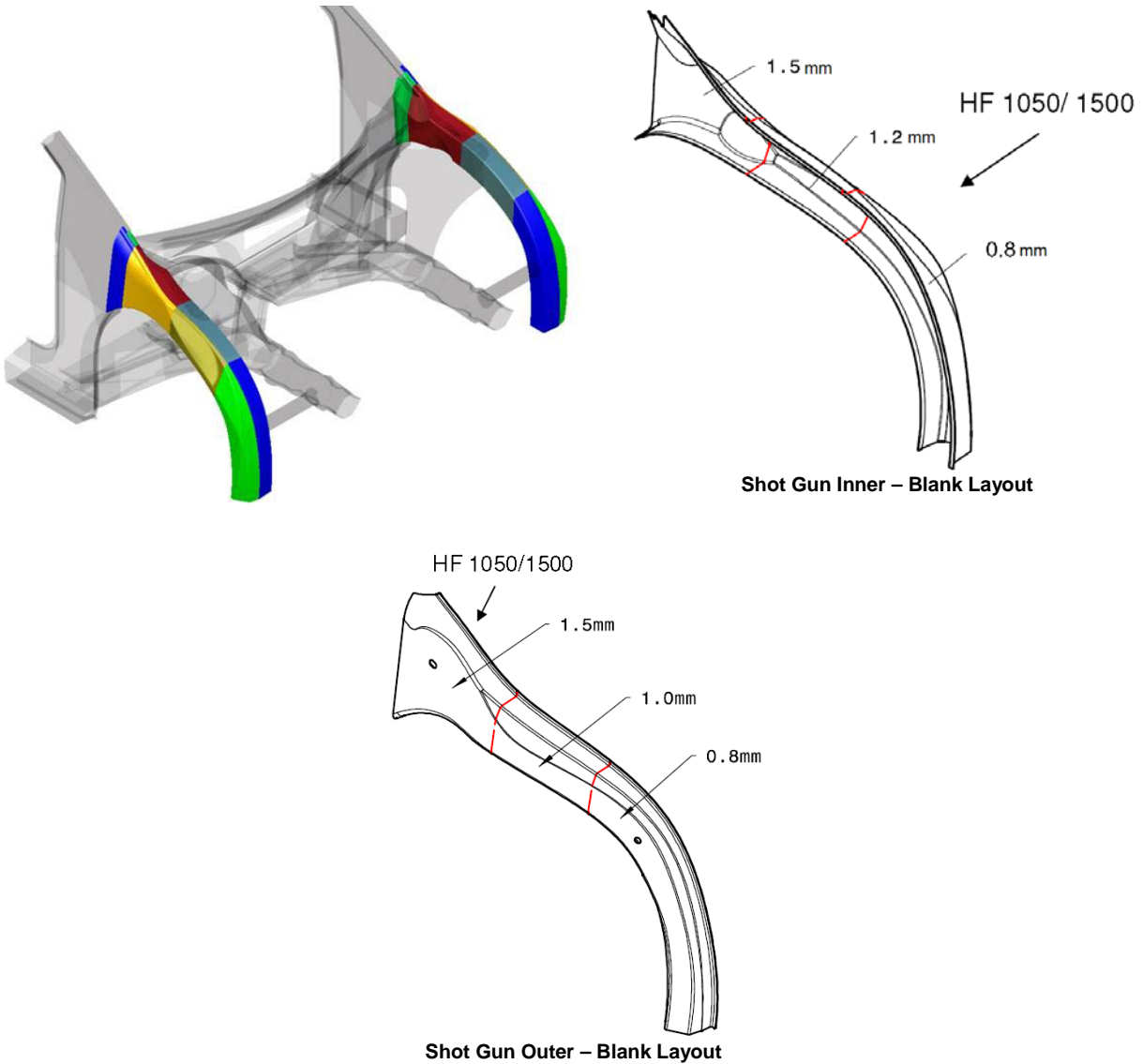


Figure 3-8 Shotgun Hot Stamped TWB

### 3.2.3 Rocker

Far from the normal box sections seen in this critical part for crash management, the FSV Rocker sub-system cross section is shown in Figure 3-9 below left. The Rockers are manufactured using roll-formed CP 1050/1470, 1.0 mm steel and has a 6.0 kg mass each. CP steels are characterised by high energy absorption and high residual deformation capacity, excellent features for crash structures. Resembling a skeletal bone, the Rocker cross-section, derived from the optimisation methodology, enabled good side crash results in four different side crash simulations: IIHS Side Impact, US SINCAP Side Impact, FMVSS 214 Pole Impact and Euro NCAP Pole Impact. See Section 3.3.2 to learn more about the Rocker's role in load paths for side crash, and Section 3.5 for a summary of crash results.

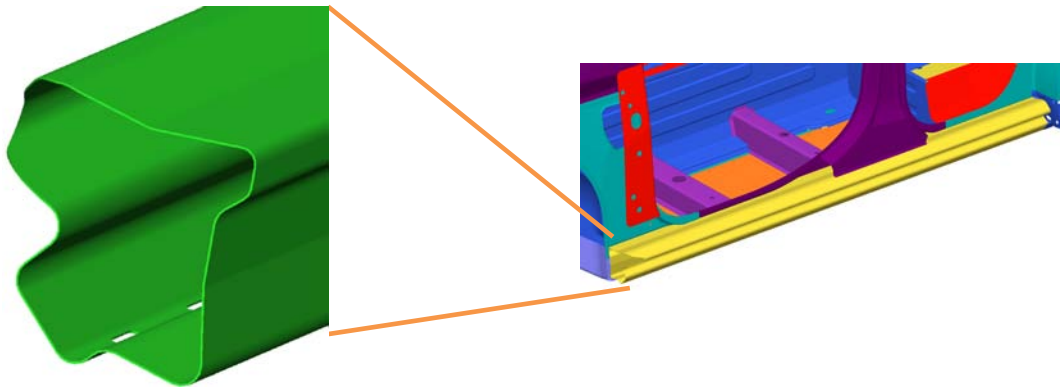


Figure 3-9: Rocker Roll-Formed Solution

## 3.3 Load Paths for Crash Management

### 3.3.1 Front End Structure for Frontal Impact

The BEV front end takes full advantage of the smaller package space required for the electric drive motor as compared to a typical ICE and transmission package. The additional packaging space allows for straighter, fully optimised front rails with larger sections as shown in Figure 3-7 in the previous section and Figure 3-10, following. The front rails (load path No. 1), shotguns (load path No. 2) and the motor cradle (load path No. 3) work together to manage frontal crash events with minimal intrusions into the passenger compartment.

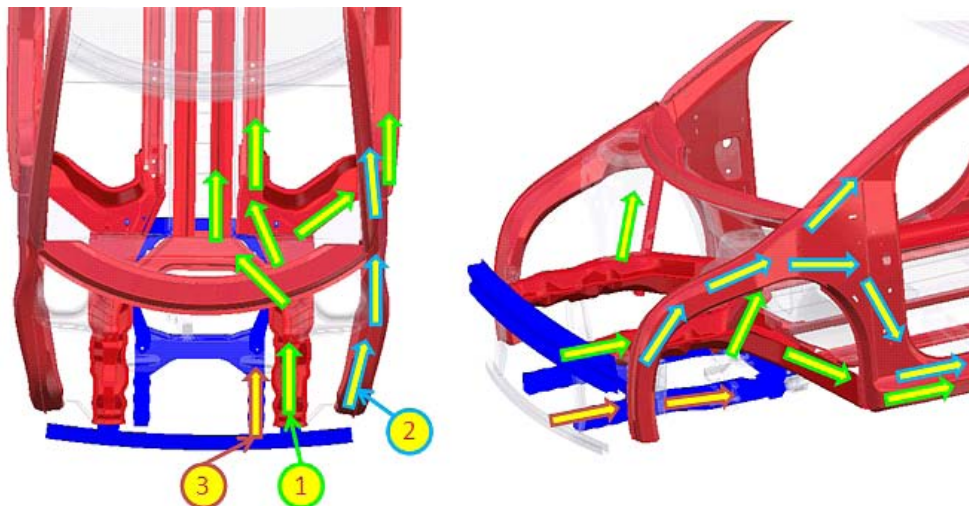


Figure 3-10: Load Paths – BEV front rails (1), shotguns (2) and motor cradle (3)

The front rail loads, illustrated in Figure 3-10's load path No. 1, are managed by the V-shaped construction through the rocker section, base and top of the tunnel. To stabilise the rear of the Front Rails, an additional load path is introduced behind the shock tower to direct the loads into the base of the A-Pillar. The BEV requires a deep tunnel to house the 30 kWh (end-of-life) battery pack. Consequently, the top and bottom of the tunnel structure, when combined with the bolt-on 207 kg, battery pack, acts as a structural "back bone" for the vehicle.

The front end's energy absorption is further enhanced with the addition of the distinctively curved upper shotgun members as shown in Figure 3-10's load path No. 2. These members absorb a significant amount of energy during USNCAP full frontal impact. The shotgun inner and outer panels also take advantage of Advanced High-Strength Steel (AHSS) grades (HF 1050/1500, LWB) similar to the front rails.

The motor mounting cradle, shown in blue in Figure 3-10's load path No. 3, also is designed to absorb energy during frontal crash load cases as well as support the motor assembly and front suspension.

With the combination of the three active load paths, the deceleration pulse of the structure can be tailored to achieve a more aggressive front end structure during the 0 to 30 millisecond crash timeframe and then a normal level during the 30 to 60 millisecond time frame when the occupant is interacting with the airbag. This approach has been shown to be beneficial for the occupants of smaller vehicles when involved in frontal crashes with larger vehicles. The deceleration pulse for the BEV (US NCAP 35MPH Rigid Barrier Impact), is shown in Figure 3-11.

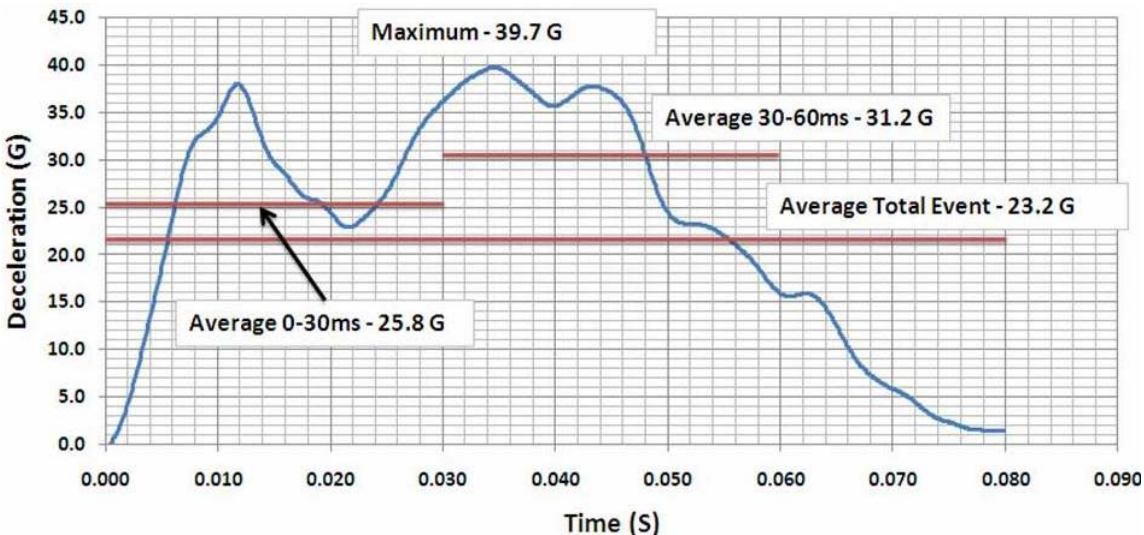
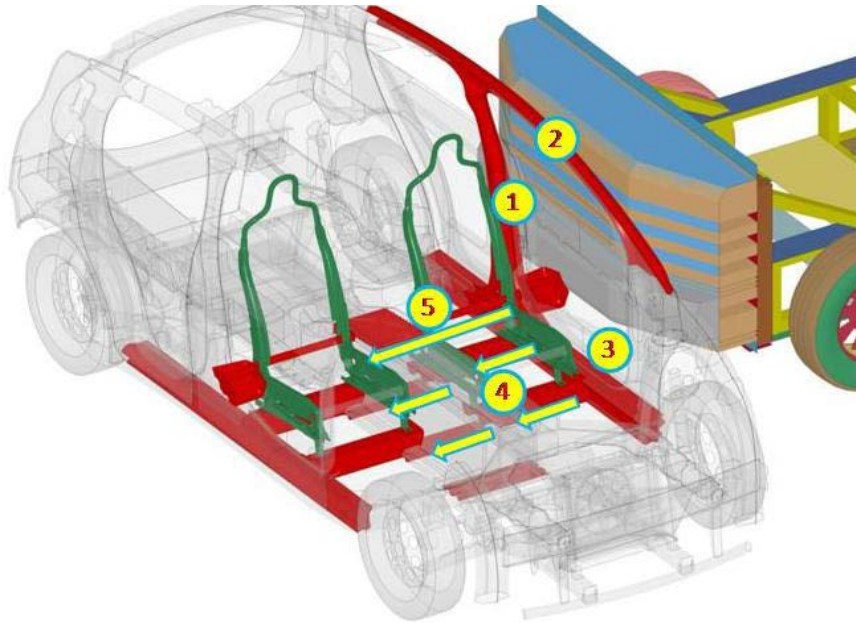


Figure 3-11: US NCAP 35 mph front rigid barrier pulse at B-Pillar

### 3.3.2 Side Structure for Side Impact

The FSV side structure's design and construction incorporate several load paths that take advantage of AHSS's very high-strength levels. The B-Pillar Inner and Outer, shown in Figure 3-12 as load path No.1, are constructed from Hot-Stamped HF1050/1500 steel. Load path No. 2, which is the Roof Rail Inner and Outer, also is Hot Stamped. Through the use of Hot Stamping, complex shapes can be manufactured with very high tensile strengths (1500 to 1600 MPa). This level of strength is highly effective in achieving low intrusions into the occupant compartment and strengthening the upper body structure for roll-over protection (roof crush). The rocker, (load path No. 3 Figure 3-11), with its unique cross section and CP1050/1470, 1.0 mm, rollformed steel, plays a major role in side impact protection, in particular for side pole impact.



**Figure 3-12: FSV Side Impact Structural Load Paths – B-Pillar Inner & Outer (1), Roof Rail Inner & Outer (2), Rocker (3), Seat Mounting Cross Members (4), Seat Back Cross Tubes (5)**

Additional side impact load paths through the body structure make use of the front seat mounting cross members, shown as load path No. 4. The two-seat mounted cross members are rollformed from Advanced High-Strength Steel's Martensitic grade (MS 950/1200, rollformed LWB). The fore-aft position of these members is aligned with bolt-on cross members that form the base of the battery structure, forming continuous load paths across the floor structure. Another unique load path for side impact is created through strengthened seat back cross tubes, shown as load path No. 5. This cross car load path is at a higher vertical height and is very effective in transferring the loads through the side structure (body and door), the driver seat and top of the tunnel. This load path can be seen in more detail in Figure 3-13.

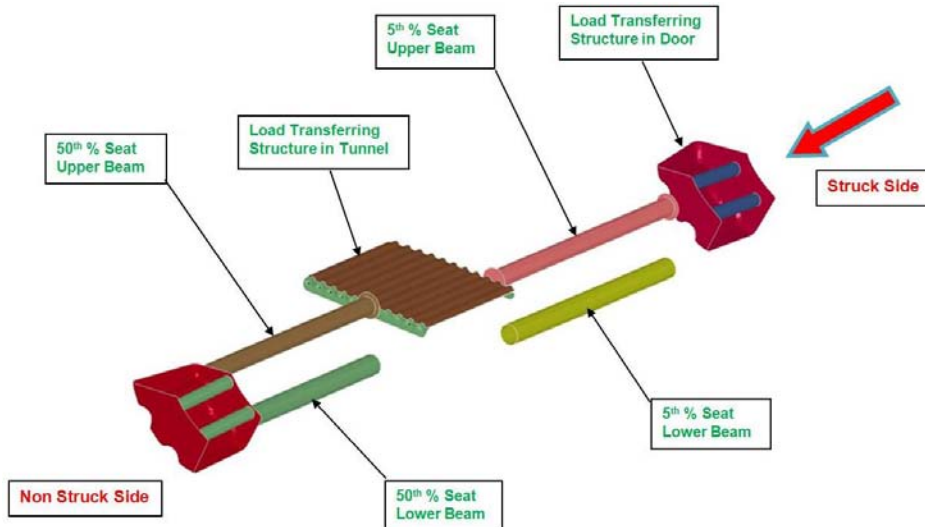


**Figure 3-13: Load Path for Transferring Load to the Non-Struck Side**

As an example of the results of one of the four side impact crash analyses (IIHS Side Impact, US SINCAP Side Impact, FMVSS 214 Pole Impact and Euro NCAP Pole Impact) conducted for the FSV BEV, the US SINCAP side B-pillar intrusion graph for the impact analysis for the FSV is shown in Figure 3-14. It shows that after the crash test the most intruding point of the B-pillar is 215 mm away from the driver seat centerline, resulting in the required "Good" rating.

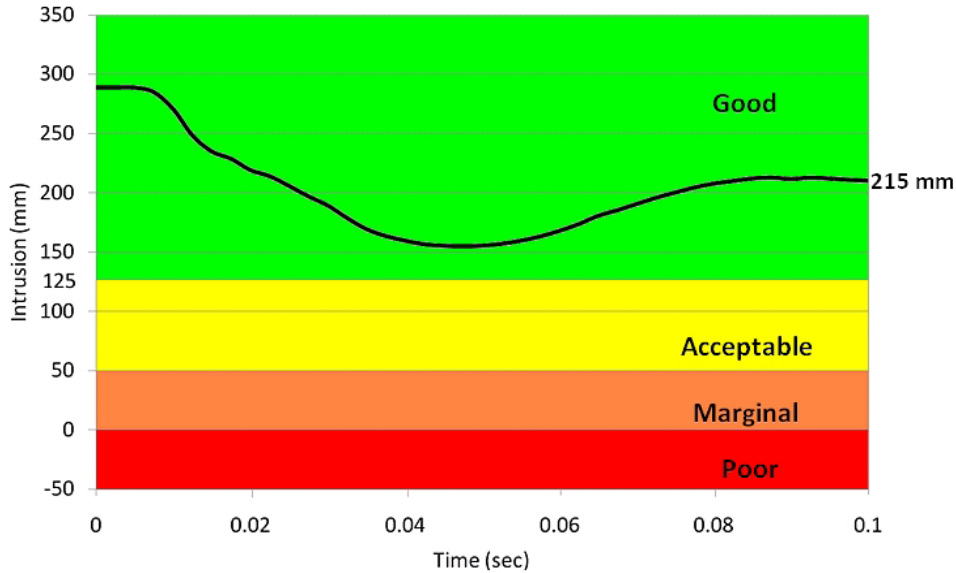


Figure 3-14: US SINCAP side impact - B-pillar intrusion graph

### 3.3.3 Rear Structure for Rear Impact

The design and construction of the FSV rear structure, incorporates two major load paths as shown in Figure 3-15. Load path No. 1 is the rear rail section that is constructed from three LWB stampings as shown in Figure 3-16. To protect the battery pack during rear impact, rollformed sections were included from the bottom of the tunnel towards the rear of the vehicle under the rear floor as shown by load path No. 2 in Figure 3-15. These two load paths, in combination with the rear cross-member, form a very rigid cage around the battery pack.

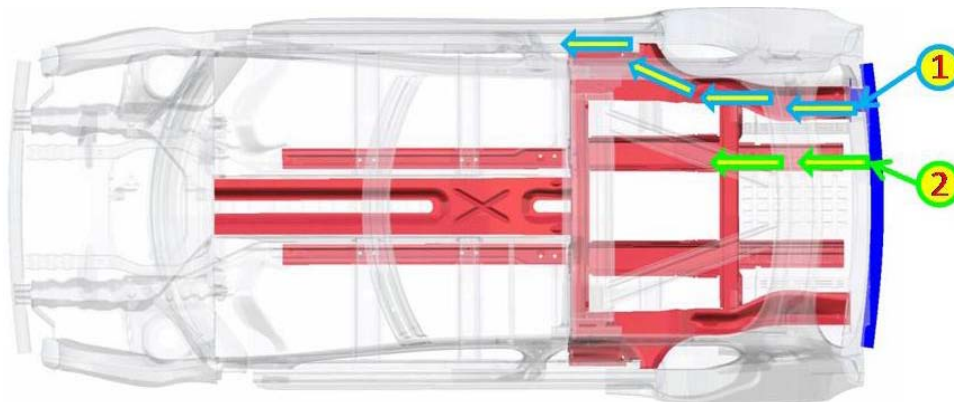
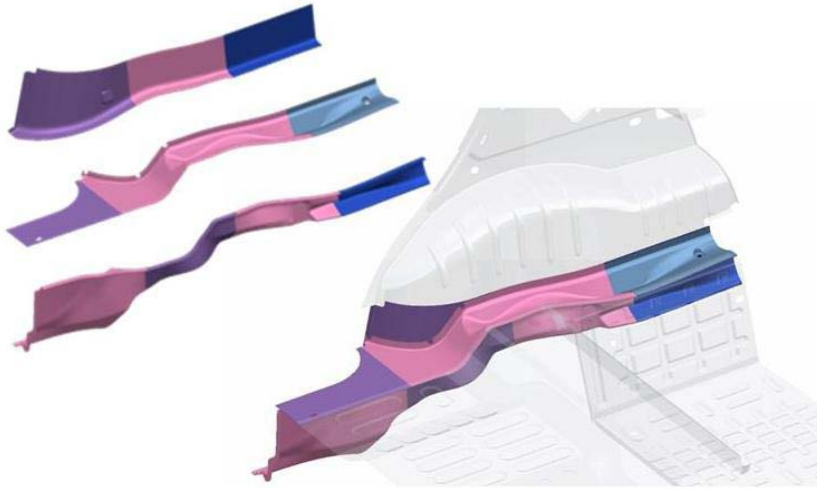


Figure 3-15: FSV Rear Impact Structural Load Paths



**Figure 3-16: FSV Rear Rail - Optimised Sections**

### 3.4 Body Structure Performance CAE Analysis

The detailed design of the FSV body structure was supported by CAE analysis, to verify the structural performance. The CAE analysis results were compared to the FSV targets to quantify the performance of the FSV body structure in terms of static stiffness, crashworthiness and durability.

Additionally, the ride and handling conditions of the FSV were evaluated with a dynamic analysis of the following tests:

- Fish-Hook test -Based on NHTSA statistics, the probability of rollover for the BEV is less than 10%, which corresponds to a 5-star rating.
- Double Lane Change Maneuver (ISO 3888-1) -The BEV remains within the boundary lines defined in the test, which is a "Pass."

As illustrated in Table 3-4 thru Table 3-6, the FSV body structure meets or surpasses all the performance targets with the additional considerations of the US NCAP Full Frontal Crash as described here. NCAP performance ratings are based on occupant injury criteria that are beyond the scope of this study. However, there is precedence for evaluating body structure performance based on cabin structure intrusion points and deceleration pulse targets, particularly at this developmental stage. Therefore, FSV crash performance was analysed for NCAP using these criteria.

The targets for the intrusion points were based on the IIHS Offset Deformable Barrier specifications since it is a similar passenger injury event to the US NCAP. A range of 35 to 38 g was set for the deceleration pulse target. This is a conservative value, with precedence in other production vehicles of exceeding 40 g and still achieving excellent frontal crash performance. Before 35 ms, higher decelerations are permitted since the passenger is not yet engaged with the passive safety systems and, as a result, does not experience B-Pillar decelerations that occur.

Table 3-7 gives the intrusion targets and results. Intrusion for the passenger compartment footwell areas' targeted points fell into the IIHS "Good" rating band, except for Toe-Center, which fell into the "Acceptable" rating band. The IIHS ODB rating system states: "When intrusion measurements fall in different rating bands, the final rating generally reflects the band with the most measures." Since the FSV results show only one intrusion measurement that fell in the "Acceptable" rating band, the overall FSV footwell intrusion rating

for the US NCAP frontal impact is "Good". This coupled with the conservative deceleration pulse target and the 39.7 g maximum deceleration pulse achieved, led the engineering team to conclude that performance is sufficient to support achievement of a five-star safety rating in conjunction with passive safety equipment.

**Table 3-4: FSV CAE analysis results – Static Stiffness**

Analysis	Target	FSV Model Results
Torsion stiffness (kN-m/deg)	20.0	19.604
Bending stiffness (N/mm)	12.0	15.552
Global Modes (Frequency Hz)		
Torsion	>40 Hz (both modes, separated by 3 Hz)	54.8
Vertical bending		60.6

**Table 3-5: FSV CAE analysis results – Crashworthiness**

Analysis	Target	FSV Model Results
US NCAP	peak pulse < 35 to 38g, footwell intrusion < 100 mm	Peak pulse 39.7 g, footwell intrusion 90.0 mm (average)
Euro NCAP	Peak pulse (driver side) <40 g, footwell intrusion < 150 mm	Peak pulse 39.2 g, footwell intrusion 113.0 mm (average)
IIHS Side Impact	B-Pillar intrusion with respect to driver seat centerline ≥ 125 mm	134mm
US SINCAP Side Impact	B-Pillar intrusion with respect to driver seat centerline ≥ 125 mm	215 mm
FMVSS 301 Rear Impact	Battery remains protected and should not contact other parts, after the crash	Battery is protected and there is no contact with other parts, after crash
ECE R32	Battery remains protected and should not contact other parts, after the crash	Battery is protected and there is no contact with other parts, after crash
FMVSS 214 Pole Impact	Door inner intrusion with respect to driver seat centerline ≥ 125 mm	159 mm
Euro NCAP Pole Impact	Door inner intrusion with respect to driver seat centerline ≥ 125 mm	169 mm
FMVSS 216a and IIHS Roof	Driver and passenger side roof structure should sustain load > 28.2 kN within the plate movement of 127 mm (FMVSS 216a), > 37.5 kN (IIHS)	Sustains load = 45 kN for driver side, = 43 kN for passenger side
RCAR/IIHS Low Speed Impact	Damage is limited to the bumper and crash box	No damage in components other than the bumper and crash box

**Table 3-6: FSV CAE analysis results – Durability**

Analysis	Target Life Cycles	FSV Model Predicted Life Cycles
3g pot hole	200,000	927,100
0.7g cornering	100,000	1,676,000
0.8g forward braking	100,000	274,700 (engine cradle life) 17,340,000 (body life)

**Table 3-7: Maximum US NCAP Dash Intrusion At Various Measuring Points**

FSV Cabin Structure Measuring Point	Intrusion Targets for "Good" Rating (mm)	Intrusion (mm)
Footrest	< 100	22.0
Toe-Left	< 100	90.2
Toe-Center	< 100	109.9
Toe-Right	< 100	51.8
IP-Left	< 100	11.7
IP-Right	< 100	11.3
A-Pillar	< 100	9.3

### 3.4.1 Crash Events

Images of select crash events can be seen in Figures 3-17 – 3-23 following:

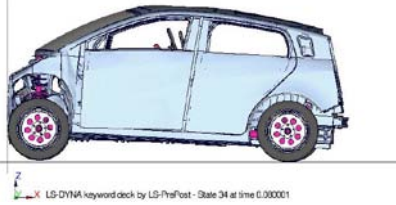


**Figure 3-17: US-NCAP Frontal Crash at 80 msec**

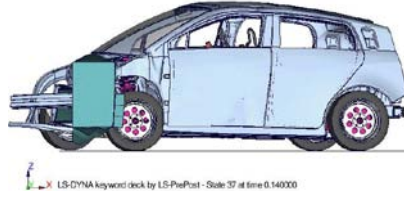


**Figure 3-18: EuroNCAP Frontal Crash at 140 msec**

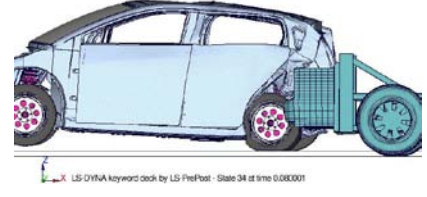


**Figure 3-19: FMVSS 301 Rear Impact**

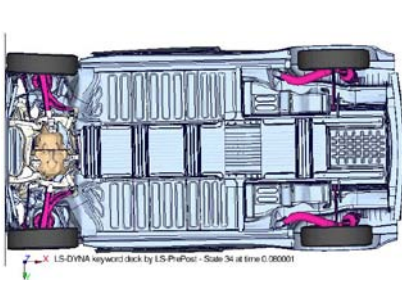


**Figure 3-20: IIHS Side Impact**

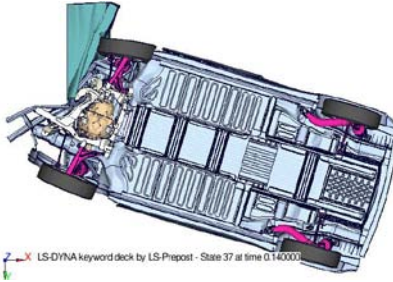


**Figure 3-21: US SINCAP Side Impact Post-Test Deformed Vehicle at 100 ms**

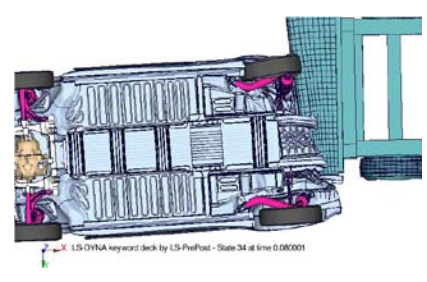


**Figure 3-22: FMVSS 214 Pole Impact at 100 ms Post-Pole Test Deformation**



**Figure 3-23: FMVSS 216-a Roof Crush Deformed passenger side-roof structure at rigid plate movement 127 mm**

### 3.5 Manufacturing Process Simulation Results

#### 3.5.1 One Step Metal Stamping Simulation

One Step simulation was conducted for all the body structure parts using Hyperform Radioss One Step (Altair Hyperworks 10.0). Most of the parts of the body structure can be made through cold forming. Parts that play an important role in crashworthiness, such as B-pillars, Shotguns and Roof Rails, are made through a hot forming process.

Although One Step simulation was completed on all the body structure parts, it cannot replace the incremental analysis process. Some parts which have complicated shapes like body side outer, front rails, rear rails and B-pillars require the incremental analysis method for predicting the manufacturing results more accurately. The Forming Limit Diagram (FLD) helps determine whether a given component will fail.

For example, the One Step stamping simulation completed on the floor panel, shown in Figure 3-24, was analysed with an FLD diagram. The floor is a two-piece laser welded blank with respective thicknesses of 0.5 and 1.5 mm. Material for these blanks is Dual Phase (DP), 300/500 and DP 500/800 steels. FLD diagrams, shown in Figure 3-24, predict no failure for the floor panel. There are very minor areas where wrinkling can occur and these can be easily improved by implementing additional design changes to the CAD data. One Step stamping simulations give the approximate results very quickly whenever there is any change in the CAD data.

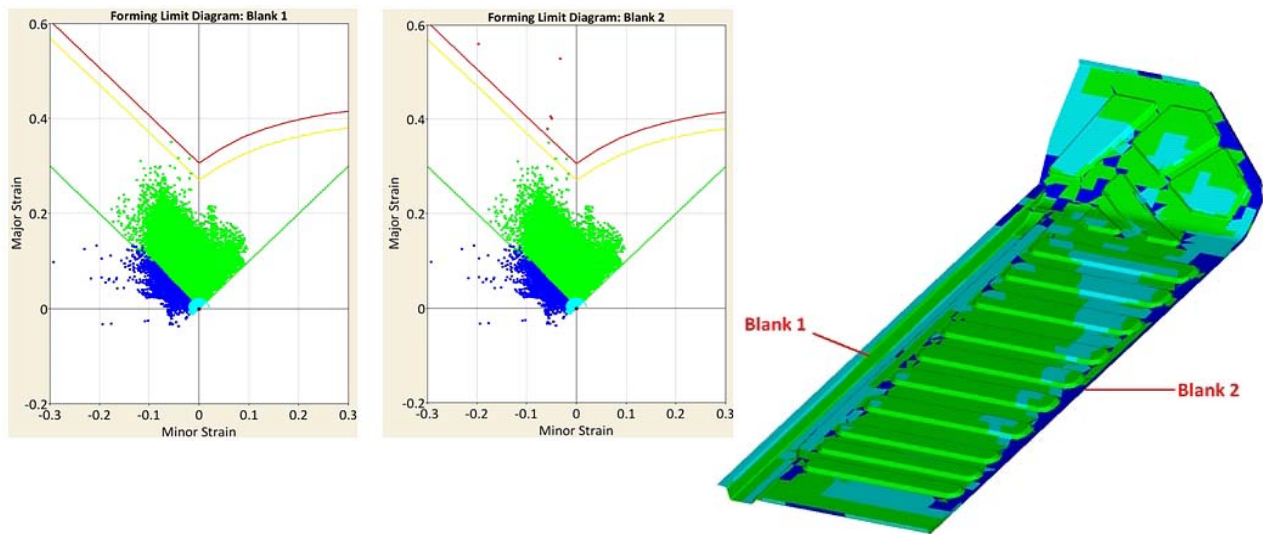
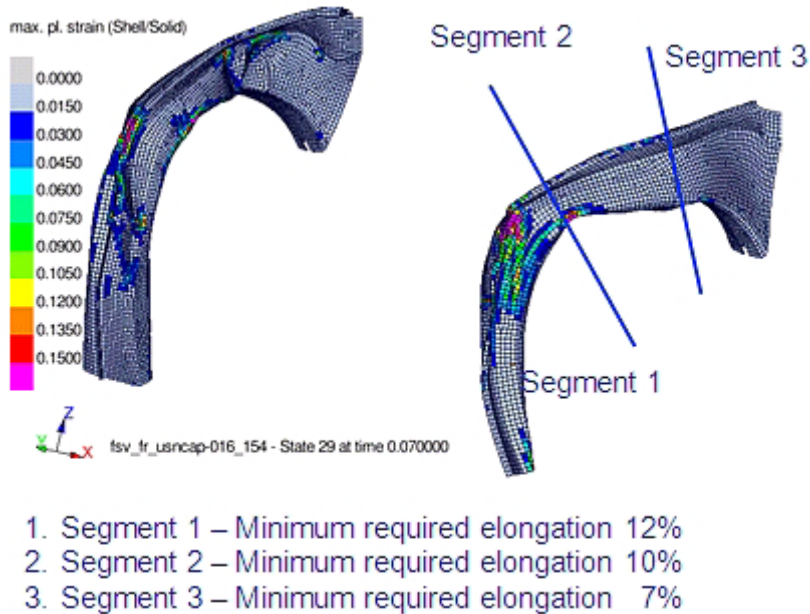


Figure 3-24: Floor Panel Single Step Forming Simulation

#### 3.5.2 One Step Hot Stamping Simulation

As discussed in Section 3.2 and 3.3, the front shot gun members form a very important part of the front end structure, absorbing significant amounts of energy during frontal crash. The shot gun inner and outer panels are hot-stamped from HF 1050/1500 steel. The formability of these parts was assessed using single step formability simulations. The predicted elongations for the front crash test case are shown in Figure 3-25.



**Figure 3-25: Front Shotgun Members - Minimum Required Elongation**

The results for the One Step Forming analysis for all other components are shown in the Bill of Materials (BOM) file, a supplementary file to the FSV Phase 2 Engineering Report.

### 3.5.3 Incremental Forming Simulations

More complex stamping parts were analysed using Incremental Forming Simulations. The following parts were considered:

- |                                                                    |                           |
|--------------------------------------------------------------------|---------------------------|
| 1. Front Shock Tower Panel (TWIP)                                  | 5. Rear Rail Outer (LWB)  |
| 2. Rear Header Reinforcement Panel                                 | 6. Rear Rail Inner (LWB)  |
| 3. Rear Floor                                                      | 7. Front Rail Lower (LWB) |
| 4. Rear Rail Reinforcement (LWB, Stamping & Indirect Hot Stamping) | 8. Front Rail Upper (LWB) |
|                                                                    | 9. Body Side (LWB)        |

All Incremental Forming Simulation results can be reviewed in detail in the FSV Phase 2 Engineering Report. Following are a few examples.

#### 3.5.3.1 Front Rail Lower

The front rail structure, shown in Figure 3-26 (left), is a unique design which was determined through the optimisation methodology. It has a V-shaped rear structure that provides paths for crash energy loads to move into the tunnel and below the vehicle and out to the rocker. It is made of Laser-Welded Blank (LWB) with TRIP material of varying thicknesses. Forming simulations were conducted on this lower portion of the Front Rail with the result of the first forming simulation iteration, Figure 3-26 (right), indicating a number of problem areas of wrinkling and material failures. Figure 3-27 indicates design changes that were made based on the first iteration results.

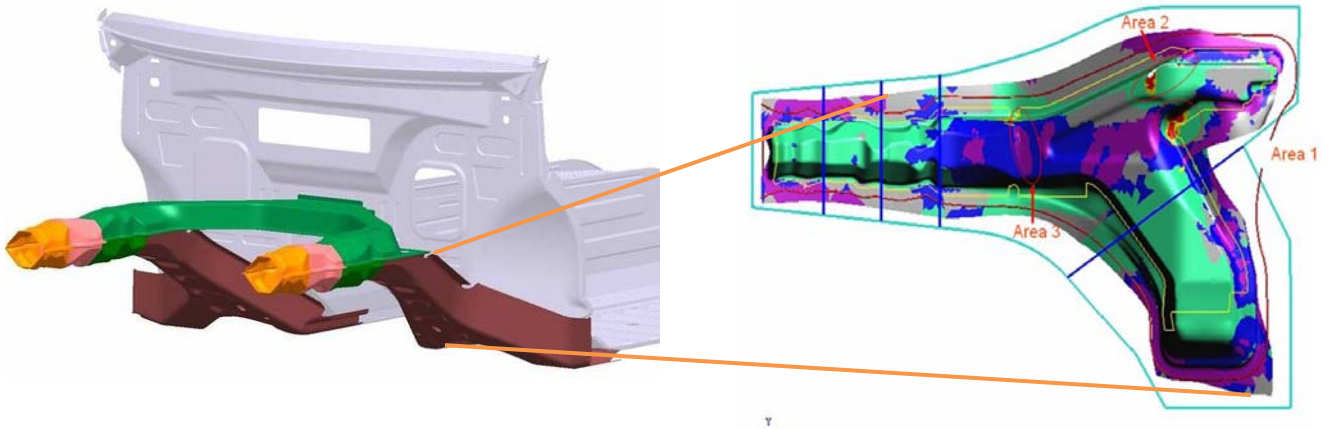


Figure 3-26: Front Rail Lower First Iteration Forming Results

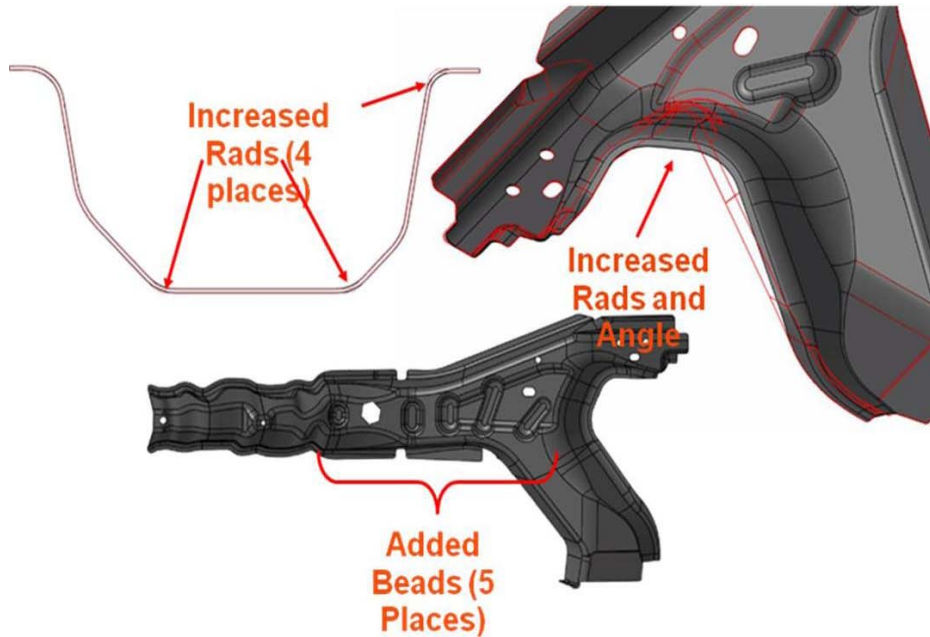


Figure 3-27: Front Rail Lower Design Changes

After several design and analysis iterations, the geometry with forming simulation results shown in Figure 3-28 indicate this part can be made using the specified TRIP 600/980 grade of steel. It can be seen that very small areas on the part show some points in the failure area. These areas can be modified and resolved with further design and analysis iterations.

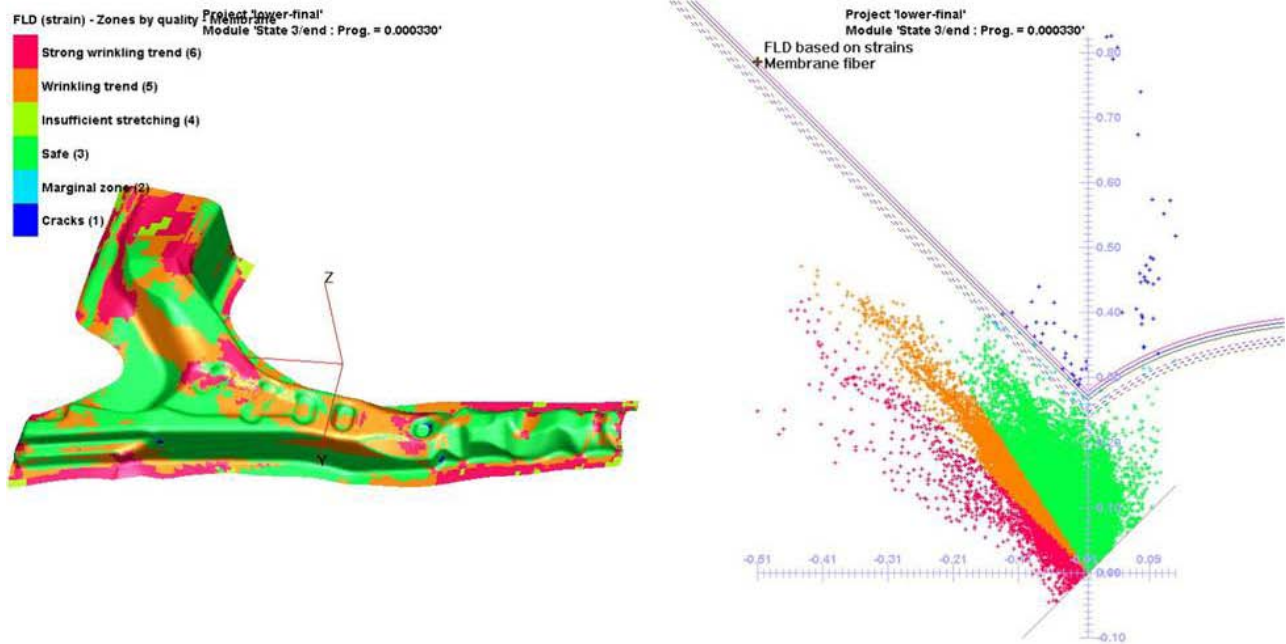


Figure 3-28: Front Rail Lower Forming Results

### 3.5.3.2 Front Rail Upper

The forming results for the first design iteration of the front rail upper (Figure 3-29) indicated several changes to this design were needed for manufacturability (also shown in Figure 3-29). The forming results are shown in Figure 3-30.

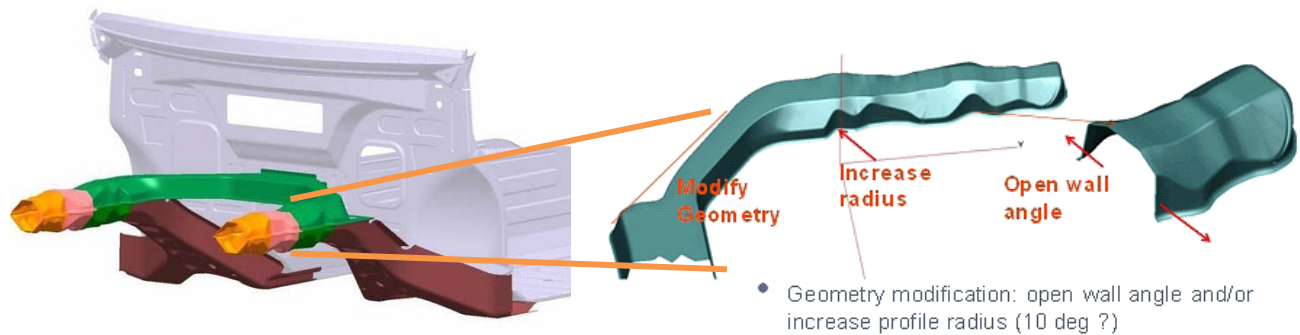
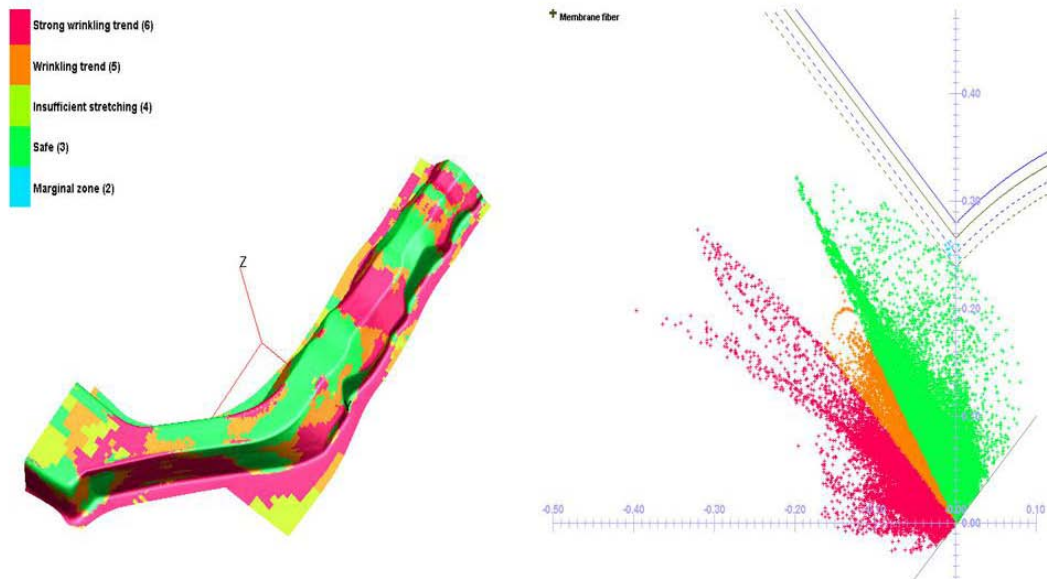


Figure 3-29: Front Rail Upper (Left) and First Iteration Recommendations (Right)



**Figure 3-30: Front Rail Upper Forming Results**

It is expected that, as noted above, areas needing modification or refinement can be resolved with further analysis iterations and with little impact on mass or performance. WorldAutoSteel member companies may provide additional application engineering assistance for adapting these concept designs to series production vehicles.

### 3.5.3.3 Body Side Outer

The body side outer is a large challenging part with multiple conflicting requirements. It includes large depths of draw, complex geometry around door openings, large Class A styling surface and contribution to strength for B-Pillar, upper rail and front body hinge pillar. This part was investigated with a two-piece Laser Welded Blank (LWB) and a four-piece LWB as shown in Figure 3-31. The results for the two-piece LWB option, shown in Figure 3-32, indicate that this part, with some additional design changes, is suitable for manufacturing. The results for the four-piece LWB option shown in Figure 3-33 indicate similar results.



**Figure 3-31: Body Side Outer Two-Piece Option (left) and Four-Piece Option (right)**

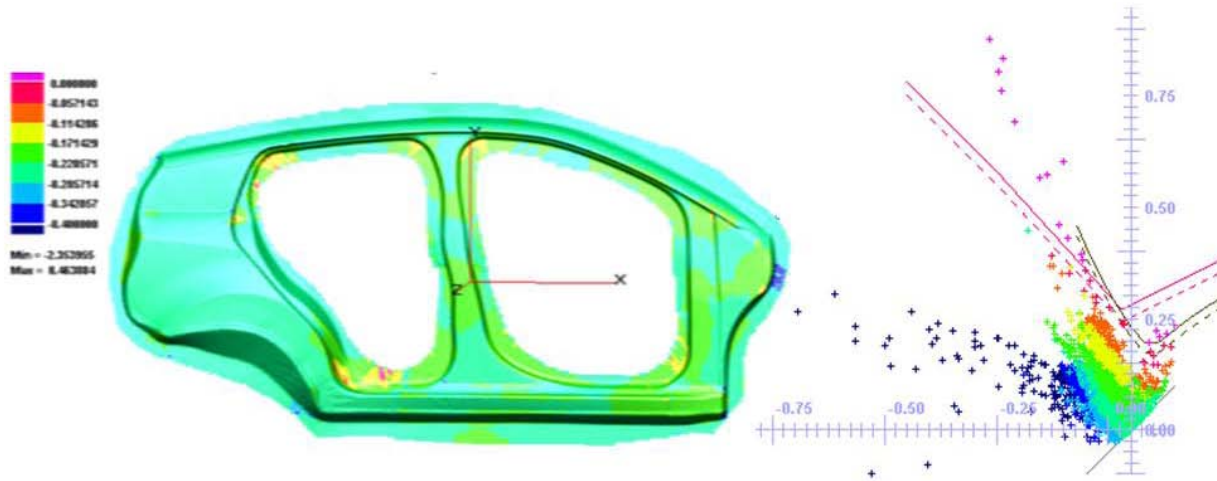


Figure 3-32: Forming Results – Body Side Outer, Two-Piece Option

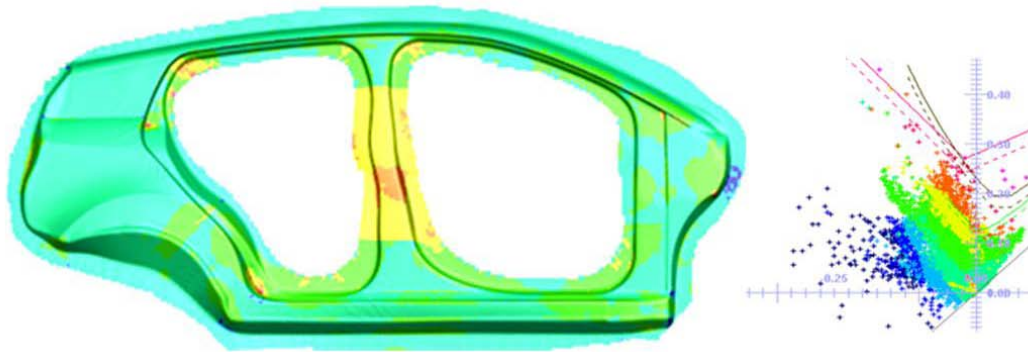


Figure 3-33: Forming Results – Body Side Outer, Four-Piece Option

Since similar results were achieved for both options, each was further evaluated for static stiffness and crashworthiness performance. The structural performance was found to be acceptable for both options, but with the addition of Front Body Hinge Pillar reinforcements (LH & RH) needed for the two-piece option. The two options were then evaluated for cost and mass, with the results shown in Table 3-8.

Table 3-8: Body Side Outer Options – Mass and Cost Comparison

Options	Mass (kg)	Cost per Side (US\$)
Body Side Outer, Two-Piece LWB	11.6	\$39
Body Side Outer, Four-Piece LWB	13.9	\$61

This evaluation led to the implementation of the two-piece option in the final BEV body structure design.

### 3.6 Body Structure Joining and Assembly

#### 3.6.1 Joining Technologies

Some of the most common assembly joining techniques were considered for the FutureSteelVehicle programme. The joining processes selected for the FutureSteelVehicle body structure assembly are the following:

- Resistance Spot Welding
- Laser Welding
- Laser Brazing
- Roller Hemming
- Adhesive Bonding

Table 3-9 summarises joining techniques and Figures 3-34 – 3-36 show their location in the vehicle.

**Table 3-9: FSV Joining Technologies Summary**

Number of spot welds	1023
Length of laser welds	83.6 m
Length of laser braze	3.4 m
Length of hem flange	2 m
Length of hem adhesive	2 m
Length of structural adhesive	9.8 m
Length of anti-flutter adhesive	6.5 m

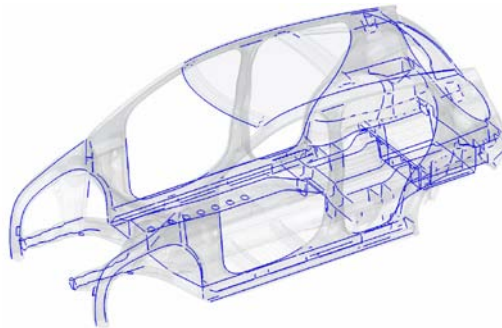


**Figure 3-34: FSV Continuous Laser Welding**

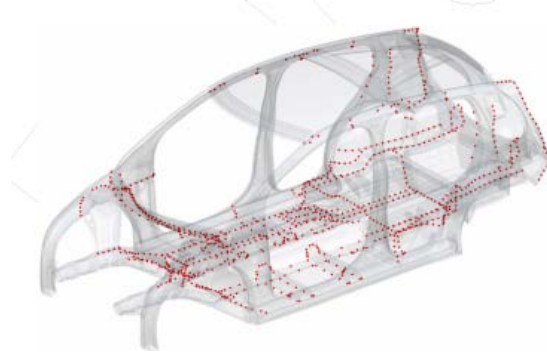


**Figure 3-35: FSV Spot Weld Spacing**

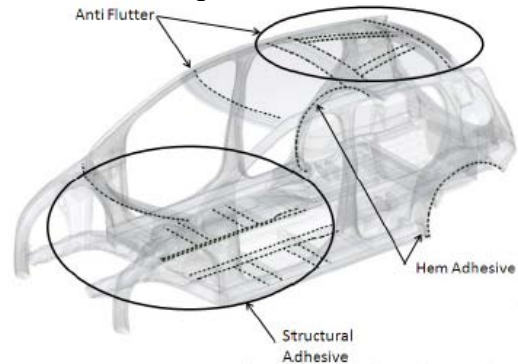


**Figure 3-36: FSV Adhesive**

### 3.6.2 Weldability of Advanced High-Strength Steels

As the yield strengths of steel continue to increase to 1000 MPa and above, there is a growing interest in using laser welding for Advanced High-Strength Steel. Generally the higher the strength of steel, the greater the sensitivity to heat input during the welding process. Due to the lower heat input of laser welding as compared to resistance spot welding, laser welding should be considered as an option to resistance spot welding. This Overview Report covers a few points concerning laser welding. More can be found in the FSV Phase 2 Engineering Report. For more comprehensive information on welding with AHSS, see the *Advanced High-Strength Steel Application Guidelines*.

#### 3.6.2.1 Laser Welding of Zinc Coated Steel

A major consideration when laser welding is the material used for the steel coating. Typically the steel is zinc coated, either hot-dip galvanised (GI), electro galvanised (EZ) or galvanized (GA) on both sides to add an effective anti-corrosion coating. The zinc coating poses no issues when laser welding a butt joint but when welding a lap joint, special techniques have to be applied due to “degassing” of the zinc coating during the welding process. Zinc vaporises at a temperature around 900°C, which is far lower than the temperature required for the laser welding process. The two layers of zinc coating between the two sheets of a lap joint generate high vapor pressure when welding. This can lead to blowouts of molten material during the welding process which would result in a weak weld joint. To prevent this, a small gap of 0.1/0.2 mm between the two sheets is required to allow the vapor pressure to dissipate. This gives excellent joint continuity without cracks, pores or non-metallic inclusions.

One of the latest ways that this can be achieved is by the process of laser dimpling along the weld flange, (see Figure 3-37). This additional process can be conducted using the same laser that is used for the welding operation and is a cost efficient method with high repetition rates.

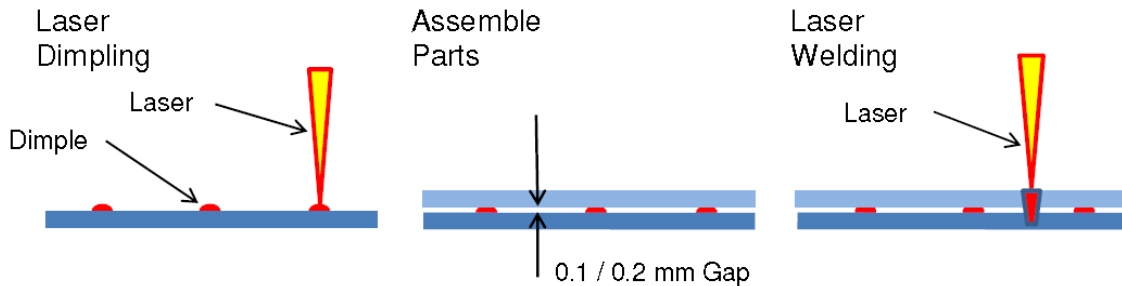


Figure 3-37: Laser Dimpling Process

#### 3.6.2.2 Laser Welding Three Material Thicknesses

Laser welding three material thickness (3T) together is presently not possible, albeit there have been a number of OEM studies that are encouraging but have not been adopted as a viable assembly process. In a 3T condition, as in the door opening, welding of the body side outer, upper roof rail, B-pillar reinforcement and body side inner assembly, a different approach needs to be taken. In this situation a two-step process is used. Laser welding has to be completed from both sides of the assembly, effectively creating two sets of two-metal thickness welds. This is achieved by using a laser weld stitch pattern of 20-40-20, where 20 is a 20 mm run of weld with a 40 mm gap and another 20 mm weld run. Welding is completed on one side of the assembly, while the same pattern is created on the opposite side of the assembly. The welding can be made simultaneously with one weld pattern staggered so that a 20 mm weld can be placed in the middle of the 40 mm gap left by the first weld pattern.

### 3.6.3 Body Assembly Flow Chart

For the purpose of this programme, the FSV body structure is considered without the closures/hang on parts (the hood, front/rear doors, liftgate and front fenders).

The FSV programme body structure assembly has been sub-divided into a number of major assemblies, as illustrated in Figure 3-38, which are as follows:

- Front structure
- Front floor
- Rear floor
- Underbody
- Body side outer LH/RH
- Upper structure and shotgun

The completed body structure assembly would then transfer to a line where the closures, front and rear doors, hood, liftgate and the front fenders would be added. This makes the complete body-in-white (BIW) which would then transfer to the vehicle paint shop.

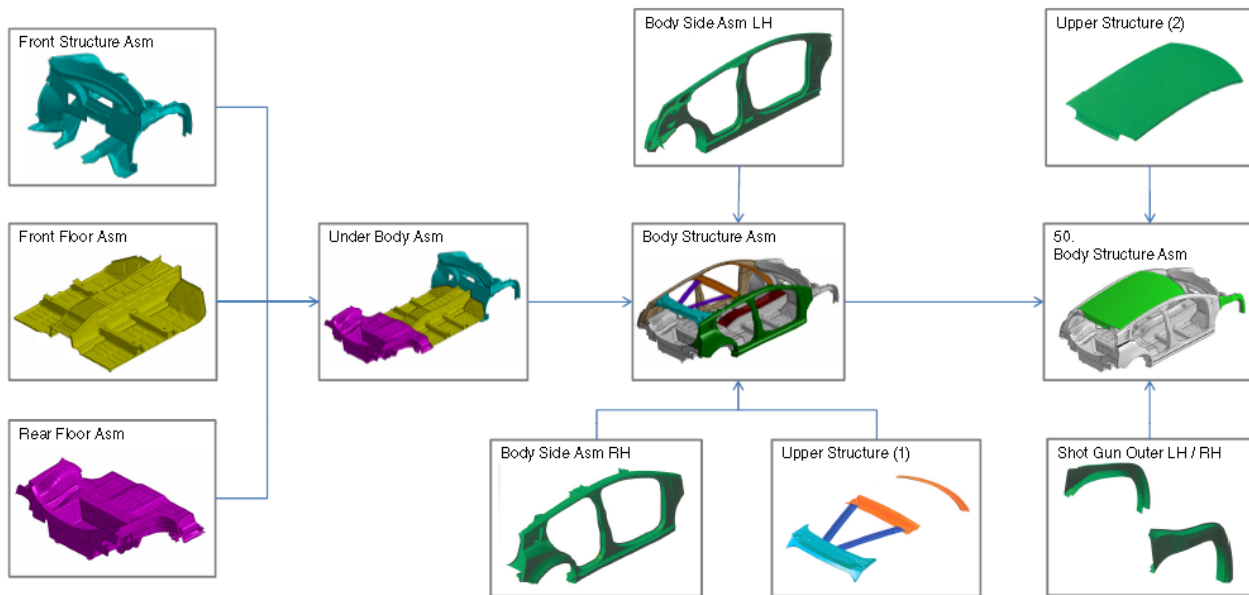


Figure 3-38: FSV Body Structure Assembly Flowchart

## 4.0 Body Structure Cost Assessment

A technical cost modeling approach was used to assess the manufacturing costs of the FSV body structure components. No supplier cost estimates were used. The technical cost modeling approach used in the cost model is similar to the one used by Massachusetts Institute of Technology (MIT) for the ULSAB-AVC programme. The manufacturing costs were estimated for all the body structure components, using the different manufacturing processes.

The cost breakdown for the steel components/systems fabrication is shown in Table 4-1, assuming an annual volume of 100,000 and a five-year production life.

**Table 4-1: Body structure manufacturing costs breakdown**

Manufacturing Technology	Parts Weight (kg)	Unit Cost Per Vehicle (\$USD)
Stamping	76.1	\$306.1
Stamping – Laser welded blanks	72.0	\$270.4
Hot Stamping	4.8	\$48.70
Hot Stamping – Laser welded blanks	16.8	\$118.5
Open Rollforming	4.5	\$7.70
Closed Rollforming	13.5	\$23.6
<b>Total Body Structure (Manufacturing)</b>	<b>187.7</b>	<b>\$775.0</b>

Each sub-assembly in the overall body structure assembly was reviewed to determine the following parameters:

- Sub-Assembly/Assembly Structure
- Joining Process
- Assembly Process Parameters
- Length of weld (Laser Welding, Laser Brazing)
- Number of welds (Resistance Spot Welding)
- Length of bond (Adhesive bonding)
- Length of hem flange (Hemming)

Based on the assembly sequence and joining specifications determined from the overall assessment, the assembly costs were estimated for each of the sub-assembly and assembly concepts, using the following:

- Laser Welding
- Laser Braze
- Adhesive Bonding
- Resistance Spot Welding
- Hemming

Table 4-2 shows the costs for the FSV body structure sub-assemblies and the total assembly.

**Table 4-2: Body structure assembly costs**

Assembly	Cost (\$USD)
Body Side Inner Sub Assembly RH	\$17.59
Body Side Inner Sub Assembly LH	\$17.59
Body Side Outer Sub Assembly RH	\$5.29
Body Side Outer Sub Assembly LH	\$5.29
Body Side Assembly RH	\$24.95
Body Side Assembly LH	\$24.95
Front Structure Assembly	\$46.53
Front Floor Sub Assembly	\$39.91
Rear Floor Assembly	\$89.63
Underbody Assembly	\$22.20
Body Structure Assembly	\$45.79
<b>Total Body Structure Assembly Cost</b>	<b>\$339.73</b>

#### 4.1 Increased Volumes and Comparison to ULSAB-AVC

Table 4-3 shows parts costs for FSV BEV's 100,000 vehicles per year production volume with 225,000 per year, as was the assumption for ULSAB-AVC. Costs shown are for the ULSAB-AVC C-Class.

**Table 4-3: FSV body structure parts costs vs. ULSAB-AVC parts costs**

Parameter	FSV		ULSAB-AVC
Body Structure Weight (kg)	188 kg		202 kg
Production Volume Scenario	100,000 /yr	225,000/yr	225,000/yr
Total Body Structure Part Costs	US\$775	US\$684	US\$620
Base Material Price	\$0.73		\$0.73
Material	50%	57%	66%
Labor	7%	7%	7%
Equipment	14%	15%	10.5%
Tooling	17%	9%	8%
Energy	3%	3%	2%
Overhead	5%	5%	4%
Building	1%	1%	0.5%
Maintenance	3%	3%	2%
Number Stamped Parts	75		64
Number of Hot Stamped Parts	16		0
Number of Tubular Parts	10 (Rollformed)		4 (Hydroformed)
Number of LWB Parts	18		11
Total Number of Parts	119		79

#### 4.2 Sensitivity Analysis

The cost model had certain assumptions made specific to the program. Sensitivity analyses were performed to demonstrate the effect on the overall vehicle cost as a result of changing certain key parameters including: production volume, product life, and steel prices.

For the FSV BEV, the yearly production volume was assumed to be 100,000 for a production life of five years, which is considerably less than a conventional vehicle production volume of 225,000 for an average product life of eight years. Hence, it was important to show the sensitivity of the overall vehicle costs when the production volume and product life were varied in this range to show how the large tooling investments associated with vehicle manufacturing could be spread out when volume or life span increases. Similarly, since material costs make up a high percentage of the overall vehicle costs, a variation in the steel prices also show a high impact on the costs. Figure 4-1 shows the results of the sensitivity analyses and the range within which the key parameters were varied.

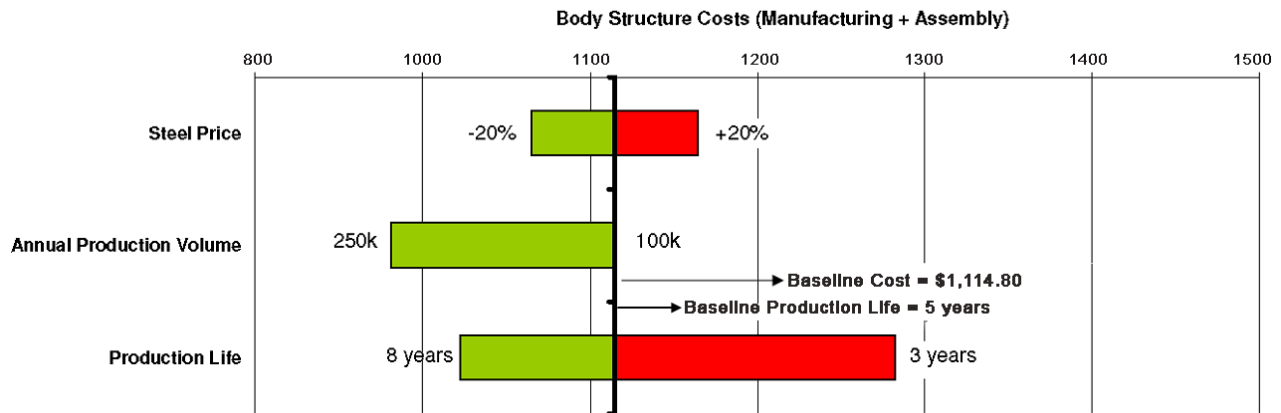


Figure 4-1: FSV body structure costs sensitivity analysis results

## 5.0 Environmental Assessments

With a fast growing automotive sector and global concern over climate change from anthropogenic GHG's (attributable to human activities), the key priorities are improving fuel economy, reducing emissions and shifting to a sustainable automotive industry. In many regions around the world, strict tailpipe carbon dioxide (CO<sub>2</sub>) emissions legislation has been passed with a view towards further reductions by 2020 and beyond as indicated in Figure 5-1 following.

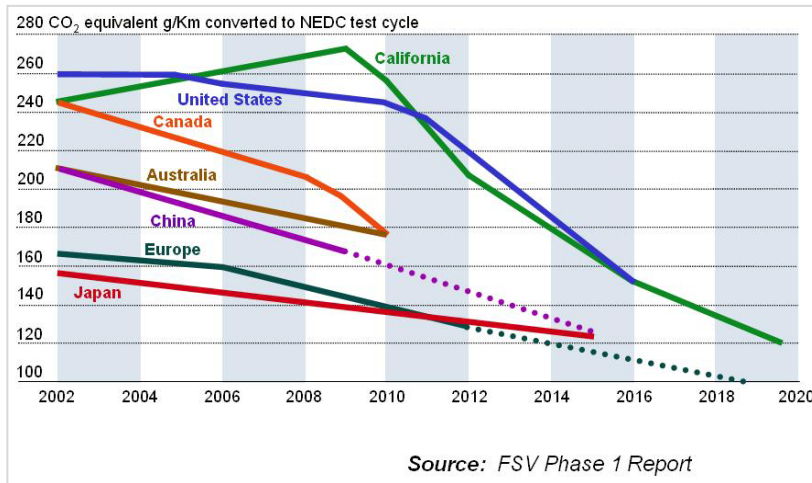
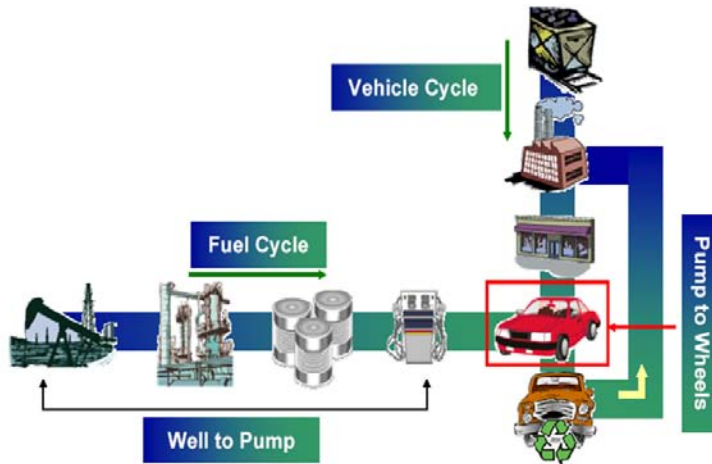


Figure 5-1: Trends in Global Fuel Economy/Vehicle Emissions Regulations

One of the challenges concerning automotive emissions regulations is to achieve the intended control without creating unintended consequences or unexpected results. Climate change and energy concerns prompt increased fuel efficiency standards or tailpipe emission regulations. And improving fuel economy and reducing tailpipe emissions during the “use” phase of a vehicle is very important.

However, the “use” phase represents only part of the total emissions associated with a vehicle throughout its life. A more comprehensive evaluation can be achieved if emissions from all phases of a vehicle's life are considered - from materials production through the end-of-life disposal (Figure 5-2). Decisions based on total life cycle data prevent the possibility of unintended consequences.



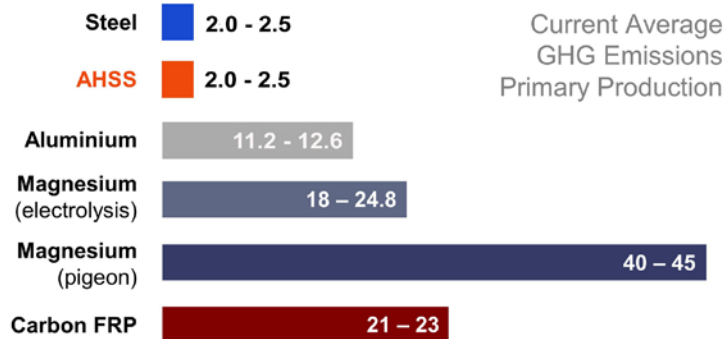
Source: Argonne National Laboratory

Figure 5-2: Vehicle Life Cycle Phases

Material production for alternative material vehicles will load the environment with significantly more GHG emissions than that of a steel vehicle, as shown in Figure 5-3 below. Mass reduction is therefore only one component of a comprehensive and effective greenhouse gas reduction strategy for the automotive industry.

**Material production** greenhouse gas (GHG) emissions:

**GHG from Production (in kg CO<sub>2</sub>eq/kg of material)**



**Figure footnotes:**

- All steel and aluminium grades included in ranges.
- Difference between AHSS and conventional steels less than 5%.
- Aluminium data - global for ingots; European only for process from ingot to final products.

**Figure 5-3: Material Production Greenhouse Gas Emissions**

Evaluating vehicle performance during the use phase only is not sufficient to properly assess vehicle emissions impact. The total life cycle – including fuel production as well as materials production and manufacturing must be taken into account. Consequently, total life cycle assessment evaluations of the FSV concept designs were conducted to assess their potential to meet CO<sub>2</sub> emissions targets. This should be a model for vehicle design materials decision making.

**5.1 Life Cycle Assessment (LCA)**

**5.1.1 Methodology**

A fully parameterised model which calculates life cycle GHG emissions attributable to vehicles as a function of their material composition and power train characteristics, was developed by Dr. Roland Geyer at the University of California, Santa Barbara (UCSB) Bren School of Environmental Science. This model enables comparisons of various body structure and component materials across all phases of the vehicle life cycle, and has been used extensively by WorldAutoSteel in their application programmes.

The UCSB Greenhouse Gas Comparison Model has been used to assess the impact of sub-systems and body structure design, steel fabrication choices, and advanced powertrains on vehicle life emissions. Section 2.5.1 BEV Sub-Systems Selection summarises the process for evaluating the various sub-system designs based on LCA methodology. Figure 5-4 recaps the sub-systems included in the LCA.

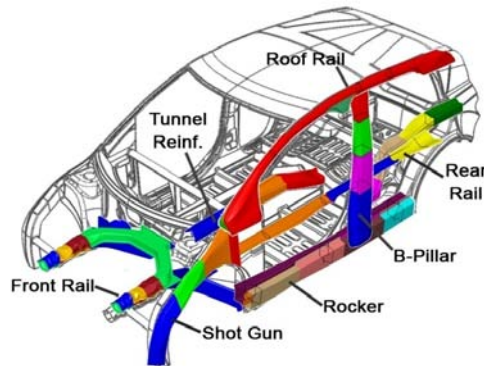


**Figure 5-4: Sub-Systems Included In LCA Review**

This same methodology used to evaluate the sub-systems applied to the full vehicle body structure to determine the life cycle emissions profile of the BEV variant. The UCSB GHG Automotive Materials Comparison model allows for advanced powertrain impact studies, including Battery-Electric (BEV) and Plug-in Hybrid (at 20 and 40 mile ranges, respectively). Key model parameters include the BEV powertrain and energy consumption factors based on vehicle size, geographic power grid emissions, driving cycle, vehicle life = 200,000 km, material processing efficiencies and recycling treatment.

The engineering team provided body structure and total vehicle masses, manufacturing emissions attributed to each subsystem fabrication process, and component manufacturing efficiencies (yields) associated with these steel fabrication methods.

### 5.1.2 Results

The results shown in Table 5-1 vividly demonstrate that the coupling of a light weight Advanced High-Strength Steel body structure combined with a battery electric powertrain results in a 40 to 70% reduction in life cycle emissions (depending on the energy source) compared to comparably-sized vehicles with conventional ICE-gasoline (ICEg) engines.

**Table 5-1: FSV LCA Results**

Vehicle	Material	Use	Recycling	Fabrication	Total CO <sub>2</sub> e
FSV-BEV	2,337	13,844	(1,009)	199	15,371

FutureSteelVehicle was compared to other benchmark vehicles: the ULSAB AVC concept vehicle from 2000, and the 2010 VW Polo V, which received the 2010 European Car of the Year award, and is distinguished for its efficient, light weight steel structure. For further comparisons the masses of the Polo V and ULSAB-AVC were modified to accommodate a battery electric propulsion system, and then their life cycle emissions were calculated. Use phase emission calculations utilised data from a study completed by Forschungsgesellschaft Kraftfahrwesen mbH Aachen (fka) entitled *Weight Influence on the Energy Consumption of Battery Electric and Plug-In Hybrid Vehicles*.

The results are shown below in Table 5-2, and corresponding charts in Figures 5-5 and 5-6. The data show that using the U.S. energy grid, AHSS combined with an electrified powertrain reduces total life cycle emissions by 56%. In regions where energy grid sources are more efficient, such as Europe, this grows to nearly 70% reduction in total life cycle emissions, as shown in Table 5-3. (Note: Fabrication CO<sub>2</sub>e is not included in the comparison since this is unknown for the Polo). The assumed vehicle life for these two graphs is 200,000 km; driving cycle used was the New European Driving Cycle (NEDC).

**Table 5-2: FutureSteelVehicle BEV and Benchmark Vehicle Comparisons (U.S. Energy Grid)**

Vehicle/Powertrain	Material Production (kg CO2e)	Use Phase (kg CO2e)	Recycling (kg CO2e)	Total Life Cycle (kg CO2e)
FSV BEV	2,337	13,844	(1,009)	15,172
ULSAB-AVC*	2,009	25,208	(841)	26,376
Polo V*	2,603	32,655	(1,124)	34,134
ULSAB-AVC BEV**	2,520	14,271	(1,088)	15,703
Polo V BEV**	2,847	15,044	(1,229)	16,662

\* With internal combustion gasoline engine  
\*\* Modified to battery electric vehicle (BEV)

**Table 5-3: Comparison between U.S. and Europe Energy Grids**

Vehicle/Powertrain	Material & Recycling (kg CO2e)	Use Phase (kg CO2e)	Total Life Cycle (kg CO2e)
Polo V ICEg	1,479	32,655	34,134
FSV BEV USA grid	1,328	13,844	15,172
FSV BEV Europe grid	1,328	9,670	10,998
FSV vs. Polo V - USA grid		<b>- 56% CO2e reduction</b>	
FSV vs. Polo V - Europe grid		<b>- 68% CO2e reduction</b>	

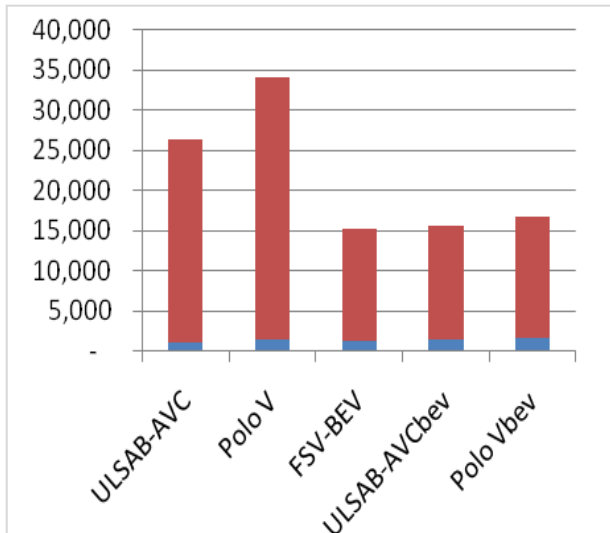


**Figure 5-5: FSV BEV Life Cycle Emissions Comparison – U.S. Grid**

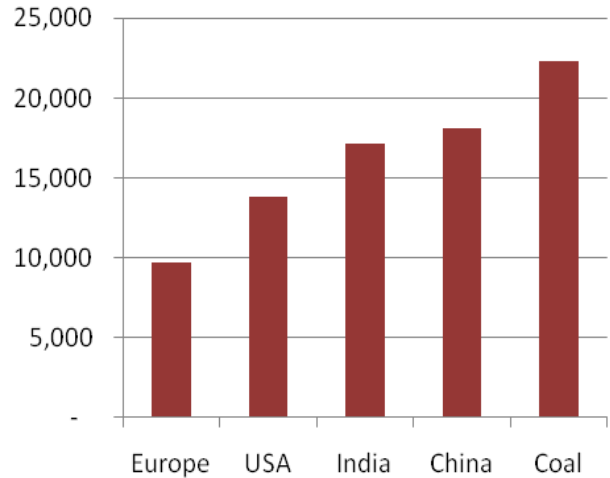


**Figure 5-6: FSV BEV Use Phase Emissions – Various Electric Grids**

It is noteworthy that, based on the new steels' light-weighting capabilities, steel is the only material to achieve reductions in *all* life cycle phases. As the automotive industry's efforts to reduce CO2e emissions are increasingly moving towards more advanced powertrains and fuel sources, material production will account for a much larger percentage of total life cycle emissions. This is due to the fact that these powertrains will greatly reduce the use phase CO2e emissions, as evidenced in the FSV results, which means that the material production phase emissions will make up a greater percentage of total vehicle emissions.

Figure 5-7 following compares Conventional steel and AHSS body structures to aluminium and sheet moulding compound (SMC) body structures along with the cumulative impact of powertrain and fuel

technology improvements on the total life cycle CO<sub>2</sub>e emissions. The comparison finds that use of these upcoming technologies can have a dramatic influence on the total vehicle LCA CO<sub>2</sub>e emissions. The use of advanced powertrains (such as hybrids), and advanced fuels (such as cellulose ethanol) can result in a dramatic reduction in the use phase CO<sub>2</sub>e emissions.

A key point, demonstrated by this graph, is that although the material production phase CO<sub>2</sub>e emissions remain the same, they become a much more significant percentage of the total LCA CO<sub>2</sub>e emissions as use phase efficiencies are achieved.

It is concluded that as other green technologies that improve vehicle CO<sub>2</sub>e emissions are implemented in mainstream vehicle designs, the emissions from material production will become more important, placing greater emphasis on selecting a low GHG-intensive material such as steel. FutureSteelVehicle demonstrates that using Advanced High-Strength Steel in tandem with more efficient powertrains and fuel sources can dramatically reduce the vehicle carbon footprint.

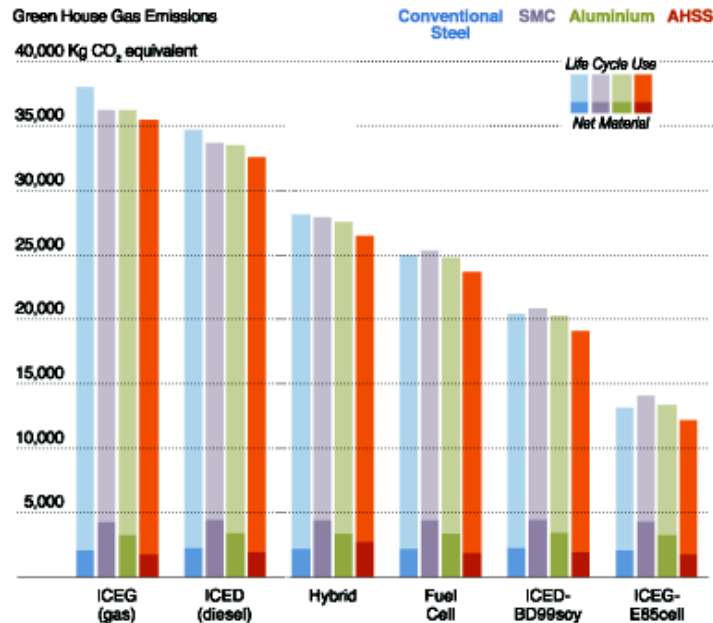


Figure 5-7: Life Cycle GHG's, Varying By Materials, Powertrains and Fuel Sources

## 5.2 Fuel Cycle Assessments

In addition to the Life Cycle Assessment (LCA) conducted, the fuel cycles for FSV designs were compared to a conventional ICE. Fuel Cycle assessments included two segments: "Well-to-Pump" and "Pump-to-Wheel." Well-to-Pump assessment of possible FSV vehicle fuel sources were conducted in FSV Phase 1, using Argonne National Lab program "Greet 1.8B." Data from these assessments were used in the Pump-to-Wheel and Well-to-Wheel analyses summarised following.

### 5.2.1 Pump-to-Wheel CO<sub>2</sub>e Emissions Assessment

The FSV-1 Pump-To-Wheel CO<sub>2</sub>e emissions are shown in Figure 5-8. The gasoline representative baseline vehicle shown is a conventional vehicle with a gasoline-powered internal combustion engine. For each PHEV, both Charge Sustaining (CS) and Charge Depleting (CD) all-electric driving modes also are shown. On a Pump-to-Wheel basis, all four FSV powertrain variants will emit less than 95g (CO<sub>2</sub>e) km, which is a

standards target currently under consideration in the European Union's and the most stringent in the world today. The PHEVs and BEV produce zero tailpipe CO<sub>2</sub>e emissions when driven in all-electric mode.

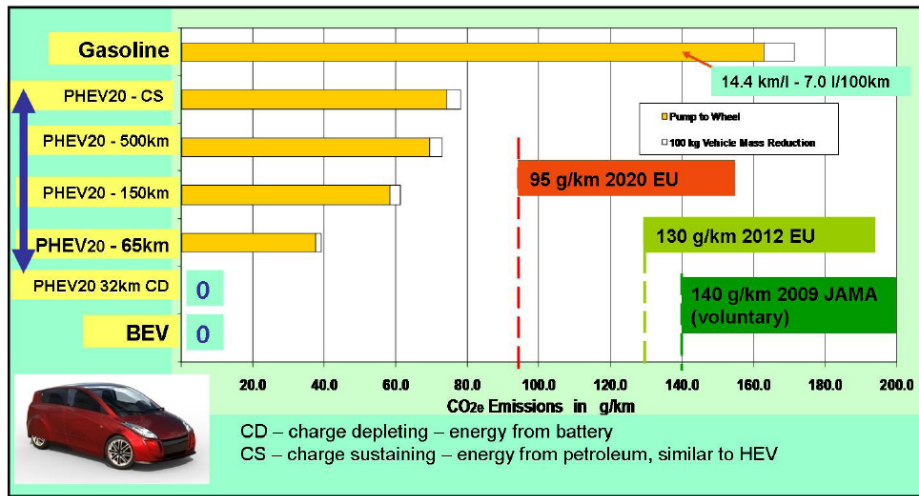


Figure 5-8: FSV-1 Pump-to-Wheel CO<sub>2</sub>e Emissions g/km (UDDS)

### 5.2.2 Well-to-Wheel Analysis

However, there are cumulative CO<sub>2</sub>e emissions from the production of fossil fuels, renewable fuel, or electricity. Therefore, a Well-to-Wheel analysis is very important for a comprehensive evaluation of vehicle emissions. Adding the Well-to-Pump emissions factor to each vehicle, the Well-to-Wheel CO<sub>2</sub>e emissions are attained, as shown in Figure 5-9. It can be observed from Figure 5-9 that, the PHEV in Charge Depleting all-electric mode, and the BEV have zero tailpipe CO<sub>2</sub>e emissions. However, their carbon footprint is not zero due to emissions from the fuel production.

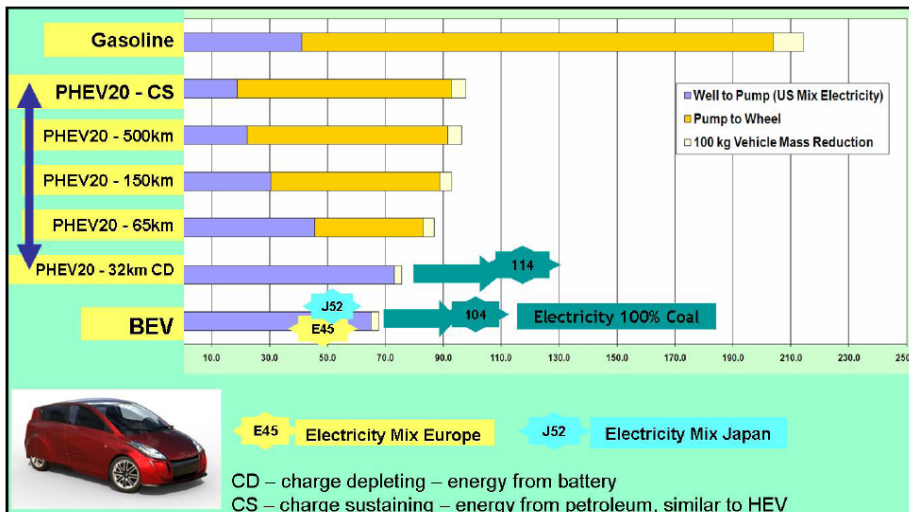


Figure 5-9: FSV-1 Well-to-Wheel CO<sub>2</sub>e Emissions g/km (UDDS)

## 6.0 Extension to Plug-In Hybrid and Fuel Cell Variants

### 6.1 FSV-1 PHEV<sub>20</sub>

The FSV-1 BEV body structure design was adapted by engineering judgement to integrate the PHEV<sub>20</sub> powertrain. FSV-1 PHEV<sub>20</sub> specifications are shown in Table 6-1.

**Table 6-1: FSV-1 PHEV 20 Powertrain Specifications**

Battery Pack	5 kWh capacity (45 kg mass, 36 liter volume)
Engine/Generator	1.0L-3 cylinder gasoline

Adaptations made:

- Engine/generator mounted ahead of rear axle, leading to 50/50 vehicle mass split between front and rear wheels.
- Underfloor adapted to accommodate battery pack in the tunnel under front floor.
- Rear floor adapted to accept modular sub-assembly including engine/generator and rear suspension.

Table 6-2 highlights powertrain and performance. Table 6-3 provides the final mass and vehicle dimensions.

**Table 6-2: FSV-1 PHEV<sub>20</sub> Powertrain and Performance**

FSV 1 A-B Class 4-door hatchback 3700 mm long	PHEV <sub>20</sub> Electric Range: 32km Total: 500km Max Speed: 150km/h 0-100 km/h 11-13 s
--------------------------------------------------------	--------------------------------------------------------------------------------------------------------

**Table 6-3: PHEV<sub>20</sub> Mass and Vehicle Dimensions**

Vehicle	Body Structure Mass (kg)	Length (mm)	Width (mm)	Height (mm)	Wheel Base (mm)	Track Front/Rear (mm)	Powertrain Mass (kg)	Curb Mass (kg)	GVW (kg)
PHEV <sub>20</sub>	176.4	3820	1705	1495	2524	1470	335.4	988	1463

The layout for the FSV-1 PHEV<sub>20</sub> is illustrated in Figure 6-1.

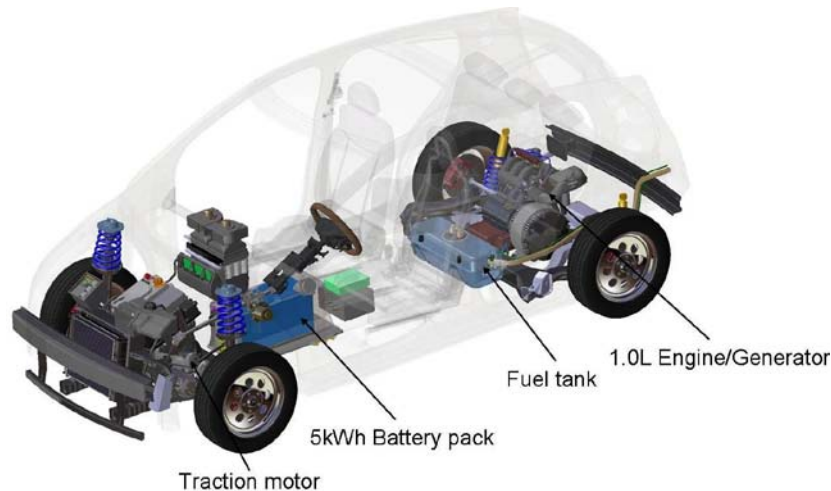


**Figure 6-1: PHEV<sub>20</sub> layout**

## 6.2 FSV-2 Variants

The FSV-1 BEV body structure design was also adapted by engineering judgement to integrate the PHEV<sub>40</sub> and Fuel Cell (FCEV) powertrains into a larger size FSV-2. Table 6-4 and 6-5 provides a summary of the variants' specifications:

**Table 6-4: FSV-2 Powertrains and Performances**

FSV 2 C-D Class 4-door sedan 4350 mm long	Plug-In Hybrid	Fuel Cell
	PHEV <sub>40</sub> Electric Range: 64km Total: 500km Max Speed: 161km/h 0-100 km/h 10-12 s	FCEV Total Range: 500km Max Speed: 161km/h 0-100 km/h 10-12 s

**Table 6-5: FSV-2 Variants - Mass and Vehicle Dimensions**

Vehicle	Body Structure Mass (kg)	Length (mm)	Width (mm)	Height (mm)	Wheel Base (mm)	Track Front/Rear (mm)	Powertrain Mass (kg)	Curb Mass (kg)	GVW (kg)
PHEV <sub>40</sub>	200.8	4350	1805	1495	2800	1570	460.7	1195	1670
FCEV	200.8	4350	1805	1495	2800	1570	293.2	1029	1504

Both powertrains share a common front-end and a common front wheel drive traction motor package. The traction motors rated peak power is 75 kW (55 kW of continuous power). The FSV-2 body structure is shown in Figure 6-2.



**Figure 6-2: FSV-2 Body Structure**

### 6.2.1 FSV-2 PHEV<sub>40</sub>

The PHEV<sub>40</sub> battery pack is a lithium-ion manganese-based cell with an 11.7 kWh capacity (105 kg mass, 86 liter volume). A rear mounted 1.4 L, 3 cylinder gasoline engine/generator set provides the PHEV<sub>40</sub> with an extended range of 500 km. The component packaging and structural characteristics for this vehicle are similar to the PHEV<sub>20</sub>. The FSV-2 PHEV<sub>40</sub> layout is shown in Figure 6-3.



Figure 6-3: FSV-2 PHEV<sub>40</sub>

### 6.2.2 FSV-2 FCEV

The FSV-2 FCEV fuel cell components (stack, battery, humidifier, hydrogen pump, compressor, etc.) are packaged in the engine compartment as shown in Figure 6-4 and 6-5. The fuel cell stack is packaged in the rear of the vehicle as shown in the Figure. The lithium-ion battery pack is positioned in front of the tunnel, behind the firewall. The hydrogen tanks are packaged in front of the rear axle under the rear passenger seats. This packaging design also allows for a common front-end with the BEV variant of the FSV.

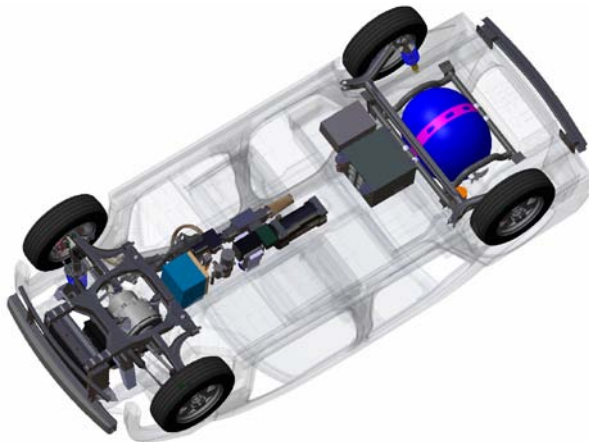


Figure 6-4: FSV-2 FCEV Underbody Packaging

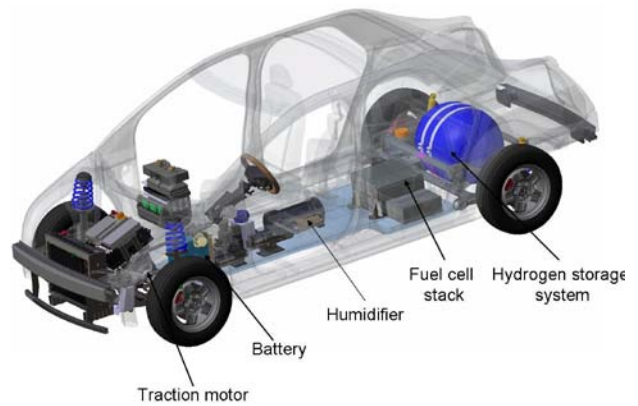


Figure 6-5: FSV-2 FCEV Layout

## References:

1. Beach, W., Kreutzer, D., Lieberman, B. & Loris, N., (2008). *The Economic Costs of the Lieberman-Warner Climate Change Legislation*, Retrieved from The Heritage Foundation website: [www.heritage.org/Research/Reports/2008/05/The-Economic-Costs-of-the-Lieberman-Warner-Climate-Change-Legislation](http://www.heritage.org/Research/Reports/2008/05/The-Economic-Costs-of-the-Lieberman-Warner-Climate-Change-Legislation)
2. Biermann, Dr.-Ing. Habil. Jan-Welm; Bröckerhoff, Dr.-Ing. Markus; Crampen, Dr.-Ing. Manfred; Schulte-Cörne, Dipl.-Ing. Claus, (2010). *Determination Of Weight Influence On The Energy Consumption Of Battery Electric Vehicles And Plugin Hybrid Vehicles*, Available by contacting the WorldAutoSteel offices, [cathyjohnson@worldautosteel.org](mailto:cathyjohnson@worldautosteel.org)
3. Blum, Jeremy J., et al, (2008). Vehicle Related Factors that Influence Injury Outcome in Head-On Collisions. 52nd AAAM Annual Conference, Annals of Advances in Automotive Medicine (reference to small vehicle crash performance.)
4. EDAG AG, (2007). Future Generation Passenger Compartment (FGPC), Available from <http://www.a-sp.org/publications.htm>
5. EDAG AG, (2009). *FutureSteelVehicle Phase 1 Engineering Report*, Available from: [www.worldautosteel.org/Projects/Future-Steel-Vehicle/Phase-1-Results-Phase-2-Launch.aspx](http://www.worldautosteel.org/Projects/Future-Steel-Vehicle/Phase-1-Results-Phase-2-Launch.aspx)
6. EDAG AG, (2010). *Phase 2 FutureSteelVehicle Steel Technology Assessment and Design Optimization Engineering Report*, Available from: [www.worldautosteel.org/Projects/Future-Steel-Vehicle/FSVInterimReport.aspx](http://www.worldautosteel.org/Projects/Future-Steel-Vehicle/FSVInterimReport.aspx)
7. Engineering Technology Associates, Inc. (ETA), (2009). *Methodology Used in Future Steel Vehicle Wins SAE Vehicle Innovation Competition*, Retrieved from The Auto Channel website: [www.theautochannel.com/news/2009/12/18/459143.html](http://www.theautochannel.com/news/2009/12/18/459143.html)
8. Florentin, J.; Durieux, F.; Kuriyama, Y.; and Yamamoto, T., (2011). *Electric Motor Noise in a Lightweight Steel Vehicle*, SAE Paper No. 2011-01-1724, [www.sae.org](http://www.sae.org)
9. Geyer, R., (2007). *Life Cycle Greenhouse Gas Emission Assessments of Automotive Material: The Example of Mild Steel, Advanced High Strength Steel and Aluminium in Body in White Applications*, Available from: [www.worldautosteel.org/Projects/LCA-Study.aspx](http://www.worldautosteel.org/Projects/LCA-Study.aspx)
10. Geyer, R., (2010). *UCSB Greenhouse Gas Materials Comparison Model – June 2010*, Available from <http://www.worldautosteel.org/Projects/LCA-Study/2010-UCSB-model.aspx>
11. Insurance Institute for Highway Safety (2002). *Frontal Offset Crashworthiness Evaluation Guidelines for Rating Structural Performance*. Available from <http://www.iihs.org/ratings/protocols/pdf/structural.pdf>
12. Keeler, Dr. Stuart (2009). *Advanced High-Strength Steels Application Guidelines*, Available from <http://www.worldautosteel.org/projects/AHSSGuidelines/AHSS-application-guidelines-version-4.aspx>
13. Porsche Engineering Services, Inc., (2002). *ULSAB-AVC (Advanced Vehicle Concepts) Engineering Report*, Retrieved from WorldAutoSteel website: [www.worldautosteel.org/Projects/ULSAB-AVC.aspx](http://www.worldautosteel.org/Projects/ULSAB-AVC.aspx)

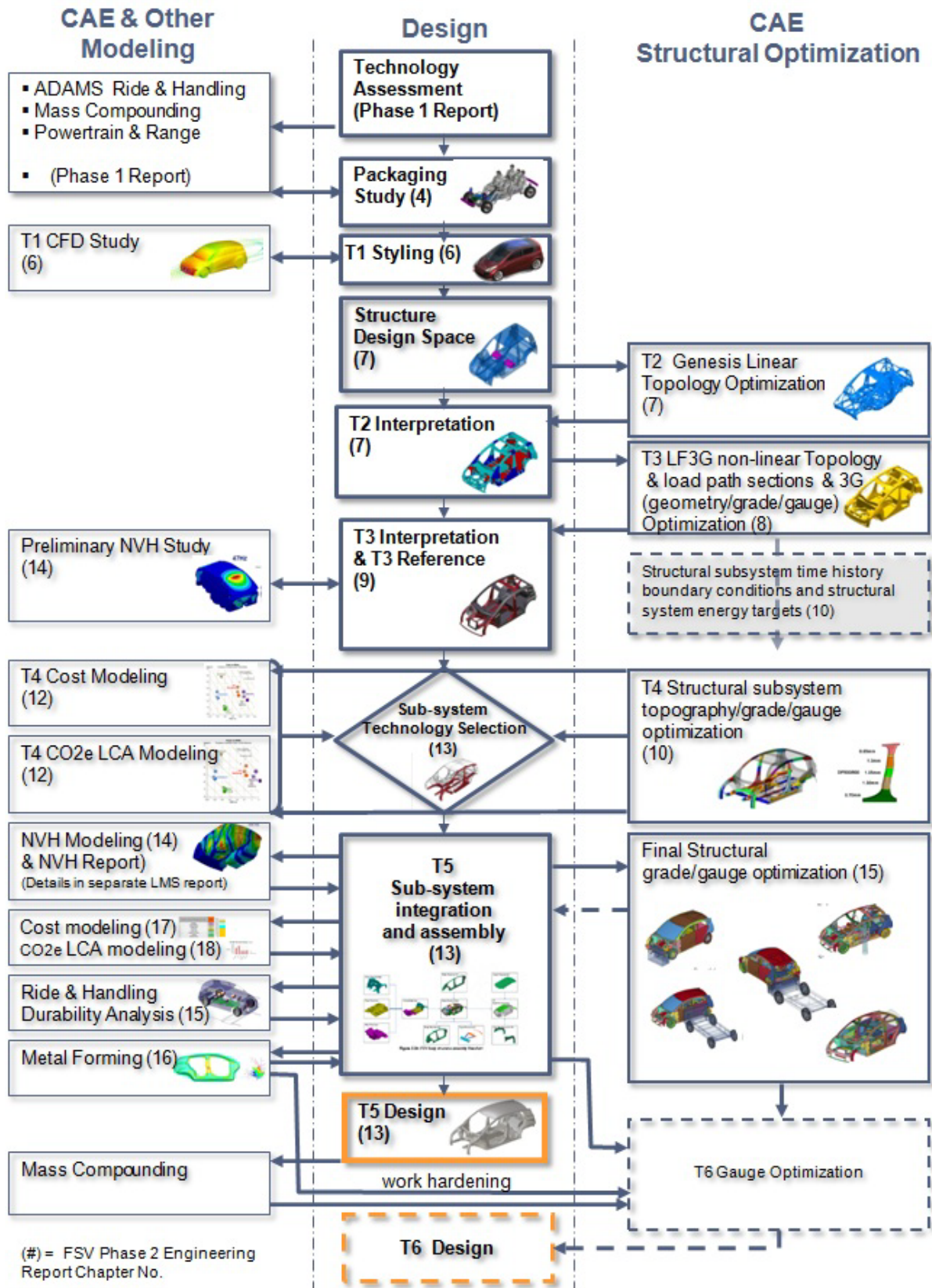
## Appendices

Appendix 1: FSV's Enhanced Steel Portfolio

Item #	Steel Grade	Thickness (mm)		Gauge Length	YS (MPa)	YS (MPa)	UTS (MPa)	UTS (MPa)	Tot EL (%)	N-value	Modulus of Elasticity (MPa)	Fatigue Strength	K Value (MPa)
		Min t	Max t		Min	Typical	Min	Typical	Typical			Typical	
1	Mild 140/270	0.35	4.60	A50	140	150	270	300	42-48	0.24	21.0 x 10 <sup>4</sup>	645	541
2	BH 210/340	0.45	3.40	A50	210	230	340	350	35-41	0.21	21.0 x 10 <sup>4</sup>	695	582
3	BH 260/370	0.45	2.80	A50	260	275	370	390	32-36	0.18	21.0 x 10 <sup>4</sup>	735	550
4	BH 280/400	0.45	2.80	A50	280	325	400	420	30-34	0.16	21.0 x 10 <sup>4</sup>	765	690
5	IF 260/410	0.40	2.30	A50	260	280	410	420	34-48	0.20	21.0 x 10 <sup>4</sup>	765	690
6	IF 300/420	0.50	2.50	A50	300	320	420	430	29-36	0.19	21.0 x 10 <sup>4</sup>	775	759
7	FB 330/450	1.60	5.00	A80	330	380	450	490	29-33	0.17	21.0 x 10 <sup>4</sup>	835	778
8	HSLA 350/450	0.50	5.00	A80	350	360	450	470	23-27	0.16	21.0 x 10 <sup>4</sup>	815	807
9	DP 300/500	0.50	2.50	A80	300	345	500	520	30-34	0.18	21.0 x 10 <sup>4</sup>	865	762
10	HSLA 420/500	0.60	5.00	A50	420	430	500	530	22-26	0.14	21.0 x 10 <sup>4</sup>	875	827
11	FB 450/600	1.40	6.00	A80	450	530	560	605	18-26	0.15	21.0 x 10 <sup>4</sup>	950	921
12	HSLA 490/600	0.60	5.00	A50	490	510	600	630	20-25	0.13	21.0 x 10 <sup>4</sup>	975	952
13	DP 350/600	0.60	5.00	A80	350	385	600	640	24-30	0.17	21.0 x 10 <sup>4</sup>	985	976
14	TRIP 350/600	0.60	4.00	A50	350	400	600	630	29-33	0.25	21.0 x 10 <sup>4</sup>	975	952
15	SF 570/640	2.90	5.00	A50M	570	600	640	660	20-24	0.08	21.0 x 10 <sup>4</sup>	1005	989
16	HSLA 550/650	0.60	5.00	A50	550	585	650	675	19-23	0.12	21.0 x 10 <sup>4</sup>	1020	1009
17	TRIP 400/700	0.60	4.00	A80	400	420	700	730	24-28	0.24	21.0 x 10 <sup>4</sup>	1075	1077
18	SF 600/780	2.00	5.00	A50	600	650	780	830	16-20	0.07	21.0 x 10 <sup>4</sup>	1175	1201
19	HSLA 700/780	2.00	5.00	A50	700	750	780	830	15-20	0.07	21.0 x 10 <sup>4</sup>	1175	1200
20	CP 500/800	0.80	4.00	A80	500	520	800	815	10-14	0.13	21.0 x 10 <sup>4</sup>	1160	1183
21	DP 500/800	0.60	4.00	A50	500	520	800	835	14-20	0.14	21.0 x 10 <sup>4</sup>	1180	1303
22	TRIP 450/800	0.60	2.20	A80	450	550	800	825	26-32	0.24	21.0 x 10 <sup>4</sup>	1170	1690
23	CP 600/900	1.00	4.00	A80	600	615	900	910	14-16	0.14	21.0 x 10 <sup>4</sup>	1255	1301
24	CP 750/900	1.60	4.00	A80	750	760	900	910	14-16	0.13	21.0 x 10 <sup>4</sup>	1255	1401
25	TRIP 600/980	0.90	2.00	A50	550	650	980	990	15-17	0.13	21.0 x 10 <sup>4</sup>	1335	1301
26	TWIP 500/980	0.80	2.00	A50M	500	550	980	990	50-60	0.40	21.0 x 10 <sup>4</sup>	1335	1401
27	DP 700/1000	0.60	2.30	A50	700	720	1000	1030	12-17	0.12	21.0 x 10 <sup>4</sup>	1375	1521
28	CP 800/1000	0.80	3.00	A80	800	845	1000	1005	8-13	0.11	21.0 x 10 <sup>4</sup>	1350	1678
29	DP 800/1180	1.00	2.00	A50	800	880	1180	1235	10-14	0.11	21.0 x 10 <sup>4</sup>	1555	1700
30	MS 950/1200	0.50	3.20	A50M	950	960	1200	1250	5-7	0.07	21.0 x 10 <sup>4</sup>	1595	1678
31	CP 1000/1200	0.80	2.30	A80	1000	1020	1200	1230	8-10	0.10	21.0 x 10 <sup>4</sup>	1575	1700
32	DP1150/1270	0.60	2.00	A50M	1150	1160	1270	1275	8-10	0.10	21.0 x 10 <sup>4</sup>	1620	1751
33	MS 1150/1400	0.50	2.00	A50	1150	1200	1400	1420	4-7	0.06	21.0 x 10 <sup>4</sup>	1765	1937
34	CP 1050/1470	1.00	2.00	A50M	1050	1060	1470	1495	7-9	0.06	21.0 x 10 <sup>4</sup>	1840	2030
35	HF 1050/1500												
	<i>Conventional Forming</i>	0.60	4.50	A80	340	380	480	500	23-27	0.16	21.0 x 10 <sup>4</sup>	845	790
	<i>Heat Treated after forming</i>	0.60	4.50	A80	1050	1220	1500	1600	5-7	0.06	21.0 x 10 <sup>4</sup>	1945	2161
36	MS 1250/1500	0.50	2.00	A50M	1250	1265	1500	1520	3-6	0.05	21.0 x 10 <sup>4</sup>	1865	2021

\* Un-notched specimens, FSc = UTS + 345 (MPa)  
Alternate approximation = 3.45\*HB

APPENDIX 2: FSV DESIGN FLOW CHART



### Appendix 3: FSV BEV Exploded View and Parts List



Figure A3-1: BEV Exploded View

FSV-1 BEV Parts List can be found in Table A3-1, following.

**Overview Report - FutureSteelVehicle Phase 2**  
30 APRIL 2011

**Table A3-1: FSV-1 BEV Parts List**

Forming Key: (HS) Hot Stamping (RF) Rollforming (S) Stamping

Part No.	Part Description	Forming	Type	Yield	Tensile	Thickness	Sub Mass	Total Mass
1	50.1 0401 Bulkhead Lower - Tunnel	S	DP	700	1000	0.80	0.679	0.679
2	50.1 0400 Bulkhead Upper - Tunnel	S	DP	700	1000	0.80	0.543	0.543
3	50.1 0402 Panel - Tunnel Side RH	S	BH	280	400	0.50	2.342	2.342
4	50.1 0404 Reinf - Tunnel Top	S	BH	280	400	0.50	1.713	1.713
5	50.1 0403 Panel - Tunnel Side LH	S	BH	280	400	0.50	2.342	2.342
6	50.1 0321 Tunnel Rail Bulkhead RH	S	DP	500	800	1.00	0.381	0.381
7	50.1 0011 Floor - Front RH	S	DP	300	500	0.50	2.84	4.61
			DP	500	800	1.50	1.77	
8	50.1 0322 Tunnel Rail Bulkhead LH	S	DP	500	800	1.00	0.381	0.381
9	50.1 0025 Floor - Front LH	S	DP	300	500	0.50	2.84	4.61
			DP	500	800	1.50	1.77	
10	50.1 0093 Crossmember - Front Seat RH Front	RF	MS	950	1200	0.50	0.542	0.542
11	50.1 0094 Crossmember - Front Seat LH Front	RF	MS	950	1200	0.50	0.542	0.542
12	50.1 0095 Crossmember - Front Seat RH Rear	RF	MS	950	1200	0.60	0.688	0.688
13	50.1 0096 Crossmember - Front Seat LH Rear	RF	MS	950	1200	0.60	0.688	0.688
14	50.1 0100 Heel Board	S	BH	210	340	0.60	1.603	1.603
15	50.1 0016 Seat Pan - Rear	S	BH	210	340	0.50	2.919	2.919
16	50.1 0099 Panel - Seat Side RH	S	DP	700	1000	0.70	0.359	0.359
17	50.1 0101 Panel - Seat Side LH	S	DP	700	1000	0.70	0.359	0.359
18	50.1 0109 Reinf - Frame Rail Rear RH	S	CP	1000	1200	1.10	0.361	1.555
			DP	700	1000	0.65	0.528	
			Mild	140	270	1.55	0.666	
19	50.1 0110 Reinf - Frame Rail Rear LH	S	CP	1000	1200	1.10	0.361	1.555
			DP	700	1000	0.65	0.528	
			Mild	140	270	1.55	0.666	
20	50.1 0015 Frame Rail - Outer Rear LH	S	CP	1000	1200	0.60	0.304	1.037
			DP	700	1000	1.40	0.469	
			HSLA	350	450	0.80	0.264	
21	50.1 0334 Mounting Plate - Crush Can Rear LH	S	DP	500	1200	1.20	0.132	0.132
22	50.1 0336 Frame Rail - Inr Rear LH	U	CP	1000	1200	0.60	0.247	2.635
			DP	700	1000	1.40	1.963	
			HSLA	350	450	0.80	0.425	
23	50.1 0014 Frame Rail - Outer Rear RH	S	CP	1000	1200	0.60	0.304	1.037
			DP	700	1000	1.40	0.469	
			HSLA	350	450	0.80	0.264	
24	50.1 0333 Mounting Plate - Crush Can Rear RH	S	DP	500	800	1.20	0.132	0.132
25	50.1 0335 Frame Rail - Inr Rear RH	U	CP	1000	1200	0.60	0.247	2.635
			DP	700	1000	1.40	1.963	
			HSLA	350	450	0.80	0.425	
26	50.1 0032 Crossmember - Battery and Suspension	S	CP	800	1000	1.00	2.944	2.944
27	50.1 0330 Panel - Cargo Box Floor	S	Mild	140	270	0.50	1.326	1.326

**Overview Report - FutureSteelVehicle Phase 2**  
**30 APRIL 2011**

Part No.	Part Description	Forming	Type	Yield	Tensile	Thickness	Sub Mass	Total Mass
28	50.1 0017 Wheelhouse Inner - Rear RH	S	BH	210	340	0.70	0.835	2.58
			BH	210	340	1.20	1.745	
29	50.1 0018 Wheelhouse Inner - Rear LH	S	BH	210	340	0.70	0.835	2.58
			BH	210	340	1.20	1.745	
30	50.1 0079 Brkt - Rear Suspension RH	S	CP	800	1000	1.00	0.342	0.342
31	50.1 0080 Brkt - Rear Suspension LH	S	CP	800	1000	1.00	0.342	0.342
32	50.1 0077 Gusset - Rear RH	S	BH	210	340	1.00	0.465	0.465
33	50.1 0078 Gusset - Rear LH	S	BH	210	340	1.00	0.465	0.465
34	50.1 0320 Rail - Side to Side	S	DP	500	800	0.80	1.074	1.074
35	50.1 0108 Rail - Longitudinal RR RH	S	DP	700	1000	1.20	2.201	2.201
36	50.1 0075 Close Off - Battery Otr RH	S	BH	210	340	0.60	0.805	0.805
37	50.1 0073 Close Off - Battery Inr RH	S	BH	210	340	0.60	1.195	1.195
38	50.1 0107 Rail - Longitudinal RR LH	S	DP	700	1000	1.20	2.201	2.201
39	50.1 0076 Close Off - Battery Otr LH	S	BH	210	340	0.60	0.805	0.805
40	50.1 0074 Close Off - Battery Inr LH	S	BH	210	340	0.60	1.195	1.195
41	50.1 0329 Pnl - Rear Liftgate Lower Inr LH	S	BH	210	340	1.00	0.585	0.585
42	50.1 0013 Pnl - Rear Liftgate Lower Inr	S	BH	210	340	0.70	1.866	1.866
43	50.1 0328 Pnl - Rear Liftgate Lower Inr RH	S	BH	210	340	1.00	0.585	0.585
44	50.1 0019 Panel - Back Outboard RH	S	BH	210	340	1.00	0.577	0.577
45	50.1 0025 Panel - Back Outboard LH	S	BH	210	340	1.00	0.577	0.577
46	50.1 0020 Panel - Back Lower	S	BH	210	340	1.00	1.405	1.405
47	50.1 2601 Mount - Rear Shock RH	S	DP	500	800	2.50	0.566	0.566
48	50.1 2602 Reinf - Rear Shock RH	S	DP	500	800	2.00	0.176	0.176
49	50.1 2701 Reinf - Rear Shock LH	S	DP	500	800	2.00	0.176	0.176
50	50.1 2702 Mount - Rear Shock LH	S	DP	500	800	2.50	0.566	0.566
51	50.1 2001 Mount - Trailing Arm LH	S	DP	500	800	2.00	0.37	0.37
52	50.1 2002 Mount - Trailing Arm RH	S	DP	500	800	2.00	0.37	0.37
53	50.1 0001 Dash - Toe Pan	S	BH	280	400	0.50	2.839	2.839
54	50.1 0002 Cowl Upper	S	BH	210	340	1.00	0.866	2.268
			BH	210	340	0.60	1.402	
55	50.1 0070 Cowl Lower	S	BH	210	340	1.20	0.709	1.494
			BH	210	340	0.60	0.785	
56	60.2 0007 Mounting Plate - Crush Can Front RH	S	DP	500	800	1.75	0.121	0.121
57	60.2 0008 Mounting Plate - Crush Can Front LH	S	DP	500	800	1.75	0.121	0.121
58	50.1 0306 Closeout - Lower Rail LH	S	DP	700	1000	0.80	0.309	0.309
59	50.1 0302 Front Rail - Lower LH	S	TRIP	600	980	1.90	0.359	5.998
			TRIP	600	980	2.00	0.419	
			TRIP	600	980	1.90	0.535	
			TRIP	600	980	1.80	4.685	
60	50.1 0305 Closeout - Lower Rail RH	S	DP	700	1000	0.80	0.309	0.309
61	50.1 0301 Front Rail - Lower RH	S	TRIP	600	980	1.90	0.359	5.998
			TRIP	600	980	2.00	0.419	
			TRIP	600	980	1.90	0.535	
			TRIP	600	980	1.80	4.685	

**Overview Report - FutureSteelVehicle Phase 2**  
**30 APRIL 2011**

Part No.	Part Description	Forming	Type	Yield	Tensile	Thickness	Sub Mass	Total Mass
62	50.1 0303 Front Rail - Upper	S	TRIP	600	980	1.80	0.667	5.743
			TRIP	600	980	2.00	0.811	
			TRIP	600	980	1.80	4.265	
63	50.1 0304 Closeout - Upper Rail	S	DP	700	1000	1.00	0.616	0.616
64	50.1 0044 Shock Tower - Frt RH	S	TWIP	700	1000	1.00	1.457	1.457
65	50.1 0063 Shock Tower - Frt LH	S	TWIP	700	1000	1.00	1.457	1.457
66	50.1 0022 Shotgun Inner LH	HS	HF	1050	1500	1.20	0.476	2.15
			HF	1050	1500	0.80	0.759	
			HF	1050	1500	1.50	0.915	
67	50.1 0021 Shotgun Inner RH	HS	HF	1050	1500	1.20	0.476	2.15
			HF	1050	1500	0.80	0.759	
			HF	1050	1500	1.50	0.915	
68	50.1 0326 A-Pillar Brace	RF	DP	700	1000	1.20	0.695	0.695
69	50.1 0326 A-Pillar Brace LH	RF	DP	700	1000	1.20	0.695	0.695
70	50.1 0318 Shotgun Brace LH	S	BH	210	340	1.20	0.206	0.206
71	50.1 0308 Shotgun Brace RH	S	BH	210	340	1.20	0.206	0.206
72	50.6 0023 Roof Rail Inner Front LH	HS	HF	1050	1500	0.70	0.84	1.171
			HF	1050	1500	0.95	0.331	
73	50.6 0064 FBHP Inner LH	S	DP	500	800	1.20	1.667	1.667
74	50.6 0056 Rocker Filler Front LH	S	BH	210	340	0.60	0.199	0.199
75	50.6 0017 B-Pillar Inner LH	HS	HF	1050	1500	0.80	0.547	1.491
			HF	1050	1500	0.60	0.944	
76	50.6 0053 Roof Rail Inner Rear LH	S	BH	210	340	1.10	0.372	0.372
77	50.1 0067 Panel - Wheel House Outer LH	S	DP	500	800	0.65	1.732	1.732
78	50.6 0004 C-Pillar Inner LH	S	DP	500	800	0.70	1.428	1.428
79	50.2 0034 Bracket - Roof Rail to Header LH	S	BH	210	340	1.00	0.103	0.103
80	50.2 0035 Bracket - Roof Rail to Roof Bow LH	S	BH	210	340	1.00	0.254	0.254
81	50.6 0018 Reinf - Roof Rail LH	HS	HF	1050	1500	0.70	2.049	2.049
82	50.6 0066 Rocker LH	RF	CP	1050	1470	1.00	6.032	6.032
83	50.6 0072 Rocker Cap LH	S	BH	210	340	0.85	0.244	0.244
84	50.6 0028 Reinf - B-Pillar LH	HS	HF	1050	1500	0.60	0.547	1.491
			HF	1050	1500	1.00	0.944	
85	50.6 0006 Body Side Outer LH	S	DP	350	600	0.80	8.189	10.928
			BH	210	340	0.60	2.739	
86	50.6 0069 Panel Rear Quarter Lwr LH	S	BH	210	340	1.20	0.198	0.198
87	50.6 0051 Panel - Gutter Rear LH	S	BH	210	340	1.00	0.795	0.795
88	50.6 0046 FBHP Inner RH	S	DP	500	800	1.20	1.667	1.667
89	50.6 0022 Roof Rail Inner Front RH	HS	HF	1050	1500	0.70	0.84	1.171
			HF	1050	1500	0.95	0.331	
90	50.6 0055 Rocker Filler Front RH	S	BH	210	340	0.60	0.199	0.199
91	50.6 0009 B-Pillar Inner RH	HS	HF	1050	1500	0.80	0.547	1.491
			HF	1050	1500	0.60	0.944	
92	50.6 0052 Roof Rail Inner Rear RH	S	BH	210	340	1.10	0.372	0.372
93	50.1 0049 Panel - Wheel House Outer RH	S	DP	500	800	0.65	1.732	1.732
94	50.6 0005 C-Pillar Inner RH	S	DP	500	800	0.70	1.428	1.428

**Overview Report - FutureSteelVehicle Phase 2**  
**30 APRIL 2011**

Part No.	Part Description	Forming	Type	Yield	Tensile	Thickness	Sub Mass	Total Mass
95	50.2 0033 Bracket - Roof Rail to Roof Bow RH	S	BH	210	340	1.00	0.254	0.254
96	50.2 0032 Bracket - Roof Rail to Header RH	S	BH	210	340	1.00	0.103	0.103
97	50.6 0012 Reinf - Roof Rail RH	S	HF	1050	1500	0.70	2.049	2.049
98	50.6 0048 Rocker RH	RF	CP	1050	1470	1.00	6.032	6.032
99	50.6 0071 Rocker Cap RH	S	BH	210	340	0.85	0.244	0.244
100	50.6 0026 Reinf - B-Pillar RH	HS	HF	1050	1500	0.60	0.547	1.491
			HF	1050	1500	1.00	0.944	
101	50.6 0050 Panel - Gutter Rear RH	S	BH	210	340	1.00	0.795	0.795
102	50.6 0068 Panel Rear Quarter Lwr RH	S	BH	210	340	1.20	0.198	0.198
103	50.6 0002 Body Side Outer RH	S	DP	350	600	0.80	8.189	10.928
			BH	210	340	0.60	2.739	
104	50.2 0007 Rear Header Reinf	S	BH	210	340	2.00	2.759	3.775
			BH	210	340	0.70	1.016	
105	50.2 0006 Rear Header	S	BH	210	340	0.70	1.662	1.662
106	50.2 0009 Support - Roof LH	S	Mild	140	270	0.50	0.463	0.463
107	50.2 0008 Support - Roof RH	S	Mild	140	270	0.50	0.463	0.463
108	50.2 0013 Roof Bow	RF	BH	210	340	0.50	0.941	0.941
109	50.2 0011 Header - Roof Front	RF	BH	210	340	0.80	1.131	1.131
110	50.1 0405 Top Panel - Tunnel	S	DP	700	1000	1.00	3.067	3.067
111	50.2 0010 Pnl - Roof Outer	S	BH	210	340	0.50	9.011	9.011
112	50.1 0069 Shotgun Outer LH	HS	HF	1050	1500	1.00	0.431	2.088
			HF	1050	1500	0.80	0.689	
			HF	1050	1500	1.50	0.968	
113	50.1 0051 Shotgun Outer RH	HS	HF	1050	1500	1.00	0.431	2.088
			HF	1050	1500	0.80	0.689	
			HF	1050	1500	1.50	0.968	
114	50.1 3002 Reinf - Shock Tower Frt	S	DP	500	980	2.00	0.69	0.69
115	50.1 3003 Reinf - Shock Tower Frt	S	DP	500	980	2.00	0.69	0.69
116	50.1 2112 Panel - Cargo Box Side RH	S	Mild	140	270	0.50	0.611	0.611
117	50.1 2113 Panel - Cargo Box Side LH	S	Mild	140	270	0.50	0.611	0.611
118	50.6 6354 Reinf - FBHP RH	S	DP	700	1000	0.80	0.453	0.453
119	50.6 1354 Reinf - FBHP LH	S	DP	700	1000	0.80	0.453	0.453
<b>Total FSV-1 BEV Body Structure Mass</b>								<b>187.7</b>

## Appendix 4: FSV-1 PHEV<sub>20</sub> Exploded View and Parts List



**Figure A4-1: FSV-1 PHEV<sub>20</sub> Exploded View**

FSV-1 PHEV<sub>20</sub> Parts List can be found in Table A4-1, following.

**Overview Report - FutureSteelVehicle Phase 2**  
**30 APRIL 2011**

**Table A4-1: FSV-1 PHEV<sub>20</sub> Parts List**

Forming Key: (HS) Hot Stamping (RF) Rollforming (S) Stamping

Part No.	Part Description	Forming	Type	Yield	Tensile	Thickness	Sub Mass	Total Mass
1	50.1 0401 Bulkhead Lower - Tunnel	S	DP	700	1000	0.80	0.679	0.679
2	50.1 0400 Bulkhead Upper - Tunnel	S	DP	700	1000	0.80	0.543	0.543
3	50.1 0402 Panel - Tunnel Side RH	S	BH	280	400	0.50	2.342	2.342
4	50.1 0404 Reinf - Tunnel Top	S	BH	280	400	0.50	1.713	1.713
5	50.1 0403 Panel - Tunnel Side LH	S	BH	280	400	0.50	2.342	2.342
7	50.1 0011 Floor - Front RH	S	DP	300	500	0.50	2.84	4.61
			DP	500	800	1.50	1.77	
9	50.1 0025 Floor - Front LH	S	DP	300	500	0.50	2.84	4.61
			DP	500	800	1.50	1.77	
10	50.1 0093 Crossmember - Front Seat RH Front	RF	MS	950	1200	0.50	0.542	0.542
11	50.1 0094 Crossmember - Front Seat LH Front	RF	MS	950	1200	0.50	0.542	0.542
12	50.1 0095 Crossmember - Front Seat RH Rear	RF	MS	950	1200	0.60	0.688	0.688
13	50.1 0096 Crossmember - Front Seat LH Rear	RF	MS	950	1200	0.60	0.688	0.688
14	50.1 0100 Heel Board	S	BH	210	340	0.60	1.603	1.603
15	50.1 0391 Seat Pan - Rear	S	BH	210	340	0.50	2.854	2.854
16	50.1 0099 Panel - Seat Side RH	S	DP	700	1000	0.70	0.359	0.359
17	50.1 0101 Panel - Seat Side LH	S	DP	700	1000	0.70	0.359	0.359
18	50.1 0109 Reinf - Frame Rail Rear RH	S	CP	1000	1200	1.10	0.361	1.555
			DP	700	1000	0.65	0.528	
			Mild	140	270	1.55	0.666	
19	50.1 0110 Reinf - Frame Rail Rear LH	S	CP	1000	1200	1.10	0.361	1.555
			DP	700	1000	0.65	0.528	
			Mild	140	270	1.55	0.666	
20	50.1 0015 Frame Rail - Outer Rear LH	S	CP	1000	1200	0.60	0.304	1.037
			DP	700	1000	1.40	0.469	
			HSLA	350	450	0.80	0.264	
21	50.1 0334 Mounting Plate - Crush Can Rear LH	S	DP	500	800	1.20	0.132	0.132
23	50.1 0014 Frame Rail - Outer Rear RH	S	CP	1000	1200	0.60	0.247	2.635
			DP	700	1000	1.40	1.963	
			HSLA	350	450	0.80	0.425	
22	50.1 0336 Frame Rail - Inr Rear LH	S	CP	1000	1200	0.60	0.304	1.037
			DP	700	1000	1.40	0.469	
			HSLA	350	450	0.80	0.264	
24	50.1 0333 Mounting Plate - Crush Can Rear RH	S	DP	500	800	1.20	0.132	0.132
25	50.1 0335 Frame Rail - Inr Rear RH	S	CP	1000	1200	0.60	0.247	2.635
			DP	700	1000	1.40	1.963	
			HSLA	350	450	0.80	0.425	
35	50.1 0001 Seat Pan-Engine Cover	S	Mild	140	270	0.60	2.38	2.38
27	50.1 0390 Cargo Box	S	Mild	140	270	0.50	0.984	0.984
28	50.1 0017 Wheelhouse Inner - Rear RH	S	BH	210	340	0.70	0.835	2.58
			BH	210	340	1.20	1.745	

**Overview Report - FutureSteelVehicle Phase 2**  
**30 APRIL 2011**

Part No.	Part Description	Forming	Type	Yield	Tensile	Thickness	Sub Mass	Total Mass
29	50.1 0018 Wheelhouse Inner - Rear LH	S	BH	210	340	0.70	0.835	2.58
			BH	210	340	1.20	1.745	
34	50.1 0320 Rail - Side to Side	S	DP	500	800	0.80	1.074	1.074
32	50.1 0004 Brkt-Fuel Tank Strap	S	BH	210	340	1.20	0.061	0.061
32	50.1 0004 Brkt-Fuel Tank Strap	S	BH	210	340	1.20	0.061	0.061
36	50.1 0003 Rail - Side to Side	S	DP	500	800	0.80	1.061	1.061
33	50.1 0005 Brkt-Fuel Tank Strap	S	BH	210	340	1.20	0.098	0.098
33	50.1 0005 Brkt-Fuel Tank Strap	S	BH	210	340	1.20	0.098	0.098
41	50.1 0329 Pnl - Rear Liftgate Lower Inr LH	S	BH	210	340	1.00	0.585	0.585
42	50.1 0013 Pnl - Rear Liftgate Lower Inr	S	BH	210	340	0.70	1.866	1.866
43	50.1 0328 Pnl - Rear Liftgate Lower Inr RH	S	BH	210	340	1.00	0.585	0.585
44	50.1 0019 Panel - Back Outboard RH	S	BH	210	340	1.00	0.577	0.577
45	50.1 0025 Panel - Back Outboard LH	S	BH	210	340	1.00	0.577	0.577
46	50.1 0020 Panel - Back Lower	S	BH	210	340	1.00	1.405	1.405
47	50.1 2601 Mount - Rear Shock RH	S	DP	500	800	2.50	0.566	0.566
48	50.1 2602 Reinf - Rear Shock RH	S	DP	500	800	2.00	0.176	0.176
49	50.1 2701 Reinf - Rear Shock LH	S	DP	500	800	2.00	0.176	0.176
50	50.1 2702 Mount - Rear Shock LH	S	DP	500	800	2.50	0.566	0.566
51	50.1 2001 Mount - Trailing Arm LH	S	DP	500	800	2.00	0.37	0.37
52	50.1 2002 Mount - Trailing Arm RH	S	DP	500	800	2.00	0.37	0.37
53	50.1 0001 Dash - Toe Pan	S	BH	280	400	0.50	2.839	2.839
54	50.1 0002 Cowl Upper	S	BH	210	340	1.00	0.866	2.268
			BH	210	340	0.60	1.402	
55	50.1 0070 Cowl Lower	S	BH	210	340	1.20	0.709	1.494
			BH	210	340	0.60	0.785	
58	50.1 0306 Closeout - Lower Rail LH	S	DP	700	1000	0.80	0.309	0.309
59	50.1 0302 Front Rail - Lower LH	S	TRIP	600	980	1.90	0.359	5.998
			TRIP	600	980	2.00	0.419	
			TRIP	600	980	1.90	0.535	
			TRIP	600	980	1.80	4.685	
60	50.1 0305 Closeout - Lower Rail RH	S	DP	700	1000	0.80	0.309	0.309
61	50.1 0301 Front Rail - Lower RH	S	TRIP	600	980	1.90	0.359	5.998
			TRIP	600	980	2.00	0.419	
			TRIP	600	980	1.90	0.535	
			TRIP	600	980	1.80	4.685	
62	50.1 0303 Front Rail - Upper	S	TRIP	600	980	1.80	0.667	5.743
			TRIP	600	980	2.00	0.811	
			TRIP	600	980	1.80	4.265	
63	50.1 0304 Closeout - Upper Rail	S	DP	700	1000	1.00	0.616	0.616
56	60.2 0007 Mounting Plate - Crush Can Front RH	S	DP	500	800	1.75	0.121	0.121
57	60.2 0008 Mounting Plate - Crush Can Front LH	S	DP	500	800	1.75	0.121	0.121
64	50.1 0044 Shock Tower - Frt RH	S	TWIP	500	980	1.00	1.457	1.457
114	50.1 3002 Reinf - Shock Tower Frt	S	DP	700	1000	2.00	0.69	0.69
65	50.1 0063 Shock Tower - Frt LH	S	TWIP	500	980	1.00	1.457	1.457
115	50.1 3003 Reinf - Shock Tower Frt	S	DP	700	1000	2.00	0.69	0.69

**Overview Report - FutureSteelVehicle Phase 2**  
**30 APRIL 2011**

Part No.	Part Description	Forming	Type	Yield	Tensile	Thickness	Sub Mass	Total Mass
66	50.1 0022 Shotgun Inner LH	S	HF	1050	1500	1.20	0.476	2.15
			HF	1050	1500	0.80	0.759	
			HF	1050	1500	1.50	0.915	
67	50.1 0021 Shotgun Inner RH	S	HF	1050	1500	1.20	0.476	2.15
			HF	1050	1500	0.80	0.759	
			HF	1050	1500	1.50	0.915	
68	50.1 0326 A-Pillar Brace	RF	DP	700	1000	1.20	0.695	0.695
69	50.1 0326 A-Pillar Brace LH	RF	DP	700	1000	1.20	0.695	0.695
70	50.1 0318 Shotgun Brace LH	S	BH	210	340	1.20	0.206	0.206
71	50.1 0308 Shotgun Brace RH	S	BH	210	340	1.20	0.206	0.206
72	50.6 0023 Roof Rail Inner Front LH	HS	HF	1050	1500	0.70	0.84	1.171
			HF	1050	1500	0.95	0.331	
73	50.6 0064 FBHP Inner LH	S	DP	500	800	1.20	1.667	1.667
74	50.6 0056 Rocker Filler Front LH	S	BH	210	340	0.60	0.199	0.199
75	50.6 0017 B-Pillar Inner LH	HS	HF	1050	1500	0.80	0.547	1.491
			HF	1050	1500	0.60	0.944	
76	50.6 0053 Roof Rail Inner Rear LH	S	BH	210	340	1.10	0.372	0.372
77	50.1 0067 Panel - Wheel House Outer LH	S	DP	500	800	0.65	1.732	1.732
78	50.6 0004 C-Pillar Inner LH	S	DP	500	800	0.70	1.428	1.428
79	50.2 0034 Bracket - Roof Rail to Header LH	S	BH	210	340	1.00	0.103	0.103
80	50.2 0035 Bracket - Roof Rail to Roof Bow LH	S	BH	210	340	1.00	0.254	0.254
81	50.6 0018 Reinf - Roof Rail LH	HS	HF	1050	1500	0.70	2.049	2.049
82	50.6 0066 Rocker LH	RF	CP	1050	1470	1.00	6.032	6.032
83	50.6 0072 Rocker Cap LH	S	BH	210	340	0.85	0.244	0.244
84	50.6 0028 Reinf - B-Pillar LH	HS	HF	1050	1500	0.60	1.189	1.491
			HF	1050	1500	1.00	0.302	
85	50.6 0006 Body Side Outer LH	HS	DP	350	600	0.80	8.359	11.098
			BH	210	340	0.60	2.739	
86	50.6 0069 Panel Rear Quarter Lwr LH	S	BH	210	340	1.20	0.198	0.198
87	50.6 0051 Panel - Gutter Rear LH	S	BH	210	340	1.00	0.795	0.795
117	50.6 6354 Reinf - FBHP LH	S	DP	700	1000	0.80	0.453	0.453
88	50.6 0046 FBHP Inner RH	S	DP	500	800	1.20	1.667	1.667
89	50.6 0022 Roof Rail Inner Front RH	HS	HF	1050	1500	0.70	0.84	1.171
			HF	1050	1500	0.95	0.331	
99	50.6 0055 Rocker Filler Front RH	S	BH	210	340	0.60	0.199	0.199
91	50.6 0009 B-Pillar Inner RH	HS	HF	1050	1500	0.80	0.547	1.491
			HF	1050	1500	0.60	0.944	
92	50.6 0052 Roof Rail Inner Rear RH	S	BH	210	340	1.10	0.372	0.372
93	50.1 0049 Panel - Wheel House Outer RH	S	DP	500	800	0.65	1.732	1.732
94	50.6 0005 C-Pillar Inner RH	S	DP	500	800	0.70	1.428	1.428
95	50.2 0033 Bracket - Roof Rail to Roof Bow RH	S	BH	210	340	1.00	0.254	0.254
96	50.2 0032 Bracket - Roof Rail to Header RH	S	BH	210	340	1.00	0.103	0.103
97	50.6 0012 Reinf - Roof Rail RH	HS	HF	1050	1500	0.70	2.049	2.049
98	50.6 0048 Rocker RH	RF	CP	1050	1470	1.00	6.032	6.032

**Overview Report - FutureSteelVehicle Phase 2**  
**30 APRIL 2011**

Part No.	Part Description	Forming	Type	Yield	Tensile	Thickness	Sub Mass	Total Mass
99	50.6 0071 Rocker Cap RH	S	BH	210	340	0.85	0.244	0.244
100	50.6 0026 Reinf - B-Pillar RH	HS	HF	1050	1500	0.60	1.189	1.491
			HF	1050	1500	1.00	0.302	
101	50.6 0050 Panel - Gutter Rear RH	S	BH	210	340	1.00	0.795	0.795
102	50.6 0068 Panel Rear Quarter Lwr RH	S	BH	210	340	1.20	0.198	0.198
103	50.6 0002 Body Side Outer RH	S	DP	350	600	0.80	8.359	11.098
			BH	210	340	0.60	2.739	
118	50.6 1354 Reinf - FBHP RH	S	DP	700	1000	0.80	0.453	0.453
104	50.2 0007 Rear Header Reinf	S	BH	210	340	2.00	2.759	3.775
			BH	210	340	0.70	1.016	
105	50.2 0006 Rear Header	S	BH	210	340	0.70	1.662	1.662
106	50.2 0009 Support - Roof LH	S	Mild	140	270	0.50	0.463	0.463
107	50.2 0008 Support - Roof RH	S	Mild	140	270	0.50	0.463	0.463
108	50.2 0013 Roof Bow	RF	BH	210	340	0.50	0.941	0.941
109	50.2 0011 Header - Roof Front	RF	BH	210	340	0.80	1.131	1.131
110	50.1 0405 Top Panel - Tunnel	S	DP	700	1000	1.00	3.067	3.067
111	50.2 0010 Pnl - Roof Outer	S	DP	300	500	0.50	9.011	9.011
112	50.1 0069 Shotgun Outer LH	HS	HF	1050	1500	1.00	0.431	2.088
			HF	1050	1500	0.80	0.689	
			HF	1050	1500	1.50	0.968	
113	50.1 0051 Shotgun Outer RH	HS	HF	1050	1500	1.00	0.431	2.088
			HF	1050	1500	0.80	0.689	
			HF	1050	1500	1.50	0.968	
<b>Total FSV-1 PHEV<sub>20</sub> Body Structure Mass</b>								<b>176.4</b>

## Appendix 5: FSV-2 Exploded View and Parts List

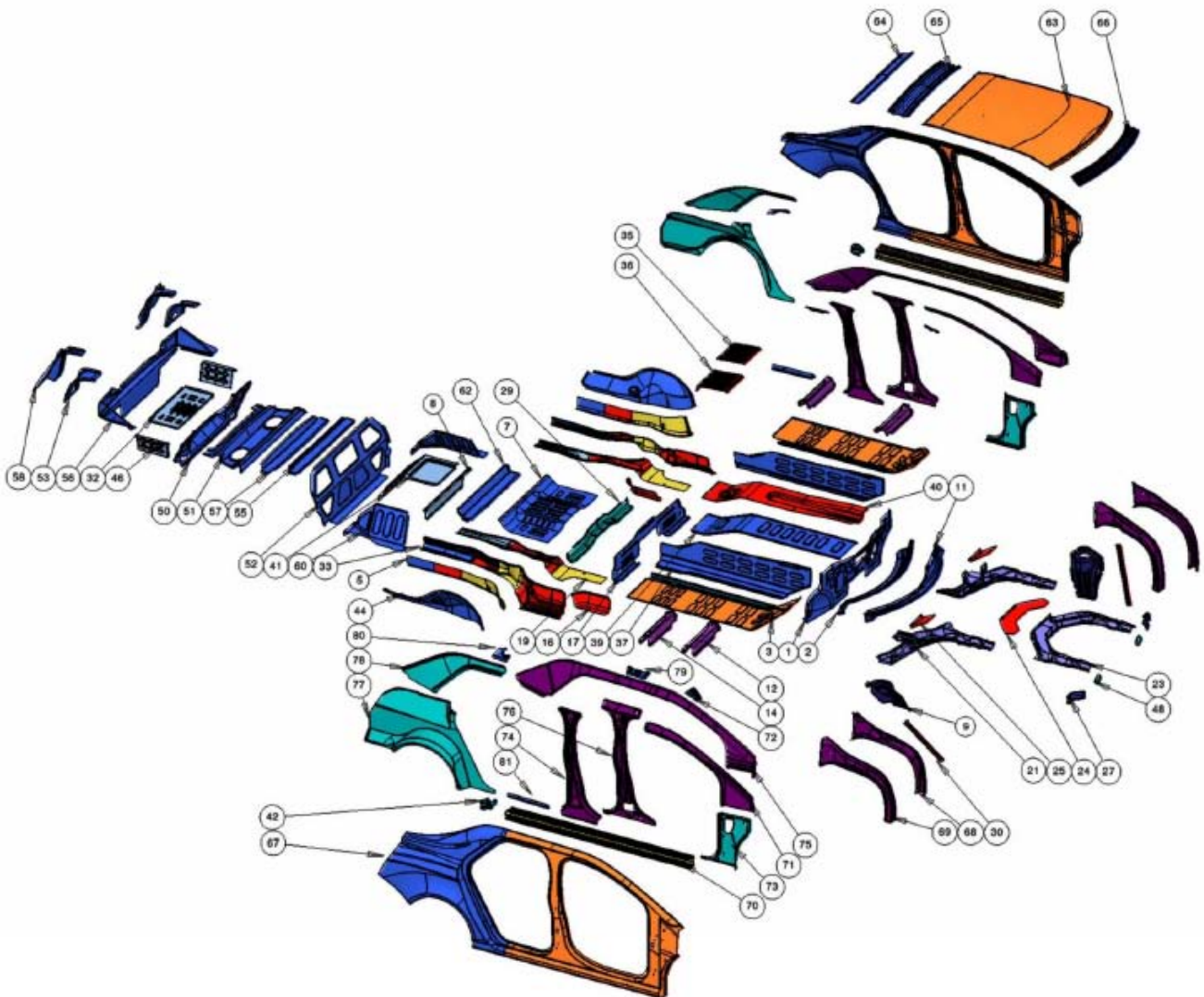


**Figure A5-1: FSV-2 Exploded View**

FSV-2 Parts List can be found in Table A5-1, following.

**Overview Report - FutureSteelVehicle Phase 2**  
**30 APRIL 2011**

**Table A5-1: FSV-2 Parts List**

Forming Key: (HS) Hot Stamping (RF) Rollforming (S) Stamping

Item	Part Description	Forming	Type	Yield	Tensile	Thickness	Sub Mass	Total Mass
1	50.1 0001 Dash Panel	S	BH	280	400	0.5	2.997	2.997
2	50.1 0002 Cowl Upper	S	BH	210	340	0.6	1.412	2.753
						1.2	1.341	
3	50.1 0011 Floor - Front RH	S	DP	300	500	0.5	2.914	4.824
			DP	500	800	1.5	1.91	
4	50.1 0025 Floor - Front LH	S	DP	300	500	0.5	2.914	4.824
			DP	500	800	1.5	1.91	
5	50.1 0014 Frame Rail Otr - Rear RH	S	CP	1000	1200	0.6	0.471	1.182
			DP	700	1000	1.4	0.456	
			HSLA	350	450	0.8	0.255	
6	50.1 0015 Frame Rail Otr - Rear LH	S	CP	1000	1200	0.6	0.471	1.182
			DP	700	1000	1.4	0.456	
			HSLA	350	450	0.8	0.255	
7	50.1 0016 Rear Seat Pan	S	BH	210	340	0.5	2.398	2.398
8	50.1 0032 Cargo Box Cross Member	S	Mild	140	270	0.5	0.791	0.791
9	50.1 0044 Apron Reinf RH	S	TWIP	500	980	1	1.462	1.462
10	50.1 0063 Apron Reinf LH	S	TWIP	500	980	1	1.462	1.462
11	50.1 0070 Cowl Lower	S	BH	210	340	0.6	0.787	1.66
						1.2	0.873	
12	50.1 0093 Frt Seat Frt Crossmember RH	RF	MS	950	1200	0.7	0.769	0.769
13	50.1 0094 Frt Seat Frt Crossmember LH	RF	MS	950	1200	0.7	0.769	0.769
14	50.1 0095 Frt Seat Rr Crossmember RH	RF	MS	950	1200	0.7	0.808	0.808
15	50.1 0096 Frt Seat Rr Crossmember LH	RF	MS	950	1200	0.7	0.808	0.808
16	50.1 0099 Side Panel RH	S	DP	700	1000	0.7	0.425	0.425
17	50.1 0100 Heel Board	S	BH	210	340	0.6	1.639	1.639
18	50.1 0101 Side Panel LH	S	DP	700	1000	0.7	0.425	0.425
19	50.1 0109 Rear Frame Rail Reinf RH	S	CP	100	1200	1.1	0.75	2.37
			DP	700	1000	0.65	0.556	
			Mild	140	720	1.55	1.064	
20	50.1 0110 Rear Frame Rail Reinf LH	S	CP	100	1200	1.1	0.75	2.37
			DP	700	1000	0.65	0.556	
			Mild	140	720	1.55	1.064	
21	50.1 0301 Front Rail - Lower RH	S	TRIP	600	980	1.8	4.685	5.995
						1.9	0.891	
						2	0.419	
22	50.1 0302 Front Rail - Lower LH	S	TRIP	600	980	1.8	4.685	5.995
						1.9	0.891	
						2	0.419	
23	50.1 0303 Front Rail - Upper	S	TRIP	600	980	0.8	0.297	5.938
						0.95	0.347	
						1.85	1.016	
						1.85	4.251	
24	50.1 0304 Closeout - Upper Rail	S	DP	700	1000	1	0.939	0.939
25	50.1 0305 Lower Rail Closeout RH	S	DP	700	1000	1	0.391	0.391
26	50.1 0306 Closeout - Lower Rail LH	S	DP	700	1000	1	0.391	0.391

**Overview Report - FutureSteelVehicle Phase 2**  
30 APRIL 2011

Part No.	Part Description	Forming	Type	Yield	Tensile	Thickness	Sub Mass	Total Mass
27	50.1 0308 Shotgun Brace RH	S	BH	210	340	0.7	0.122	0.122
28	50.1 0318 Shotgun Brace LH	S	BH	210	340	0.7	0.122	0.122
29	50.1 0320 Side to Side Rail	S	DP	500	800	0.8	1.149	1.149
30	50.1 0326 A-Pillar Brace RH	RF/T	DP	700	1000	0.7	0.401	0.401
31	50.1 0327 A-Pillar Brace LH	RF/T	DP	700	1000	0.7	0.401	0.401
32	50.1 0330 Cargo Box Floor Panel	S	IF	140	270	0.5	1.139	1.139
33	50.1 0335 Rear Frame Rail Inner RH	S	DP	700	1000	1.4	3.321	4.255
			CP	1000	1200	0.6	0.314	
			HSLA	350	450	0.8	0.62	
34	50.1 0336 Rear Frame Rail Inner LH	S	DP	700	1000	1.4	3.321	4.255
			CP	1000	1200	0.6	0.314	
			HSLA	350	450	0.8	0.62	
35	50.1 0400 Tunnel Bulkhead Upper	S	DP	700	1000	0.8	0.772	0.772
36	50.1 0401 Tunnel Bulkhead Lower	S	DP	700	1000	0.8	0.961	0.961
37	50.1 0402 Tunnel Side Panel RH	S	BH	280	400	0.5	2.403	2.403
38	50.1 0403 Tunnel Side Panel LH	S	BH	280	400	0.5	2.403	2.403
39	50.1 0404 Tunnel Top Reinforcement	S	BH	280	400	0.5	2.509	2.509
40	50.1 0405 Tunnel Top Panel	S	DP	700	1000	0.6	2.949	2.949
41	50.1 0500 Rear Floor Panel	S	Mild	140	210	0.5	1.667	1.667
42	50.1 2002 Suspension Mount RH	S	DP	500	800	2	0.37	0.37
43	50.1 2001 Suspension Mount LH	S	DP	500	800	2	0.37	0.37
44	50.1 2017 Rear Wheelhouse Inner RH	S	BH	210	340	1.2	1.727	2.473
						0.7	0.75	
45	20.1 0217 Wheelhouse Inner Rear LH	S	BH	210	340	1.2	1.727	2.473
						0.7	0.75	
46	50.1 2112 Cargo Box Side Panel RH	S	Mild	140	210	0.5	0.33	0.33
47	50.1 2113 Cargo Box Side Panel LH	S	Mild	140	210	0.5	0.33	0.33
48	60.2 0007 Frt Crush Can Mntg Plate RH	S	DP	500	800	1.75	0.121	0.121
49	60.2 0008 Frt Crush Can Mntg Plate LH	S	DP	500	800	1.75	0.121	0.121
50	50.1 0501 Back Panel Inner	S	BH	210	340	0.7	2.124	2.124
51	50.1 8675 Package Shelf	S	BH	210	340	0.7	3.307	3.307
52	50.1 3090 Seat Back Panel	S	BH	210	340	0.5	2.81	2.81
53	50.1 0502 Back Panel Inner Upper RH	S	BH	210	340	0.7	0.524	0.524
54	50.1 0503 Back Panel Inner Upper LH	S	BH	210	340	0.7	0.524	0.524
55	50.1 1999 Package Shelf Front Support	S	BH	210	340	0.7	0.898	0.898
56	50.1 0271 Back Panel	S	BH	210	340	0.7	3.521	3.521
57	50.1 5789 Package Shelf Rear Support	S	BH	210	340	0.7	1.359	1.359
58	50.1 7685 Lamp Can RH	S	BH	210	340	0.8	1.259	1.259
59	50.1 7785 Lamp Can LH	S	BH	210	340	0.8	1.259	1.259
60	50.1 0510 Rear Floor Side Panel RH	S	BH	210	340	0.5	1.038	1.038
61	50.1 0517 Rear Floor Side Panel LH	S	BH	210	340	0.5	1.038	1.038
62	50.1 0420 Seat Back Lwr Crossmember	S	BH	210	340	0.5	1.215	1.215
63	50.2 5332 Roof Panel	S	DP	350	600	0.5	7.48	7.48
64	50.2 5334 Rear Header	RF	BH	210	340	0.8	1.24	1.24
65	50.2 0013 Roof Bow	RF	BH	210	340	0.5	1.11	1.11
66	50.2 0011 Roof Front Header	S	BH	210	340	0.8	1.223	1.223

**Overview Report - FutureSteelVehicle Phase 2**  
**30 APRIL 2011**

Item	Part Description	Forming	Type	Yield	Tensile	Thickness	Sub Mass	Total Mass
67	50.6 2002 Body Side Outer RH	S	DP	350	600	0.8	8.074	13.116
			BH	210	340	0.6	5.042	
68	50.1 0021 Shotgun Inner RH	HS	HF	1050	1500	1.5	0.92	2.675
						1.2	0.476	
						0.8	1.278	
69	50.1 0051 Shotgun Outer RH	HS	HF	1050	1500	0.8	0.689	2.09
						1	0.431	
						1.5	0.968	
70	50.6 0048 Rocker RH	RF	CP	1050	1470	1.2	8.434	8.434
71	50.6 0022 Roof Rail Inner Front RH	HS	HF	1050	1500	0.7	0.812	1.086
						0.95	0.275	
72	50.2 0032 Brkt - Roof Rail to Header RH	S	BH	210	340	1	0.103	0.103
73	50.6 0046 FBHP Inner RH	S	DP	500	700	1.2	1.666	1.666
74	50.6 2026 B-Pillar Reinf RH	HS	HF	1050	1500	0.6	1.11	1.749
						1	0.64	
75	50.6 2012 Roof Rail Reinf RH	HS	HF	1050	1500	0.7	2.576	2.576
76	50.6 2009 B-Pillar Inner RH	HS	HF	1050	1500	0.6	0.696	1.54
						0.8	0.844	
77	50.1 2049 Wheel House Outer Panel RH	S	DP	500	800	0.65	3.808	3.808
78	50.6 2052 C-Pillar Inner RH	S	DP	500	800	0.7	1.368	1.368
79	50.2 2033 Roof Bow to Roof Rail Brkt RH	S	BH	210	340	0.5	0.149	0.149
80	50.6 6482 Rear Header Bracket RH	S	BH	210	340	0.8	0.134	0.134
81	50.6 5413 Rear Door Closeout Panel RH	S	BH	210	340	0.5	0.109	0.109
82	50.6 0064 FBHP Inner LH	S	DP	500	700	1.2	1.666	1.666
83	50.6 0066 Rocker LH	RF	CP	1050	1470	1.2	8.434	8.434
84	50.6 2023 Roof Rail Inner Front LH	HS	HF	1050	1500	0.7	0.812	1.086
						0.95	0.275	
85	50.1 0069 Shotgun Outer LH	HS	HF	1050	1500	0.8	0.689	2.09
						1	0.431	
						1.5	0.968	
86	50.1 0022 Shotgun Inner LH	HS	HF	1050	1500	1.5	0.92	2.675
						1.2	0.476	
						0.8	1.278	
87	50.6 2003 Body Side Outer LH	S	DP	350	600	0.8	8.074	13.116
			BH	210	340	0.6	5.042	
88	50.2 2633 Roof Rail to Header Brkt LH	S	BH	210	340	1	0.103	0.103
89	50.6 2626 B-Pillar Reinf LH	HS	HF	1050	1500	0.6	1.11	1.749
						1	0.64	
90	50.6 2612 Roof Rail Reinf LH	HS	HF	1050	1500	0.7	2.576	2.576
91	50.6 2609 B-Pillar Inner LH	HS	HF	1050	1500	0.6	0.696	1.54
						0.8	0.844	
92	50.1 2649 Wheel House Outer Panel RH	S	DP	500	800	0.65	3.808	3.808
93	50.6 2652 C-Pillar Inner LH	S	DP	500	800	0.7	1.368	1.368
94	50.2 7633 Roof Bow to Roof Rail Brkt LH	S	BH	210	340	0.5	0.149	0.149
95	50.6 4682 Rear Header Bracket LH	S	BH	210	340	0.8	0.134	0.134
96	50.6 4513 Rear Door Closeout Panel LH	S	BH	210	340	0.5	0.109	0.109
<b>Total FSV-2 Body Structure Mass</b>								<b>200.8</b>